

Aalto University
School of Science
Master's Programme in Mathematics and Operations Research

Pekka Huhtala

Loop $O(n)$ models: a numerical transfer matrix study of long range order and s-holomorphicity

Master's Thesis
Espoo, March 19, 2021

Supervisor: Professor Nuutti Hyvönen
Advisor: Professor Nuutti Hyvönen

Author:	Pekka Huhtala	
Title:	Loop $O(n)$ models: a numerical transfer matrix study of long range order and s-holomorphicity	
Date:	March 19, 2021	Pages: 102
Major:	Mathematics	Code: SCI3054
Supervisor:	Professor Nuutti Hyvönen	
Advisor:	Professor Nuutti Hyvönen	
<p>This work studies $O(n)$ models, which are classical spin hamiltonians defined in a two-dimensional lattice. From the $O(n)$ models, it is possible to derive $O(n)$ loop models. For these, it is possible to express expectation values of observables as sums of graphs in the lattice.</p> <p>At the critical points, at the continuum limit, some of these models are expected converge to conformally invariant models. Then the expectation values would be holomorphic functions of the space variable. It is expected that there are loop $O(n)$ models in finite lattices, that have related properties. Such properties may be discrete holomorphicity and s-holomorphicity.</p> <p>I study these questions numerically, with transfer matrices. I first construct the transfer matrices for the loop $O(n)$ models in the hexagonal lattice, for its partition function and the expectation value of the parafermionic observable.</p> <p>I use the partition function transfer matrix in the numerical study of long range order. This gives a new way of understanding the results of the renormalization group studies on the $O(n)$ models.</p> <p>I use the transfer matrices for parafermions in the numerical study of s-holomorphicity, which is expected to be a sufficient property for the convergence of expectation values of the parafermionic observable. The numerical transfer matrix approach gives meaningful results, for which parameter values n, K the s-holomorphicity would be possible.</p>		
Keywords:	$O(n)$ models, loop $O(n)$ models, conformal invariance, renormalization group, parafermionic observable, s-holomorphicity, transfer matrix	
Language:	English	

Tekijä:	Pekka Huhtala		
Työn nimi:	$O(n)$ rengasmallien korrelaatio- ja s -holomorfinisuusominaisuudet : numeerinen siirtomatriisitutkimus		
Päiväys:	19. maaliskuuta 2021	Sivumäärä:	102
Pääaine:	Matematiikka	Koodi:	SCI3054
Valvoja:	Professor Nuutti Hyvönen		
Ohjaaja:	Professor Nuutti Hyvönen		
<p>Tämä työ käsittelee $O(n)$-malleja, jotka ovat kaksiulotteisissa hiloissa määriteltyjä klassisia spin-malleja (Hamiltonin funktioita). $O(n)$-mallista voidaan johtaa $O(n)$-rengasmalli. $O(n)$-rengasmallien observaabelien odotusarvot voidaan esittää graafisesti, renkaiden ja polkujen summana hilassa.</p> <p>Kriittisissä pisteissä ja hilavakion lähestyessä nollaa, näiden mallien uskotaan lähestyvän konformi-invariantteja malleja. Tällöin observaabelien odotusarvot ovat paikkamuuttujan holomorfinisia funktioita. On arveltu, että äärellisen hilan $O(n)$-rengasmalleilla on vastaavia diskreettejä rakenteita, kuten diskreetti holomorfinisuus ja s-holomorfinisuus.</p> <p>Näitä asiota tutkitaan numeerisesti, siirtomatriisien avulla. Korrelaatiofunktioiden laskeminen vahvistaa renormalisaatioryhmän avulla saadut tulokset, mutta antaa myös uuden lähestymistavan.</p> <p>Myös s-holomorfinisuuden ja konvergenssin tutkiminen numeerisesti siirtomatriisien avulla antaa järkeviä tuloksia.</p>			
Asiasanat:	$O(n)$ mallit, $O(n)$ rengasmallit, konformi-invarianssi, renormalisaatioryhmä, parafermioni, s -holomorfinisuus, siirtomatriisi		
Kieli:	Englanti		

Acknowledgements

I thank my wife Kaija, for the warm hugs that cured my heart, for the good life together.

I thank prof. Kalle Kytölä for giving me a good research topic. Actually, prof. Kytölä gave me three optional topics to choose from. All three were very fine, giving a possibility to write a good publication. Very few professors can do that, I have learned.

Hämeenlinna, March 19, 2021

Pekka Huhtala

Contents

1	Introduction	7
2	The $O(n)$ and $O(n)$ loop models	10
2.1	A lattice model of classical spins	10
2.2	Integrals over one spin	14
2.3	From $O(n)$ model to $O(n)$ loop model	16
2.4	Correlation functions in the $O(n)$ loop model	19
3	Parafermionic observable for the $O(n)$ loop model	22
3.1	Parafermionic observable in a hexagonal lattice	23
3.2	Solutions with $n = 2$, $n = 3/2$ and $n = 1$	26
4	Theoretical physics at the scaling limit	29
4.1	Renormalization group (RG) basics	29
4.2	Transfer matrix	36
4.2.1	General introduction	37
4.2.2	Long range order	38
4.2.3	Parafermionic observable	40
5	Proving conformal invariance at the scaling limit	43
5.1	Complex analysis in \mathbb{C}	44
5.2	Complex analysis in lattices	47
5.3	Proofs and proof ideas of conformal invariance	51
5.3.1	$O(1)$ is conformally invariant at the scaling limit . . .	51
5.3.2	Studying conformal invariance with transfer matrices .	58
6	Constructing the transfer matrices for the loop $O(n)$ model	60
6.1	Transfer matrix for the $O(n)$ loop model, the Blöte-Nienhuis -construction	60
6.2	Transfer matrix for the $O(n)$ loop model, the $ \cdot$ -row V -row construction	62

6.3	Transfer matrix for the $O(n)$ loop model with a parafermionic observable	66
7	Loop $O(n)$ model transfer matrix calculations I: the long range order	71
8	Loop $O(n)$ model transfer matrix calculations II: testing the s-holomorphicity of the parafermionic observable	83
9	Conclusions	88
A	Algorithms	91
B	Additional figures for chapter 8 (s-holomorphicity)	93
C	Additional figures for chapter 8 (parafermion)	98

Chapter 1

Introduction

The $O(n)$ model is a classical spin hamiltonian defined in a two-dimensional lattice. A lattice is a repeated arrangement of points. There is a length scale a determining the distance between lattice points. If a is decreased, in a finite domain $\Omega \subset \mathbb{R}^2$ covered by lattice, the amount of lattice points is increasing. There will be finer and finer lattices in fixed domain Ω , as a is decreased.

What happens to physics [1], described by the $O(n)$ model, when $a \rightarrow 0$? A key physical quantity is the correlation length ξ . In this case ξ means the maximal distance where spins are correlated: if a spin at point A has a certain direction, the direction of spin at point B is related to this. The directions of uncorrelated spins are independent. So we have two length scales, a and ξ .

If ξ is finite, the limit $a \rightarrow 0$ of the model is taken keeping D and ξ constant. If the limit exists, it is expected to be a field theory, a Hamiltonian, where the degrees of freedom are defined at every point of $D \subset \mathbb{R}^2$. The correlation length may diverge at certain temperatures, called critical temperatures. These are points for second order phase transitions. The resulting field theory is expected to be a conformal field theory. Observables in conformal field theories are complex, holomorphic functions. This raises questions related to the lattice model. When do such limits exist? What are the discrete structures that will have such limits?

In this work, I will try to answer these questions by studying a special model, called the $O(n)$ loop model, in two-dimensional hexagonal lattice. After defining this discrete model and some mathematical structures related to it, I turn to results from the known renormalization group studies. This is necessary for defining and correctly approaching criticality and the scaling limit. Universality, a central result of the renormalization group, states for example that the critical properties of lattice models are independent

of lattice details. I then turn to the second central subject of this work, preholomorphicity and parafermionic observables.

The idea of preholomorphicity is that, as the observables at the scaling limit at criticality are expected to be holomorphic functions of the space coordinates, there should be related structures in the discrete model. Parafermionic observables are functions of dynamic variables of the discrete model, and also preholomorphic functions of position in the two-dimensional complex coordinates. Here the preholomorphicity means essentially discretisation of Morera's theorem.

The task is then to show that the parafermionic observable F becomes a holomorphic function at the scaling limit. This has been done famously for the Ising model (which is the $O(1)$ model), by Smirnov [2]. The proof is based on formulating a related Riemann problem, which is to determine a holomorphic function in a domain from its values on the boundary. Part of Smirnov's work relies on showing that the square F^2 of the parafermionic observable is also preholomorphic. Reason for studying F^2 is that the boundary condition is easily given for F^2 , which is even constant on the boundary of Ω . The Riemann problem for F^2 can be solved to give a holomorphic function.

Smirnov introduced for parafermion F a stricter condition called s-holomorphicity. Then, for the Ising model, the needed holomorphicity for F^2 is achieved, and thus the parafermionic function F is shown to be holomorphic at the scaling limit.

It is fairly easy to define preholomorphic observables F for any $O(n)$ -loop model. For the similar proof (as for the Ising model) of holomorphicity at the scaling limit, it would be necessary to find that quantities $F^{1/s}$ are also holomorphic. Here s is called the parafermionic spin, and for a given n and a given $O(n)$ -loop model, there are two possible spin values. I will study holomorphicity and s-holomorphicity of F with a very straightforward calculation, using transfer matrices.

This work begins by the definition of the $O(n)$ -model in chapter 2. In the same section, the loop $O(n)$ -models are derived from the $O(n)$ -models. Chapter 2 ends with an expression for the 2-point correlation function for the $O(n)$ loop model. Chapter 3 defines the parafermionic observable and function $F(z)$ as its expectation value. The preholomorphicity condition then gives equations for the model parameters. Chapter 4 introduces some general ideas in the renormalization group and the concept of transfer matrix. Chapter 5 is essentially a part of Smirnov's reviews, and the idea is to show the importance and role of s-holomorphicity in the proof of conformal invariance.

Chapter 6 represents my construction for the transfer matrix of loop $O(n)$ -models in a hexagonal lattice. Using this transfer matrix, I calculate

numerically correlation functions in chapter 7, confirming and expanding the views by the renormalization group in chapter 4. In chapter 6, I also construct transfer matrices for the parafermionic function $F(z)$. In chapter 8 I do a numerical study of the s-holomorphicity of the loop $O(n)$ model in the hexagonal lattice.

Chapter 2

The $O(n)$ and $O(n)$ loop models

A classical hamiltonian H is a real function of the dynamical degrees of freedom (for particles, coordinates and their conjugate momenta). A hamiltonian, its functional form, determines the dynamics of a system, how it behaves in time. Using the Poisson brackets, this can be formulated so that H is the generator of translations in time. Usually the value of a classical Hamiltonian is the energy of the system.

Statistical physics uses often word model for the word hamiltonian, like Anderson model, Heisenberg model or the $O(n)$ models. These are all hamiltonians, with different degrees of freedom and functional forms. A model is a simplification of some real system.

There are many $O(n)$ -models, several in quantum field theory, for example. However I will here use the name $O(n)$ -model for the spin model, defined in 2.1.2 below.

Loop $O(n)$ models were introduced by Nienhuis [3]. The understanding of $O(n)$ loop model physics has not changed substantially since then.

2.1 A lattice model of classical spins

The $O(n)$ model is a model (a Hamiltonian) of classical spins in a usually two-dimensional lattice. A lattice is a repeated arrangement of points, so that the surroundings of each point is the same. An example of such Bravais lattice is the quadratic lattice.

Definition 2.1.1. (*Bravais lattice*)

Let $\tilde{a}_1, \tilde{a}_2 \in \mathbb{R}^2$ and $\tilde{a}_1 \cdot \tilde{a}_2 \neq 0$. A two-dimensional Bravais lattice B is defined as

$$B = \{n\tilde{a}_1 + m\tilde{a}_2, \quad n, m \in \mathbb{Z}\}. \quad (2.1)$$

A crystal lattice consists of identical copies of the same physical unit, called the crystal basis, located at all the points of the Bravais lattice. Usually crystal basis is defined by a finite set of points relative to a Bravais lattice point.

An example of a crystal lattice with a two-point crystal basis is the hexagonal lattice. Vectors a_1 and a_2 generating the bravais lattice and vector b defining the two-point crystal basis can be chosen as in Figure 2.1 below.

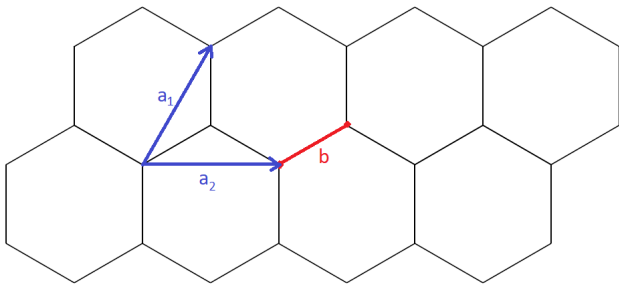


Figure 2.1: Hexagonal lattice, lattice generating vectors a_1 and a_2 and the crystal basis b .

Then the hexagonal lattice is the following set of points:

$$C_{hex} = \{n\tilde{a}_1 + m\tilde{a}_2 + kb \mid n, m \in \mathbb{Z}, k \in \{0, 1\}\}. \quad (2.2)$$

Figure 2.1 also defines vectors a_1 and $a_2 \in \mathbb{R}^2$. I will use a for the distance of nearest neighbours in the hexagonal lattice. I will refer to a hexagonal lattice point (n, m, k) with a single index $k \in C_{hex}$.

Lattice models are Hamiltonians, where the degrees of freedom are defined at the lattice points. In the $O(n)$ model, these degrees of freedom are classical (they all commute) spin vectors $S_k \in \mathbb{R}^n$ of unit length, $|S_k|^2 = 1$, for each lattice point k . $O(n)$ is a model of interacting spins, where each spin S_i interacts with its nearest neighbour.

Let Λ be a finite, simply connected subset of \mathbb{R}^2 covered by some finite lattice C^Λ . Let G^Λ be a graph, whose vertices are the lattice points, and bonds are the lines between nearest neighbours. (I reserve the word edge for a different purpose). In a hexagonal lattice C_{hex}^Λ graph G^Λ looks like a honeycomb. For a general lattice (C^Λ) and the hexagonal lattice (C_{hex}^Λ) the set of bonds can be written as

$$B^\Lambda = \left\{ \{v_1, v_2\} \mid v_1, v_2 \in C^\Lambda, \quad v_1, v_2 \text{ nearest neighbours} \right\}. \quad (2.3)$$

$$B_{hex}^\Lambda = \left\{ \{v_1, v_2\} \mid v_1, v_2 \in C_{hex}^\Lambda, \quad |v_1 - v_2| = a \right\}, \quad (2.4)$$

where a is the lattice constant in the hexagonal lattice.

We will study classical spin models in a lattice. That means we have at each lattice point $k \in C^\Lambda$ a spin $S_k \in \mathbb{R}^n$ (or at each vertex in graph terms). In $O(n)$ -models there is a further condition that $|S_k|^2 = 1$, $k \in C^\Lambda$. The meaning of a spin configuration S is simple: just give each spin in the lattice a value. Formally a spin configuration S can be defined as

$$S = \{ \{S_k\} \mid k \in C^\Lambda, S_k \in \mathbb{R}^n, |S_k|^2 = 1 \}. \quad (2.5)$$

The set of $O(n)$ spin configurations Ω (so that $S \in \Omega$) can be written as

$$\Omega = \{ S_i \in \mathbb{R} \mid S_i^2 = 1 \}^{|C_{hex}^\Lambda|}. \quad (2.6)$$

Now we are ready to define the lattice $O(n)$ -spin model.

Definition 2.1.2. (*$O(n)$ spin model in a general lattice*)

Let Λ be a finite, simply connected subset of \mathbb{R}^2 . Let Λ be covered by some lattice C^Λ . Let G^Λ be a graph, whose vertices are the lattice points, and B^Λ the set of bonds between nearest neighbours. Let S be a configuration of spins in the lattice, so that at each lattice point k there is a spin $S_k \in \mathbb{R}^n$, $|S_k|^2 = 1$. Let Ω be the set of spin configurations. Then the $O(n)$ -model is $H_{O(n)}^\Lambda : \Omega \rightarrow \mathbb{R}$,

$$H_{O(n)}^\Lambda(S) = -J \sum_{\{i,j\} \in B^\Lambda} S_i \cdot S_j. \quad (2.7)$$

The sum in equation (2.7) is simply over nearest neighbour -pairs in a lattice. $J \in \mathbb{R}$ is called the coupling constant of this model. For this model, the value of hamiltonian $H_{O(n)}^\Lambda(S)$ is the energy of spin configuration S . Thus

$$E_{O(n)}^\Lambda(S) = -J \sum_{\{i,j\} \in B^\Lambda} S_i \cdot S_j. \quad (2.8)$$

The name of the model, $O(n)$, refers to its symmetry. Symmetries are transformations that leave the hamiltonian (now $H_{O(n),hex}^\Lambda$) invariant. Starting from any spin configuration S , if every spin is rotated in the same way, the value of $H_{O(n),hex}^\Lambda$ does not change: $H_{O(n),hex}^\Lambda(S) = H_{O(n),hex}^\Lambda(RS)$, where R is a symbol for this rotation. As rotations in \mathbb{R}^n form a group called $O(n)$, we have an $O(n)$ -model.

For the $O(n)$ model in hexagonal lattice C_{hex}^Λ we get

$$H_{O(n),hex}^\Lambda(S) = -J \sum_{\{v_1,v_2\} \in B_{hex}^\Lambda} S_{v_1} \cdot S_{v_2}. \quad (2.9)$$

$H_{O(n),hex}^\Lambda(S)$ can be written in another way. An inner (not a boundary) lattice point $k \in C_{hex}^\Lambda$ has three nearest neighbours, in directions a_1 , a_2 and a_3 . I will call these points A_k , B_k and C_k . The $O(n)$ model in C_{hex}^Λ can then be written as

$$H_{O(n),hex}^\Lambda(S) = -\frac{J}{2} \sum_{k \in C_{hex}^\Lambda} (S_k \cdot S_{A_k} + S_k \cdot S_{B_k} + S_k \cdot S_{C_k}), \quad (2.10)$$

Compared to (2.9), each bond is counted twice in this sum. For that reason, there is a factor $\frac{1}{2}$.

In addition, I will represent the following four spin models, which may be analyzed with the methods given in this work. First is a generalization of the $O(n)$ model, which I call $O_{xxz}(n)$ model. Physically, the idea for this model is to change the geometry of the lattice.

$$H_{O_{xxz}(n),hex}^\Lambda(S) = -\frac{1}{2} \sum_{k \in C_{hex}^\Lambda} (J_1 S_k \cdot S_{A_k} + J_2 S_k \cdot S_{B_k} + J_2 S_k \cdot S_{C_k}). \quad (2.11)$$

For this model, there are then two groups of bonds in the hexagonal lattice C_{hex}^Λ . Let $B_{hex}^{\Lambda_1}$ be the set of J_1 -bonds and $B_{hex}^{\Lambda_2}$ the set of J_2 -bonds (see definition (2.4) for set B_{hex}^Λ). We get

$$H_{O_{xxz}(n),hex}^\Lambda(S) = -J_1 \sum_{\{v_1, v_2\} \in B_{hex}^{\Lambda_1}} S_{v_1} \cdot S_{v_2} - J_2 \sum_{\{v_1, v_2\} \in B_{hex}^{\Lambda_2}} S_{v_1} \cdot S_{v_2}. \quad (2.12)$$

Second modification keeps the lattice and interactions in $H_{O(n),hex}^\Lambda(S)$ intact, but changes the space of spins by cutting away some part of the unit sphere in \mathbb{R}^n , $n > 1$. So at each lattice point k there is a spin $S_k \in \mathbb{R}^n$, but now the spin is zero if the azimuthal angle ϕ is smaller than some chosen $\phi_0 \in (0, \pi/2)$:

$$S_k^2 = \begin{cases} 0, & |\phi - \pi/2| < \phi_0 \\ 1, & |\phi - \pi/2| \geq \phi_0. \end{cases} \quad (2.13)$$

I call the resulting model $H_{O(\phi_0),hex}^\Lambda$. This model has not the $O(n)$ symmetry.

Third model would be to use two spins S_k and s_k , with $S_k^2 = 1$, $s_k^2 = p$.

Fourth interesting model is the Blume-Capel -model:

$$H_{BC}(S) = -J \sum_{\{v_1, v_2\} \in B_{hex}^\Lambda} S_{v_1} \cdot S_{v_2} + \Delta \sum_{k \in C_{hex}^\Lambda} S_k - \tilde{H} \sum_{k \in C_{hex}^\Lambda} S_k. \quad (2.14)$$

H_{BC} is a reduced hamiltonian, to be properly defined in chapter 4. $\Delta \in \mathbb{R}$ is the chemical potential for vacancies and \tilde{H} the external magnetic field.

In the following, I will write H^Λ for $H_{O(n),hex}^\Lambda$, and H_{xxz}^Λ for $H_{O_{xxz}(n),hex}^\Lambda$. Thus a hexagonal lattice is assumed, if not otherwise stated. Otherwise the formulas would become unnecessarily messy.

2.2 Integrals over one spin

In the partition function, there are sums or integrations over all possible values for the degrees of freedom. For the $O(n)$ -model, the degrees of freedom are the spins $S_i \in \mathbb{R}^n$, $|S_i|^2 = 1$ at the lattice points i . In this subsection I will derive some useful integration rules for one spin variable. Material in this subsection is the engine room for exact calculations.

For spin S_i , in spherical coordinates $(r, \phi_1, \phi_2, \dots, \phi_{n-2}, \theta)$, $\phi_k \in [0, \pi]$, $\theta \in [0, 2\pi]$ we have (with $r = 1$)

$$\begin{aligned}
 dS_i &= \sin^{n-2}(\phi_1)d\phi_1 \cdot \sin^{n-3}(\phi_2)d\phi_2 \cdot \dots \cdot \sin(\phi_{n-2})d\phi_{n-2} \cdot d\theta \quad (2.15) \\
 S_i^1 &= \cos \phi_1 \\
 S_i^2 &= \sin \phi_1 \cos \phi_2 \\
 S_i^3 &= \sin \phi_1 \sin \phi_2 \cos \phi_3 \\
 S_i^{n-1} &= \sin \phi_1 \dots \sin \phi_{n-2} \cos \theta \\
 S_i^n &= \sin \phi_1 \dots \sin \phi_{n-2} \sin \theta \quad (2.16)
 \end{aligned}$$

Lemma 2.2.1. *Let $S_i \in \mathbb{R}^n$, $|S_i|^2 = 1$. Let Ω_n be the volume of an n -sphere, $\Omega_n := \int dS_i = \frac{\pi^{n/2}}{\Gamma(\frac{n}{2}+1)}$. Then*

$$\int dS_i S_i^a = 0, \quad a \in \{1, 2, \dots, n\}. \quad (2.17)$$

$$\int dS_i S_i^a S_i^b = \frac{\Omega_n}{n} \delta_{a,b}, \quad a, b \in \{1, 2, \dots, n\}. \quad (2.18)$$

Proof. As

$$\int_0^{2\pi} \cos \theta d\theta = 0, \quad \int_0^{2\pi} \sin \theta d\theta = 0, \quad \int_0^\pi \sin^k \phi \cos \phi d\phi = 0, \quad (2.19)$$

we get

$$\int dS_i S_i^a = 0, \quad a = 1, 2, \dots, n.$$

The volume of an n -sphere is $\int dS_i = \frac{\pi^{n/2}}{\Gamma(\frac{n}{2}+1)} =: \Omega_n$. Then, by symmetry

$$\int dS_i (S_i^a)^2 = \frac{\Omega_n}{n}, \quad a \in \{1, 2, \dots, n\}.$$

Using the trigonometric integration formulas above, we get

$$\int dS_i S_i^a S_i^b = 0, \quad a, b \in \{1, 2, \dots, n\}, \quad a \neq b.$$

From these we get the useful result

$$\int dS_i S_i^a S_i^b = \frac{\Omega_n}{n} \delta_{a,b}.$$

□

Then also $\int dS_i S_i^a S_i^b S_i^c S_i^d = 0$, since there must be one unpaired $\cos \theta$, or $\sin \theta$, or $\cos \phi$ in the product, each of which give zero when integrated over $[0, 2\pi]$ and $[0, \pi]$, respectively.

The next nonvanishing (with even order for $\cos \phi$) has integrals $\int dS_i (S_i^a)^2 (S_i^a)^2$ and $\int dS_i (S_i^a)^4$. Then the following result is useful:

Lemma 2.2.2. *Let $S_i \in \mathbb{R}^n$, $|S_i|^2 = 1$. Let Ω_n be the volume of an n -sphere, $\Omega_n := \int dS_i = \frac{\pi^{n/2}}{\Gamma(\frac{n}{2}+1)}$. Then*

$$\begin{aligned} \int dS_i S_i^a S_i^b S_i^c S_i^d &= \frac{\Omega_n}{n(n+4)} (\delta_{a,b} \delta_{c,d} + \delta_{a,c} \delta_{b,d} + \delta_{a,d} \delta_{b,c}) + \\ &+ \frac{3\Omega_n}{(n+1)(n+4)} (\delta_{a,b} \delta_{a,c} \delta_{a,d}), \quad a, b, c, d \in \{1, 2, \dots, n\} \end{aligned} \quad (2.20)$$

Proof. The following result is useful here:

$$\int_0^{\pi/2} \sin^{2p-1} \phi \cos^{2q-1} \phi d\phi = \frac{\Gamma(p)\Gamma(q)}{2\Gamma(p+q)}. \quad (2.21)$$

Then

$$\begin{aligned} \int dS_i (S_i^1)^2 (S_i^2)^2 &= \Omega_{n-2} \int_0^\pi \cos^2 \phi_1 \sin^2 \phi_1 \sin^{n-2} \phi_1 d\phi_1 \cdot \\ &\cdot \int_0^\pi \cos^2 \phi_2 \sin^{n-3} \phi_2 d\phi_2 \\ &= \Omega_{n-2} \cdot \frac{\Gamma(\frac{n}{2} + \frac{1}{2})\Gamma(\frac{3}{2})}{\Gamma(\frac{n}{2} + 2)} \cdot \frac{\Gamma(\frac{n}{2} - 1)\Gamma(\frac{3}{2})}{\Gamma(\frac{n}{2} + \frac{1}{2})} \\ &= \frac{\Omega_n}{n(n+4)}. \end{aligned}$$

Moreover,

$$\begin{aligned} \int dS_i (S_i^1)^4 &= \Omega_{n-1} \int_0^\pi \cos^4 \phi_1 \sin^{n-2} \phi_1 d\phi_1 \\ &= \frac{\Gamma(\frac{n}{2} - \frac{1}{2})\Gamma(\frac{5}{2})}{\Gamma(\frac{n}{2} + 2)} \frac{\pi^{\frac{n}{2} - \frac{1}{2}}}{\Gamma(\frac{n}{2} + \frac{1}{2})} \\ &= \frac{3\Omega_n}{(n+1)(n+4)}. \end{aligned}$$

By the $O(n)$ symmetry

$$\begin{aligned}\int dS_i (S_i^a)^2 (S_i^b)^2 &= \frac{\Omega_n}{n(n+4)}, & a, b \in \{1, 2, \dots, n\}, \\ \int dS_i (S_i^a)^4 &= \frac{3\Omega_n}{(n+1)(n+4)}, & a \in \{1, 2, \dots, n\}.\end{aligned}$$

All other integrals of this order have cos in odd order, and are therefore zero. Thus we get

$$\begin{aligned}\int dS_i S_i^a S_i^b S_i^c S_i^d &= \frac{\Omega_n}{n(n+4)} (\delta_{a,b}\delta_{c,d} + \delta_{a,c}\delta_{b,d} + \delta_{a,d}\delta_{b,c}) + \\ &+ \frac{3\Omega_n}{(n+1)(n+4)} (\delta_{a,b}\delta_{a,c}\delta_{a,d}).\end{aligned}$$

□

Finally some shorthand notation: for the integration over all degrees of freedom, I will use the following notation:

$$\int dS^N := \int dS_1 dS_2 \dots dS_N, \quad (2.22)$$

for a lattice with N vertices.

2.3 From $O(n)$ model to $O(n)$ loop model

The $O(n)$ model 2.1.2 is a hamiltonian function $H_{O(n),hex}^\Lambda(S)$, where S is a spin configuration. For spin models the energy of configuration S is $H(S)$, so we can write $E_{O(n),hex}^\Lambda(S) = H_{O(n),hex}^\Lambda(S)$. Knowing the energies for all configurations, it is possible to calculate various thermodynamic quantities using the methods of statistical physics [1].

In general, there are two reasons for turning to these methods. First, it enables us to calculate quantities for very large systems, and hopefully even at the scaling limit (I will define this later). Second, a physical system is not completely isolated (with the exception of all universe).

Depending on how a system is connected to its surroundings, statistical physics introduces different ensembles, which means that each configuration (for example Q_k , $k = 1, 2, \dots, N$) is given a certain statistical weight. In the canonical ensemble, this weight is $W(Q_k, T) = e^{-\beta E(Q_k)}$, where $\beta = 1/(k_B T)$. Then a key quantity is the canonical partition function

$$Z(T) = \sum_{k=1}^N e^{-\beta E(Q_k)}. \quad (2.23)$$

$Z(T)$ is a normalization factor: probability for configuration Q_k is $W(Q_k, T)/Z(T)$. From $Z(T)$, it is possible to calculate various expectation values and further thermodynamic quantities, by differentiating function $Z(T)$ with respect to T .

For $O(n)$ -model 2.1.2, the hamiltonian is

$$H^\Lambda(S) = -J \sum_{\{v_1, v_2\} \in B^\Lambda} S_{v_1} \cdot S_{v_2}. \quad (2.24)$$

The partition function of the $O(n)$ -model is then

$$\begin{aligned} Z_{O(n)}(T) &= \int dS^N e^{-\beta H^\Lambda(S)} = \int dS^N \exp\left(\beta J \sum_{\{v_1, v_2\} \in B^\Lambda} S_{v_1} \cdot S_{v_2}\right) \\ &= \int dS^N \prod_{\{v_1, v_2\} \in B^\Lambda} e^{\beta J S_{v_1} \cdot S_{v_2}}. \end{aligned} \quad (2.25)$$

Factors in the product are not independent, since a spin in the hexagonal lattice point interacts with three, not one neighbouring spins.

The following approximation, combined with result (2.18), is the key for obtaining a graphical expansion.

$$e^{\beta J S_i \cdot S_j} \simeq 1 + K S_i \cdot S_j. \quad (2.26)$$

Inserting this to (2.25) gives

$$\begin{aligned} Z_{O(n)} &= \int dS^N \prod_{\{v_1, v_2\} \in B^\Lambda} (1 + K S_{v_1} \cdot S_{v_2}) \\ &= \int_S dS^N \left[1 + K \cdot \sum_{\{v_1, v_2\} \in B^\Lambda} S_{v_1} \cdot S_{v_2} + \right. \\ &\quad \left. + K^2 \cdot \sum_{\substack{\{v_1, v_2\} \in B^\Lambda \\ \{v_3, v_4\} \in B^\Lambda \\ \{v_3, v_4\} \neq \{v_1, v_2\}}} (S_{v_1} \cdot S_{v_2})(S_{v_3} \cdot S_{v_4}) + \dots \right]. \end{aligned} \quad (2.27)$$

The first sum in (2.27) is over one edge -graphs in the hexagonal lattice. The second in (2.27) is over two edge -graphs in the hexagonal lattice, and so on.

In hexagonal lattice, a spin S_v interacts with three neighbours. Thus, S_k may appear in products 0, 1, 2, or 3 times. By Lemma 2.2.1, we get nonzero contributions only if S_k appears 0 or 2 times in the product.

As an example, take the term with three pairs in (2.27):

$$Z_{O(n)}^{3pairs} := K^3 \int dS^N \sum_{\{v_1, v_2\} \in B^\Lambda} \sum_{\substack{\{v_3, v_4\} \in B^\Lambda \\ \{v_3, v_4\} \neq \{v_1, v_2\}}} \sum_{\substack{\{v_5, v_6\} \in B^\Lambda \\ \{v_5, v_6\} \neq \{v_3, v_4\} \\ \{v_5, v_6\} \neq \{v_1, v_2\}}} (S_{v_1} \cdot S_{v_2})(S_{v_3} \cdot S_{v_4})(S_{v_5} \cdot S_{v_6}).$$

By Lemma 2.2.1, S_{v_1} must appear two times in the product:

$$Z_{O(n)}^{3pairs} = K^3 \int dS^N \sum_{\{v_1, v_2\} \in B^\Lambda} \sum_{\substack{\{v_1, v_3\} \in B^\Lambda \\ v_3 \neq v_2}} \sum_{\substack{\{v_5, v_6\} \in B^\Lambda \\ \{v_5, v_6\} \neq \{v_1, v_3\} \\ \{v_5, v_6\} \neq \{v_1, v_2\}}} (S_{v_1} \cdot S_{v_2})(S_{v_1} \cdot S_{v_3})(S_{v_5} \cdot S_{v_6}).$$

Also S_{v_2} and S_{v_3} must appear two times in the product. This means that $\{v_2, v_3\}$ must also be a bond.

$$Z_{O(n)}^{3pairs} = K^3 \int dS^N \sum_{\{v_1, v_2\} \in B^\Lambda} \sum_{\substack{\{v_1, v_3\} \in B^\Lambda \\ v_3 \neq v_2}} (S_{v_1} \cdot S_{v_2})(S_{v_1} \cdot S_{v_3})(S_{v_2} \cdot S_{v_3}).$$

We thus sum over graphs, where there are bonds $\{v_1, v_2\}$, $\{v_1, v_3\}$ and $\{v_2, v_3\}$. That makes a loop with three spins, so we can write

$$Z_{O(n)}^{3pairs} = K^3 \int dS^N \sum_{\substack{3\text{-loops } \{v_1, v_2, v_3\} \\ v_1, v_2, v_3 \in C^\Lambda}} (S_{v_1} \cdot S_{v_2})(S_{v_1} \cdot S_{v_3})(S_{v_2} \cdot S_{v_3}),$$

where the sum is over all 3-loops in the lattice (in a hexagonal lattice, there can be no 3-loops, of course). Let us calculate the integral over spins. By Lemma 2.2.1

$$\begin{aligned} Z_{O(n)}^{3pairs} &= \\ &= K^3 (\Omega_n)^{N-3} \sum_{\substack{3\text{-loops } \{v_1, v_2, v_3\} \\ v_1, v_2, v_3 \in C^\Lambda}} \int dS_{v_1} dS_{v_2} dS_{v_3} (S_{v_1} \cdot S_{v_2})(S_{v_1} \cdot S_{v_3})(S_{v_2} \cdot S_{v_3}). \end{aligned}$$

By Lemma 2.2.1

$$\begin{aligned} \int dS_{v_1} (S_{v_1} \cdot S_{v_2})(S_{v_1} \cdot S_{v_3}) &= \sum_{i,j=1}^n \int dS_{v_1} S_{v_1}^i S_{v_2}^i S_{v_1}^j S_{v_3}^j \\ &= \frac{\Omega_n}{n} \sum_{i=1}^n S_{v_2}^i S_{v_3}^i = \frac{\Omega_n}{n} S_{v_2} \cdot S_{v_3}, \end{aligned}$$

and

$$\begin{aligned} \int dS_{v_2} (S_{v_2} \cdot S_{v_3})(S_{v_2} \cdot S_{v_3}) &= \sum_{i,j=1}^n \int dS_{v_2} S_{v_2}^i S_{v_3}^i S_{v_2}^j S_{v_3}^j \\ &= \frac{\Omega_n}{n} \sum_{i=1}^n S_{v_3}^i S_{v_3}^i = \frac{\Omega_n}{n} S_{v_3} \cdot S_{v_3}, \end{aligned}$$

and finally

$$\int dS_{v_3} (S_{v_3} \cdot S_{v_3}) = \Omega_n.$$

We have thus got the result

$$Z_{O(n)}^{3 \text{ bonds}} = K^3 (\Omega_n)^{N-3} \sum_{3\text{-loops}} n \left(\frac{\Omega_n}{n} \right)^3 = \sum_{3\text{-loops}} n \left(\frac{K}{n} \right)^3.$$

If we have six spins, they can be paired into one big loop with six spins or two smaller loops with three spins:

$$Z_{O(n)}^{6 \text{ bonds}} = (\Omega_n)^N \left(\sum_{\substack{\text{graphs with} \\ \text{two 3-loops}}} n^2 \left(\frac{K}{n} \right)^6 + \sum_{\substack{\text{graphs with} \\ \text{one 6-loop}}} n \left(\frac{K}{n} \right)^6 \right).$$

I use the following terminology. Any $\{v_1, v_2\}$, where v_1 and v_2 are nearest neighbour vertices in the lattice, is called a *edge*. If an edge $\{v_1, v_2\}$ is occupied by a loop, so that a loop goes through points v_1 and v_2 , it is called a *bond* $\{v_1, v_2\}$. So a bond is part of some loop. Some authors use names occupied and non-occupied bonds.

Then the partition function can be written over all possible loop graphs in the lattice:

$$Z_{O(n)} = (\Omega_n)^N \sum_{\text{loop graphs}} n^L \cdot \tilde{K}^\epsilon, \quad (2.28)$$

L is the number of loops in the graph,

ϵ is the number of bonds in the graph.

where the sum is over all possible loop configurations in the lattice and $\tilde{K} := K/n$. I omit $(\Omega_n)^N$ and the "tilde" above K in the following sections, since K is a free parameter, and a common factor will not be important. Using the other notation explained above,

$$Z_{O(n)} = \sum_{\text{loop graphs}} n^L \cdot K^\epsilon, \quad (2.29)$$

L is the number of loops in the graph,

ϵ is the number of bonds in the graph.

2.4 Correlation functions in the $O(n)$ loop model

There are several ways of defining correlation functions, for example

$$\langle S_0 \cdot S_k \rangle = \frac{\int dS^N S_0 \cdot S_k e^{-\beta H_{O(n)}}}{Z_{O(n)}} = \frac{1}{Z_{O(n)}} \int dS^N \prod_{\substack{\text{edges } E \\ \text{in lattice}}} S_0 \cdot S_k e^{\beta J S_{E_a} \cdot S_{E_b}}, \quad (2.30)$$

where $Z_{O(n)}$ is the partition function (2.29) for the $O(n)$ model. It is important to understand, that S_0 and S_k are fixed values for spins at sites 0 and k . Therefore there is no integration over them, and thus the measure dS^N does not include dS_0 and dS_k .

Inserting this to (2.25) gives

$$\begin{aligned}
\langle S_0 \cdot S_k \rangle &= \frac{1}{Z_{O(n)}} \int dS^N \prod_{\{v_1, v_2\} \in B^\Lambda} (S_0 \cdot S_k)(1 + K S_{v_1} \cdot S_{v_2}) \\
&= \frac{1}{Z_{O(n)}} \int_S dS^N \left[1 + K \cdot \sum_{\{v_1, v_2\} \in B^\Lambda} (S_0 \cdot S_k)(S_{v_1} \cdot S_{v_2}) + \right. \\
&\quad \left. + K^2 \cdot \sum_{\{v_1, v_2\} \in B^\Lambda} \sum_{\substack{\{v_3, v_4\} \in B^\Lambda \\ \{v_3, v_4\} \neq \{v_1, v_2\}}} (S_0 \cdot S_k)(S_{v_1} \cdot S_{v_2})(S_{v_3} \cdot S_{v_4}) + \dots \right].
\end{aligned} \tag{2.31}$$

Results (2.17) and (2.18) will again lead to a useful graphical expansion. A graph giving a nonzero contribution has a path from vertex 0 to vertex k , and (possibly) loops.

At order K^3 , let us calculate the contribution from the following integral:

$$K^3 \int dS^N (S_0 \cdot S_k)(S_{v_1} \cdot S_{v_2})(S_{v_3} \cdot S_{v_4})(S_{v_5} \cdot S_{v_6}), \tag{2.32}$$

where $\{v_1, v_2\}, \{v_1, v_2\}, \dots, \{v_5, v_6\}$, are edges in the lattice, which means nearest neighbours. As noted many times in the previous section, the spins S_{v_k} must appear 0 or 2 times in the product, for a nonzero contribution. We can pair the spins v_1, v_2, \dots, v_6 as in the previous chapter, giving the term $(S_0 \cdot S_k)Z_{O(n)}$. But now, if two of the spins v_1, v_2, \dots, v_6 are S_0 and S_k , we have additional pairings, like (S_0 and S_k are still in the hamiltonian)

$$\begin{aligned}
&K^3 \int dS^N (S_0 \cdot S_k)(S_0 \cdot S_{v_2})(S_{v_2} \cdot S_{v_3})(S_{v_3} \cdot S_k) \\
&= K^3 (S_0 \cdot S_k) \Omega_n^{N-2-2} \sum_{a,b,c=1}^n \int dS_{v_2} dS_{v_3} S_0^a S_{v_2}^a S_{v_2}^b S_{v_3}^b S_{v_3}^c S_k^c \\
&= K^3 (S_0 \cdot S_k) \Omega_n^{N-4} \frac{\Omega_n}{n} \sum_{b,c=1}^n \int dS_{v_3} S_0^b S_{v_3}^b S_{v_3}^c S_k^c \\
&= K^3 (S_0 \cdot S_k) \Omega_n^{N-4} \left(\frac{\Omega_n}{n} \right)^2 (S_0 \cdot S_k).
\end{aligned} \tag{2.33}$$

More generally, we would have

$$\begin{aligned}
& K^a \int dS^N (S_0 \cdot S_k)(S_0 \cdot S_{v_2})(S_{v_2} \cdot S_{v_3}) \cdots (S_{v_a} \cdot S_k) \\
&= K^a (S_0 \cdot S_k)^2 \Omega_n^{N-2-(a-1)} \left(\frac{\Omega_n}{n} \right)^{a-1} \\
&= n (S_0 \cdot S_k)^2 \Omega_n^{N-2} \left(\frac{K}{n} \right)^a. \tag{2.34}
\end{aligned}$$

Factor $n(S_0 \cdot S_k)^2 \Omega_n^{N-2}$ does not depend on the order a . Such common factors are not important, at least in this work. Graphically, this term is a path from vertex 0 to vertex k .

Forming the possible pairings in $(S_0 \cdot S_{v_2})(S_{v_2} \cdot S_{v_3}) \cdots (S_{v_a} \cdot S_k)$, we can always form loops from some pairs of spins, in addition to the $0 \rightarrow k$ path from some pairs of spins. Again, writing $\tilde{K} = K/n$, and setting the constant factors to be 1, we get

$$\langle S_0 \cdot S_k \rangle = \frac{\sum_{\substack{\text{graphs with} \\ \text{path from 0 to } k \\ \text{and loops}}} \tilde{K}^{|\gamma|} \cdot \tilde{K}^\epsilon \cdot n^L}{\sum_{\text{loop graphs}} n^L \cdot \tilde{K}^\epsilon}, \tag{2.35}$$

where the sum in the numerator is over all graphs that have a path γ from 0 to k and loops. $|\gamma|$ is the number of bonds in the path, ϵ is the number of bonds in the loops, and L is the number of loops. Sum in the denominator is the partition function, calculated in the previous section.

Chapter 3

Parafermionic observable for the $O(n)$ loop model

There are three approaches to (or aspects of) two-dimensional lattice models and their continuum limits at criticality: conformal field theory (CFT) at the continuum, integrability as a lattice model, and holomorphicity, at the continuum limit and as a lattice model. The uniting thing could therefore be related to holomorphicity, but the full picture is still forming.

In CFT, the correlation functions of certain observables are holomorphic functions of $z = x + iy$, where x and y are the cartesian coordinates in \mathbb{R}^2 . The goal here is to find for the finite model related discrete objects which are discretely holomorphic or preholomorphic functions, in other words. The latter means that taking the continuum limit produces a holomorphic function. Parafermionic observables are such objects, defined for the discrete model. It seems that they can be preholomorphic only at the critical points, which makes sense.

Cardy [5] defines a discretely holomorphic function in the following way

Definition 3.0.1. *Let G be a planar graph embedded in \mathbb{R}^2 , for example the hexagonal lattice. Let $F(z_{ij})$ be a complex valued function defined at the midpoints z_{ij} of each edge (ij) . Then F is discretely holomorphic on G if*

$$\sum_{(ij) \in \mathcal{F}} F(z_{ij})(z_j - z_i) = 0, \quad (3.1)$$

where the sum is over the edges of each face \mathcal{F} of G .

This can be understood as a discrete version of Morera's theorem. It is known [15], that this is a condition for just a part of the Cauchy-Riemann relations.

3.1 Parafermionic observable in a hexagonal lattice

The following definition is again by John Cardy [5]. For $O(n)$ -loop model in hexagonal lattice the parafermionic observable is a discrete contour integral. A directed path starts from a lattice point at boundary, goes through hexagonal lattice points and ends at z_{ij} , in the middle of two lattice points z_i and z_j . Each right turn gives a factor $e^{is\pi/3}$, each left turn $e^{-is\pi/3}$, where s is a parameter called fractional spin. Thus the parafermionic observable reminds the two-point correlation function (2.35). A formal definition is then as follows:

Definition 3.1.1. (*Parafermionic observable in hexagonal lattice*)

Let γ be a directed path in the hexagonal lattice from boundary point $z = 0$ to point z_{ij} , which is in the middle of lattice points z_i and z_j . Let $s \in \mathbb{R}$ and $\lambda = e^{is\pi/3}$. Let t_l and t_r be the number of left and right turns in the path, and let $|\gamma|$ be the number of bonds in the path. Then the parafermionic observable is

$$O(\gamma) = K^{|\gamma|} \lambda^{t_r} \bar{\lambda}^{t_l} \quad (3.2)$$

We will be working with the ensemble average of the parafermionic observable, function $F(z)$:

$$F(z) = \frac{\sum_{\substack{\text{graphs with} \\ \text{path from } 0 \text{ to } z \\ \text{and loops}}} K^\epsilon n^L K^{|\gamma|} \lambda^{t_r} \bar{\lambda}^{t_l}}{\sum_{\text{loop graphs}} n^L K^\epsilon}, \quad (3.3)$$

where the sum in the numerator is over all graphs that have a path from 0 to z , and loops, like the correlation function (2.35). z is defined above: $z = x + iy$, where $(x, y) \in \mathbb{R}^2$ are the coordinates of a two-dimensional space. $F(z)$ can be expressed in a shorter notation as

$$F(z) = \langle K^{|\gamma|} \lambda^{t_r} \bar{\lambda}^{t_l} \rangle. \quad (3.4)$$

Cardy [5] then proves that $F(z)$ is a discretely holomorphic function:

Theorem 3.1.1. *In hexagonal lattice the function*

$$F(z) = \langle K^{|\gamma|} \lambda^{t_r} \bar{\lambda}^{t_l} \rangle \quad (3.5)$$

is discretely holomorphic in a related triangular lattice, when (α is a real parameter)

$$\begin{aligned} n &= -2 \cos(4\pi/\alpha), \\ s &= (6 - \alpha)/2\alpha, \\ K &= \left(2 \pm \sqrt{2 - n}\right)^{-1/2}. \end{aligned} \quad (3.6)$$

The ensemble average here means the ensemble average in the $O(n)$ loop model with the difference that a parafermionic path has first been drawn in the lattice. So in a configuration there are loops with the $O(n)$ weights and a parafermion line with parafermion weights, nonintersecting all.

Proof. The centers of hexagons in the hexagonal lattice form a triangular lattice. As noted in figure 3.1 below, the midpoints to edges in the hexagonal lattice are also midpoints of edges in a triangular lattice. The discrete holomorphism is proved for the triangles.

Let $\{z_1, z_2, z_3\}$ be such a triangle. Then the center of this triangle belongs to the hexagonal lattice. Let the center be at $z_0 \in \mathbb{Z}$. In an equilateral triangle, the corners are at the same distance, from z_0 . Let d be this distance. Let the corner points be $\{z_1, z_2, z_3\}$ in anticlockwise order. Then $z_1 = z_0 + de^{i\phi}$, $z_2 = z_0 + de^{i\phi}e^{i\frac{2\pi}{3}}$, $z_3 = z_0 + de^{i\phi}e^{i\frac{4\pi}{3}}$. The differences and midpoints of differences are translationally invariant:

$$z_{12} = \frac{1}{2}(z_2 - z_1) = \frac{1}{2}de^{i\phi}(e^{i\frac{2\pi}{3}} - 1) \quad (3.7)$$

$$z_{23} = \frac{1}{2}(z_3 - z_2) = \frac{1}{2}de^{i\phi}(e^{i\frac{4\pi}{3}} - e^{i\frac{2\pi}{3}}) = e^{i\frac{2\pi}{3}}z_{12} \quad (3.8)$$

$$z_{31} = \frac{1}{2}(z_1 - z_3) = \frac{1}{2}de^{i\phi}(1 - e^{i\frac{4\pi}{3}}) = e^{i\frac{4\pi}{3}}z_{12}. \quad (3.9)$$

Defining $\omega = e^{2\pi i/3}$, $z_{23} = \omega \cdot z_{12}$ and $z_{31} = \omega \cdot z_{12}^2$. The condition for discrete holomorphicity is then

$$F(z_{12}) + \omega F(z_{23}) + \omega^2 F(z_{31}) = 0.$$

Let the parafermionic path enter the triangle at point z_{12} . Let the parafermionic path end at this triangle, at z_{12} , or z_{23} , or z_{31} . The center point of the triangle belongs to the hexagonal lattice. There are six possibilities to end the path in this triangle (see figure 3.1 below).

The first possibility is that the path ends where it enters, and there are no loops through the center point. Then, summing over all possible loop configurations consistent with (no overlapping) this path, gives $F_s(z_{12})$.

The second possibility is to end at z_{23} , by an extra turn right from the center. It is clear, that the possible loop configurations are the same as for $F_s(z_{12})$, so $F_s(z_{23}) = K \lambda F_s(z_{12})$.

Third possibility is to end at z_{31} , by an extra turn left from the center. It is clear, that the possible loop configurations are the same as for $F_s(z_{12})$, so $F_s(z_{31}) = K \bar{\lambda} F_s(z_{12})$.

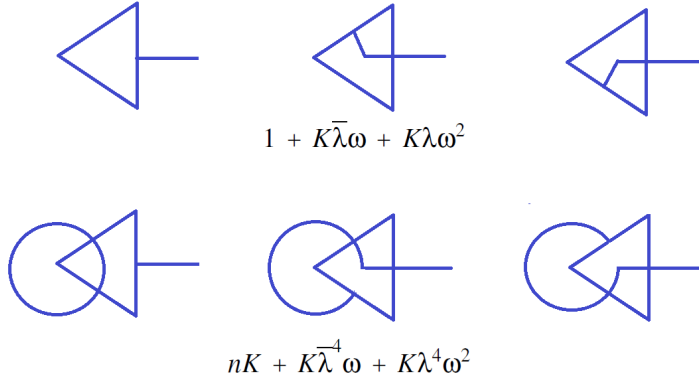


Figure 3.1: The six possibilities for a parafermionic path entering a triangle, to end in the triangle.

Then let the center point be occupied by some loop so that the parafermionic path ends at z_{12} . Then, summing over all possible loop configurations consistent with (no overlapping) this path, gives $F_l(z_{12})$.

The same loop going through the center point can almost be drawn as a parafermionic path. There is just a small distance missing inside the triangle, from the endpoint of path to the center point (see figure 3.1, the last two possibilities). A loop gives a factor nK^ϵ to the partition function. The related path to z_{13} gives a factor $K^\epsilon\lambda^4$ instead, so $F_l(z_{13}) = F_l(z_{12})\frac{\lambda^4}{n}$. Similarly $F_l(z_{23}) = F_l(z_{12})\frac{\bar{\lambda}^4}{n}$.

$$\text{As } F(z_{12}) = F_s(z_{12}) + F_l(z_{12}),$$

$$\begin{aligned} & F(z_{12}) + \omega F(z_{23}) + \omega^2 F(z_{31}) \\ &= F_s(z_{12}) + F_l(z_{12}) + \omega(F_s(z_{23}) + F_l(z_{23})) + \omega^2(F_s(z_{31}) + F_l(z_{31})) \\ &= F_s(z_{12}) (1 + K\lambda\omega + K\bar{\lambda}\omega^2) + F_l(z_{12}) \left(1 + \frac{\lambda^4}{n}\omega + \frac{\bar{\lambda}^4}{n}\omega^2\right). \end{aligned}$$

Thus we have a sufficient condition for discrete holomorphicity:

$$\begin{cases} 1 + K\lambda\omega + K\bar{\lambda}\omega^2 = 0, \\ 1 + \frac{\lambda^4}{n}\omega + \frac{\bar{\lambda}^4}{n}\omega^2 = 0. \end{cases}$$

This has a solution for $n \in [0, 2]$, when (where α is a parameter)

$$\begin{aligned} n &= -2 \cos(4\pi/\alpha), \\ s &= (6 - \alpha)/2\alpha, \\ K &= \left(2 \pm \sqrt{2 - n}\right)^{-1/2}. \end{aligned}$$

□

3.2 Solutions with $n = 2$, $n = 3/2$ and $n = 1$

I will now generalize Cardy's approach by writing the parafermionic observable as $O(\gamma) = R^{t_r} L^{t_l}$, with $R, L \in \mathbb{Z}$. I also make no assumptions on the symmetry of the triangle, so z_{23} and z_{31} are free variables. As the equations can be divided by z_{12} , I will set $z_{12} = 1$. There will then be six complex equations, as there is no rotational symmetry and thus $F_s(z_{12})$ may not be equal to $F_s(z_{23})$ or $F_s(z_{31})$, for example.

This approach results in a system of two equations, which were solved exactly with Mathematica. All these results belong to the group of results given by equations (3.6). So this subsection achieves only to prove (3.6) and find a way to exactly solve it. I found no solutions for $n > 0$, and give here the solutions for $n = 2$, $n = 3/2$ and $n = 1$.

First pair of equations for a path entering the triangle at point z_{12} , are derived as in the proof of theorem 3.1.1 above. In the loop part, ϵ is the number of edges in the loop through the center of the triangle.

$$\begin{aligned} F_s(z_{12})z_{12} + R \cdot F_s(z_{12})z_{23} + L \cdot F_s(z_{12})z_{13} &= 0, \\ nK^\epsilon F_l(z_{12})z_{12} + (R \cdot L)^{\frac{\epsilon}{2}-3} L \cdot R^5 F_l(z_{12})z_{23} + (R \cdot L)^{\frac{\epsilon}{2}-3} L^5 \cdot R F_l(z_{12})z_{13} &= 0. \end{aligned}$$

We can't have dependence on ϵ , so we must have $RL/K^2 = 1$. If $R = r e^{i\phi}$, $r, \phi \in \mathbb{R}$, it follows that $L = \frac{K^2 e^{-i\phi}}{r}$. We have first

$$\begin{aligned} z_{12} + R z_{23} + L z_{31} &= 0, \\ n z_{12} + \frac{R^2}{L^2} z_{23} + \frac{L^2}{R^2} z_{31} &= 0, \end{aligned}$$

or in polar form

$$\begin{aligned} r z_{12} + r^2 e^{i\phi} z_{23} + K^2 \cdot e^{-i\phi} z_{31} &= 0, \\ n K^4 r^4 z_{12} + r^8 e^{i4\phi} z_{23} + K^8 e^{-i4\phi} z_{31} &= 0. \end{aligned}$$

The system of six equations, for entering at z_{12} , z_{23} and z_{31} , is then

$$\begin{aligned}
z_{12} + Rz_{23} + Lz_{31} &= 0, \\
nz_{12} + \frac{R^2}{L^2}z_{23} + \frac{L^2}{R^2}z_{31} &= 0, \\
z_{31} + Rz_{12} + Lz_{23} &= 0, \\
nz_{31} + \frac{R^2}{L^2}z_{12} + \frac{L^2}{R^2}z_{23} &= 0, \\
z_{23} + Rz_{31} + Lz_{12} &= 0, \\
nz_{23} + \frac{R^2}{L^2}z_{31} + \frac{L^2}{R^2}z_{12} &= 0,
\end{aligned}$$

I then made several calculations with Mathematica, using $RL = K^2 \in \mathbb{R}_+$ as an additional equation. First, the symmetric case

$$\begin{aligned}
z_{12} + Rz_{23} + Lz_{31} &= 0, \\
nz_{12} + \frac{R^2}{L^2}z_{23} + \frac{L^2}{R^2}z_{31} &= 0,
\end{aligned} \tag{3.10}$$

To my disappointment I found no solutions for $n > 2$. But, with given $n \in [0, 2]$, there seems to be two possible values for s , and this is to my knowledge, a new result. As an example, I take $n = 2$, $K = 1/\sqrt{2}$. Then solutions to (3.10) are

$$\begin{aligned}
L_1 &= (-(1/2) - i/2)(-1)^{1/6}, & R_1 &= (1/2 + i/2)(-1)^{1/3}, \\
L_2 &= (1/2 - i/2)(-1)^{1/6}, & R_2 &= (1/2 - i/2)(-1)^{1/3}.
\end{aligned} \tag{3.11}$$

The absolute values of all these are $1/\sqrt{2}$. The arguments are $\phi_1 = 7\pi/12$ and $\phi_2 = \pi/12$. If $\phi = s\pi/3$, this means $s_1 = 7/4$ and $s_2 = 1/4$.

For $n = 3/2$ there are the following four solutions:

$$\begin{aligned}
K_1 &= \sqrt{\frac{(4 + \sqrt{2})}{7}} \simeq 0.8795, \\
L_1 &= \frac{1}{28}(7 + \sqrt{21} + 2\sqrt{42} + i(-7\sqrt{3} + \sqrt{7} + 2\sqrt{14})) \simeq 0.876573 - 0.0712603i, \\
R_1 &= \frac{1}{28}(7 + \sqrt{21} + 2\sqrt{42} - i(-7\sqrt{3} + \sqrt{7} + 2\sqrt{14})) \simeq 0.876573 + 0.0712603i, \\
s_1 &\simeq 0.07746,
\end{aligned} \tag{3.12}$$

where s is calculated from R :

$$\begin{aligned}
R_1 &\simeq 0.876573 + 0.0712603i = 0.879465 \cdot e^{-i0.0811159} \\
&= K_1 \cdot e^{-i0.0811159} = K_1 e^{-is\pi/3},
\end{aligned} \tag{3.13}$$

so that $s_1 = 3 \cdot 0.0811159/\pi \simeq 0.07746$.

$$\begin{aligned}
K_2 &= \sqrt{\frac{(4 + \sqrt{2})}{7}} \simeq 0.8795, \\
L_2 &= \frac{1}{28}(7 - \sqrt{21} - 2\sqrt{42} + i(-7\sqrt{3} - \sqrt{7} - 2\sqrt{14})) \simeq -0.376573 - 0.794765i, \\
R_2 &= \frac{1}{28}(7 - \sqrt{21} - 2\sqrt{42} - i(-7\sqrt{3} - \sqrt{7} - 2\sqrt{14})) \simeq -0.376573 + 0.794765i, \\
s_2 &\simeq 1.9225,
\end{aligned} \tag{3.14}$$

$$\begin{aligned}
K_3 &= \sqrt{\frac{(4 - \sqrt{2})}{7}} \simeq 0.6078, \\
L_3 &= \frac{1}{28}(7 + \sqrt{21(9 - 4\sqrt{2})}) + i\left(-\frac{\sqrt{3}}{4} - \frac{1}{4\sqrt{7}} + \frac{1}{\sqrt{14}}\right) \simeq 0.549247 - 0.260243i, \\
R_3 &= \frac{1}{28}(7 + \sqrt{21(9 - 4\sqrt{2})}) - i\left(-\frac{\sqrt{3}}{4} - \frac{1}{4\sqrt{7}} + \frac{1}{\sqrt{14}}\right) \simeq 0.549247 + 0.260243i, \\
s_3 &\simeq 0.4225,
\end{aligned} \tag{3.15}$$

$$\begin{aligned}
K_4 &= \sqrt{\frac{(4 - \sqrt{2})}{7}} \simeq 0.6078, \\
L_4 &= \frac{1}{28}(7 + \sqrt{21} - 2\sqrt{42} + i(-7\sqrt{3} + \sqrt{7} - 2\sqrt{14})) \simeq -0.0492466 - 0.605783i, \\
R_4 &= \frac{1}{28}(7 + \sqrt{21} - 2\sqrt{42} - i(-7\sqrt{3} + \sqrt{7} - 2\sqrt{14})) \simeq -0.0492466 + 0.605783i, \\
s_4 &\simeq 1.5775.
\end{aligned} \tag{3.16}$$

For $n = 1$ there are the following four solutions:

$$\begin{aligned}
K_1 &= 1, & L_1 &= 1, & R_1 &= 1, & s_1 &= 0, \\
K_2 &= 1, & L_2 &= 1/2(-1 - \sqrt{3}i), & R_2 &= 1/2(-1 + \sqrt{3}i), & s_2 &= 2, \\
K_3 &= 1/\sqrt{3}, & L_3 &= -i/\sqrt{3}, & R_3 &= i/\sqrt{3}, & s_3 &= 3/2, \\
K_4 &= 1/\sqrt{3}, & L_4 &= 1/6(3 - i\sqrt{3}), & R_4 &= 1/6(3 + i\sqrt{3}), & s_4 &= 1/2.
\end{aligned} \tag{3.17}$$

Chapter 4

Theoretical physics at the scaling limit

This section mainly considers renormalization group and transfer matrices. These give us general concepts, ideas and rules, how the physics of lattice systems can be treated, when the size of the system is increased in a controlled way. Renormalization group can seldom be done analytically, and not every critical system is conformally invariant. However, they give us the best available language and understanding, leaving us the task to test these ideas with the $O(n)$ loop models, for example.

Renormalization group, applied on a lattice model, can give us information about the effective field theory at the continuum limit. Universality is another important concept related to the renormalization group. For example, the continuum limit results are usually same if we define the discrete model in a hexagonal or a square lattice. For loop models there is an important universality result which states that the critical properties for $O(n)$ and $O(n)$ loop models are the same [10].

4.1 Renormalization group (RG) basics

With renormalization group (RG) [6], [7], it is possible to study physical systems at and near the points of second order phase transitions. There it is possible to gain results for the limit when lattice constant approaches zero, keeping the domain Λ fixed. As the number of degrees of freedom then approaches infinity, it is not possible to calculate all physics, like the limit of the hamiltonian. Instead, RG calculates the low-energy physics at this limit, asymptotics of the correlation functions (these determine all observations of a physical system), how correlation functions behave when distances approach

infinity.

Correlation length ξ is the length scale below which the physics of the microscopic constituents is apparent. In classical spin models, two spins outside the range of correlation length are effectively disconnected from each other. Cardy [6] defines correlation length related to the asymptotic behaviour of the (spin) correlation function:

Definition 4.1.1. (*Correlation length I*) Let d be the dimension of space and $G(r)$ the correlation function

$$G(r) = \langle S(r)S(0) \rangle.$$

The correlation length ξ is defined by the asymptotic behaviour of G :

$$G(r) \sim \frac{e^{-\frac{r}{\xi}}}{r^{\frac{d-1}{2}}}, \quad \text{for } r \gg \xi. \quad (4.1)$$

For classical spin models, another definition for the correlation length can be given as [9]:

Definition 4.1.2. (*Correlation length II*) Let $i, j \in \Lambda$ be two lattice points and let r_{ij} be their distance. Let Γ_2 be the spin-spin correlation function

$$G_2(S_i, S_j, H) = \langle S_i S_j \rangle - \langle S_i \rangle \langle S_j \rangle \quad (4.2)$$

Then the correlation length $\tilde{\xi}$ is

$$(\tilde{\xi})^2 = \frac{\sum_{i,j} r_{ij}^2 \Gamma_2(S_i, S_j)}{\sum_{i,j} \Gamma_2(S_i, S_j)}. \quad (4.3)$$

Near a critical point the correlation length is much greater than lattice spacing a . Although I do not write it explicitly, all ensemble averages depend on the free thermodynamic variables. Thus, for spin models ξ is a function of temperature and magnetic field.

Correlation length ξ can be used as an indicator for second order phase transitions. When matter approaches (changing the values of parameters like T and p) a point of second order phase transition, correlation length increases, approaching infinity at the transition point. Usually the correlation function at the transition point is a polynomial in $-r/\xi$. If there is a second order phase transition at critical temperature T_c , we have

$$\lim_{T \rightarrow T_c} \xi(T) = \infty.$$

Far away from T_c , correlation length is of the order of lattice constant: $\xi \sim d$.

RG ideas are effective when ξ is large. Therefore we will work near a point of the second order phase transition. Then the following definitions are useful. Thermodynamic state variables at the critical point are written with a subscript c , like the temperature T_c or the magnetic field H_c . In RG, state variables are often written in a dimensionless form, with respect to the critical point. Thus we will use the following variables for temperature and magnetic field:

$$t := \frac{T - T_c}{T_c}, \quad h := \frac{H - H_c}{H_c}. \quad (4.4)$$

In lattice models, a RG transformation is usually done in two steps [7]. First is called cross graining (or averaging). It can be best explained by taking an example of Ising-model in a two dimensional square lattice. Let the lattice constant be a , and let the spins S_i at lattice sites have some values in $\{-1, 1\}$. Then change the lattice constant to $2a$. In each $2a \times 2a$ square there will be nine spins S_i from the original lattice. Determine by some majority rule a spin $S'_c \in \{-1, 1\}$ for this group of spins, and attach this to the site at the center. Then we have cross-grained the configuration $\{S_i\}$ in a -lattice to configuration $\{S'_i\}$ in $2a$ -lattice. The same idea can be applied to all lattice models. From a model $H_a(K)$ in a lattice with lattice constant a , this coarse graining produces a model $H'_{2a}(K')$.

The second step is called rescaling, which scales the model $H'_{2a}(K')$ back to the original lattice with lattice constant a (which enables us to compare hamiltonians before and after a RG-transformation). Thus all lengths, like the lattice size L , are divided by 2. Quantities like spins that are independent of lengths are invariant. Formally

$$r \rightarrow r/2, \quad S'_i \rightarrow S_i, \quad K' \rightarrow K'. \quad (4.5)$$

The system size L is therefore also transformed to $L/2$. The result of RG=coarse graining + rescaling is therefore model $H'_a(S', K')$.

For the 1-dimensional Ising model it can be shown [6] that the result of a RG transformation is just a change in the values of coupling constants K . However, this is a special case. In general, the transformation results in new couplings (like next to nearest neighbour) between the lattice spins. In all cases, a series of transformations forms a path in the space of coupling constants, and if the transformations are infinitesimal ($a \rightarrow ab$, b infinitesimal), the path will be a continuous curve. An example of such RG-paths is given in Figure 4.1 below, with only two coupling constants.

In a general RG process there would be cross graining from lattice a to ba , followed by a rescaling from ba to a . The correlation function then transforms

as

$$e^{-r/\xi(K)} = e^{-r'/\xi(K')}. \quad (4.6)$$

As $r' = r/b$, we have

$$\xi(K') = \frac{\xi(K)}{b}, \quad (4.7)$$

which enables us to calculate the temperature behaviour of correlation length. Many ideas of RG and scaling are related to such scale transformations (from a to ba). Main assumption is, that large length scale, or small energy scale, physics is invariant in such transformations.

The coupling parameters change in the process, from K to K' . Generally, there may be new types of interactions in H' , compared to H . In the two-dimensional Ising model, a RG step would produce next to nearest neighbour and further, interactions. This is described in RG as

$$\{K'\} = R\{K\}, \quad (4.8)$$

which means that a RG transformation R transforms a set of interaction parameters $\{K\}$ into set $\{K'\}$. All possible interactions must be included: if some interaction parameter in $\{K\}$ is zero, it may be nonzero in $\{K'\}$. This makes an analytic approach impossible, in general.

Repeating a RG transformation (4.8) we will end up in a fixed point model with parameters $\{K^*\}$:

$$\{K^*\} = R\{K^*\}. \quad (4.9)$$

The RG process is often described as a RG-flow diagram in $\{K\}$ -space (space of model parameters) or space of thermodynamic variables like T, p, h . A RG-flow diagram has flows from unstable fixed points to stable fixed points.

Linearizing RG equations about a fixed point gives

$$K'_a - K_a^* \sim \sum_b T_{ab}(K_b - K_b^*). \quad (4.10)$$

For matrix T , denote the left eigen values as λ^i and left eigenvectors as ϕ^i :

$$\sum_a \phi_a^i T_{ab} = \lambda^i \phi_b^i. \quad (4.11)$$

Then define scaling variables, which have a simple transform property in RG:

$$u_i := \sum_a \phi_a^i (K_a - K_a^*). \quad (4.12)$$

$$u'_i = \lambda^i u_i. \quad (4.13)$$

It is useful (for deriving critical exponents) to write the eigenvalues as $\lambda^i = b^{y_i}$, where y_i are called renormalization group eigenvalues. These determine how a scaling variable behaves in a RG transformation. We define:

$$\begin{aligned} \text{if } y_i > 0, & \quad u_i \text{ is relevant,} \\ \text{if } y_i < 0, & \quad u_i \text{ is irrelevant,} \\ \text{if } y_i = 0, & \quad u_i \text{ is marginal.} \end{aligned} \tag{4.14}$$

Near a fixed point, the linear space spanned by the irrelevant eigenvectors is called the critical surface. In a reduced hamiltonian, the model parameters $\{K\}$ depend on the thermodynamic variables like p, T, h . RG flow in coupling constant space ($\{K\}$ -space) describes the behaviour of a whole universality class. For a model, RG-flow is usually given in the space of thermodynamic variables.

Example 4.1.1. *RG-flows in a two-dimensional $\{K\}$ -space near a fixed point with one relevant and one irrelevant eigenvalue.*

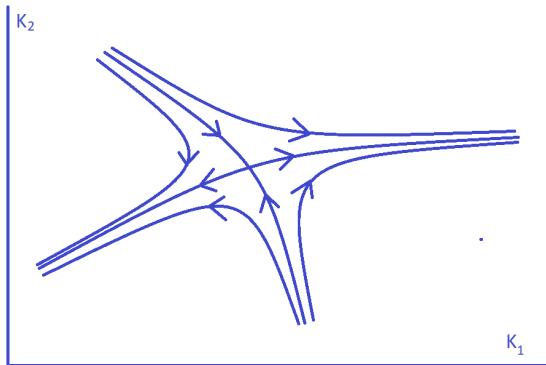


Figure 4.1: RG flows in a two-dimensional example near a fixed point with one relevant and one irrelevant eigenvalue.

Example 4.1.2. *The following RG-flow is for the $O(n)$, $-2 < n \leq 2$ [8]. The $O(n)$ loop model is expected to have the same RG-flow (by the universality hypothesis, see [6]). The parameter space is now 1-dimensional and the flow has four fixed points. The interesting fixed points are the repelling fixed point K_{c1} and the attractive point K_{c2} . For the names of the fixed points, see [8].*



Figure 4.2: RG-flow for the $O(n)$ model, $-2 < n \leq 2$.

As noted above, RG -flow diagrams like in Figure 4.1 above, describe how the coupling constants of the models behave in RG-transformations. The point where a model curve intersects critical surface, is the critical point of the model. The long distance physics near this critical point is common to many models, explaining the phenomenon of universality.

We can drive a system to critical surface using thermodynamic variables like p, t and h . If there are n scaling variables u_i , of which n' are relevant and $n - n'$ irrelevant, it is clear that the number of free thermodynamic variables must also be n' . Near a fixed point, relevant scaling variables are proportional to thermodynamic variables [6] like the relevant thermal scaling variable u_t :

$$u_t = \frac{t}{t_0} + O(t^2, h^2), \quad (4.15)$$

where t_0 is a non-universal constant.

Using this machinery, it is possible to calculate scaling behaviour of free energy and the critical exponents. Correlation functions determine how a physical system behaves. Using RG, we can determine the asymptotic behaviour of correlation functions. For the calculations, some assumption of invariance in a RG-transformation must be made. These assumptions are physically motivated by the idea that long scale (low energy) physics is kept invariant in the transformation.

Cardy writes the condition as

$$Z = Tr_S e^{-H(S)} = Tr_{S'} e^{-H'(S')}. \quad (4.16)$$

Potentials like free energy have a smooth and a singular part when approaching a critical point [6]. The singular part contains terms that are nonsmooth at the critical point. For a potential F , we have

$$F(\{K\}) = F_{smooth}(\{K\}) + F_{sing}(\{K\}). \quad (4.17)$$

From condition (4.16), it follows that the singular part of free energy (F_{sing}) is invariant in a RG-transformation. As the number of sites changes as $N' = N/b^d$, the free energy per site f transforms as

$$f_{sing}(\{K\}) = b^{-d} f_{sing}(\{K'\}). \quad (4.18)$$

In addition, Lavis and Bell [9] use the idea that correlation length ξ is the only measure of distance from the critical point. Written in this way,

$$f_{sing}(\xi) = b^{-d} \cdot f_{sing}(b^{-d}\xi). \quad (4.19)$$

Condition (4.18) leads to several interesting relations between critical exponents and eigenvalues y_i . More important to this work is the behaviour of correlation functions.

For that purpose, following [10], consider a system of linear size L . Let the model parameters be u_1, u_2, \dots, u_k . Let us choose for these parameters values so that they are separated from the fixed point only in the u_j -direction. Let Q_j be the operator conjugate to u_j [9]. Define

$$G(u_j, L) := \langle Q_j Q_j \rangle - \langle Q_j \rangle^2 = L^d \frac{\partial^2 f_L(u_j)}{\partial u_j^2}. \quad (4.20)$$

Using the scaling relations $u'_j = b^{y_j} u_j$, $f_L(u_j) = b^{-d} f(u_j b^{y_j})$, we get

$$G(u_j, L) = L^d \frac{b^{-d} \partial^2 f(u'_j)}{b^{-2y_j} \partial u_j'^2} = b^{2y_j} G(u'_j, L/b), \quad (4.21)$$

so that $G(0, L) \propto L^{2y_j}$. Let Q_j be written as a sum (or integral) over local operators

$$Q_j = \int_{L^d} d^d r q_j(r). \quad (4.22)$$

Then $G(0, L)$ can be written as

$$G(0, L) = \int_{L^d} d^d r \int_{L^d} d^d r' \langle q_j(r) q_j(r') \rangle - \langle q_j(r) \rangle \langle q_j(r') \rangle. \quad (4.23)$$

As $G(0, L) \propto L^{2y_j}$, we expect

$$\langle q_j(r) q_j(r') \rangle - \langle q_j(r) \rangle \langle q_j(r') \rangle \propto |r|^{2(y_j-d)}. \quad (4.24)$$

Thus, if correlation functions like (4.24) decay faster than $|r|^{-2d}$, the operator Q_j is irrelevant, and if they decay slower, the operator Q_j is relevant.

The purpose of this work is to find results for the scaling limit of $O(n)$ loop models. Cardy [11] defines the scaling limit in the following way:

Definition 4.1.3. (*Scaling limit*)

Scaling limit of a lattice model at the point of second order phase transition, is the limit when lattice constant $a \rightarrow 0$, keeping all other lengths fixed. This means that the correlation length and Λ are fixed.

The limit $a \rightarrow 0$ means that the dimensionless correlation length ξ (measured in a) must go to infinity. Thus we must work near a point of a second order phase transition. As

$$\xi \sim |\beta - \beta_c|^{-\nu}, \quad (4.25)$$

we understand that β must approach β_c as a power of a . To have finite correlation functions at the scaling, they must be multiplied by a correct function of a . This is called renormalization.

For correlation functions, let us introduce (see (4.24))

$$x_j := d - y_j, \quad (4.26)$$

and divide the reduced hamiltonian to smooth and singular parts, so that singular part of hamiltonian produces the singular part of free energy. Then the singular part can be written as a linear combination of relevant scaling variables u_i , $i = 1, 2, \dots, m$. The coefficients ϕ_i , $i = 1, 2, \dots, m$ are called scaling operators:

$$H_{sing}(\{K\}, S) = \sum_{\{r\}} \sum_{j=1}^m \phi_j(r) u_j, \quad (4.27)$$

where the first sum is over all lattice points and m is the number of relevant scaling variables. The following renormalization is suggested for the spin-spin- and more general correlation functions:

$$a^{-2x_s} \langle S(r_1) S(r_2) \rangle_{lattice}, \quad (4.28)$$

$$a^{-x_{j_1} - x_{j_2} \dots} \langle \phi_{j_1}(r_1) \phi_{j_2}(r_2) \cdot \dots \rangle_{lattice}. \quad (4.29)$$

The finite limit, which then should exist, defines the following, called the scaling limit of the correlation function:

$$\langle \phi_{j_1}(r_1) \phi_{j_2}(r_2) \cdot \dots \rangle := \lim_{a \rightarrow 0} a^{-x_{j_1} - x_{j_2} \dots} \langle \phi_{j_1}(r_1) \phi_{j_2}(r_2) \cdot \dots \rangle_{lattice}, \quad (4.30)$$

which could be a correlation function of some field theory. However, showing all this and understanding the limit is a very demanding task. Parts of it has been done for the Ising model, rewarding Stanislav Smirnov the Fields medal [2].

4.2 Transfer matrix

Transfer matrix is a fine numerical and theoretical tool for calculating the partition function or other similar quantities in statistical physics. It

enables useful studies of statistical physics at the continuum limit, and in some cases even exact solutions for the ground states, for example. Here, after a general introduction, I study the possibilities to make transfer matrix studies of long range order and the convergence of parafermionic observables, in spin systems.

4.2.1 General introduction

Let us take a lattice with M rows and N columns. At each lattice point let there be a degree of freedom that can have p values. Then, there are p^N configurations for each row. We can write each such row configuration as an N -dimensional vector. There are then p^N such vectors, or states. I call a spin configuration for a row shortly for state.

Let T be a $t \times t$ -dimensional matrix ($t = p^N$ for p local states). Each row or column index i corresponds to the i :th state, which is an N -dimensional vector. Then $\sum_{i_k}^t$ is a sum over all states in row k .

With periodic boundary conditions (so that row 1 is next to row M , in the lattice), we get

$$\begin{aligned} \text{Tr}(T^M) &= \sum_{i_1=1}^t \sum_{i_2=1}^t \dots \sum_{i_M=1}^t T_{i_1 i_2} \cdot T_{i_2 i_3} \cdot \dots \cdot T_{i_{M-1} i_M} \cdot T_{i_M i_1} \\ &= \sum_{\substack{\text{states } i_1 \\ \text{in row 1}}} \sum_{\substack{\text{states } i_2 \\ \text{in row 2}}} \dots \sum_{\substack{\text{states } i_M \\ \text{in row } M}} T_{i_1 i_2} \cdot T_{i_2 i_3} \cdot \dots \cdot T_{i_{M-1} i_M} \cdot T_{i_M i_1} \end{aligned} \quad (4.31)$$

So this gives a new way of writing sums over all possible states in a lattice, a common task in statistical physics, for example. For that use, T_{ab} must be the statistical weight for adding a row with state b on top of a row with state a (or vice versa).

For finding what quantities could be written in this way, let us take one state Ψ in the lattice, so that the quantity has value $A(\Psi)$. Then

$$A(\Psi) := T_{i_1 i_2} \cdot T_{i_2 i_3} \cdot \dots \cdot T_{i_{M-1} i_M}, \quad (4.32)$$

$$\ln(A(\Psi)) = \ln T_{i_1 i_2} + \ln T_{i_2 i_3} + \dots + \ln T_{i_{M-1} i_M}, \quad (4.33)$$

which means that $\ln A$ is an additive quantity, determined by $T_{i_k, j_{k+1}}$.

The most useful additive quantity for statistical physics in a lattice is energy. The most famous example is the Ising model in a square lattice:

Example 4.2.1. *Take a square $M \times N$ lattice Λ with periodic boundary conditions so that row 1 and column 1 are next to row M and column N , respectively. Let the local variables, at each point of the lattice, be classical spins*

$\sigma_{k,j}, (k,j) \in \Lambda$ with two values, $\sigma_{k,j} \in \{-1, 1\}$. Thus, a row with N spins has now 2^N possible states. The Ising model hamiltonian is

$$H(\sigma) = -J \sum_{\substack{\text{nearest} \\ \text{neighbours} \\ (k_1,j_1), (k_2,j_2)}} \sigma_{k_1,j_1} \sigma_{k_2,j_2},$$

and it can be rewritten row-wise as

$$H(\sigma) = -J \sum_{i=1}^M \sum_{j=1}^N (\sigma_{i,j} \sigma_{i,j+1} + \sigma_{i,j} \sigma_{i+1,j}),$$

so that, for states $\phi_i = (\sigma_1, \sigma_2, \dots, \sigma_N)$ for row i and $\phi_{i+1} = (\sigma'_1, \sigma'_2, \dots, \sigma'_N)$ for row $i+1$

$$T_{\phi_i, \phi_{i+1}} = \exp \left(K \sum_{k=1}^N (\sigma_k \sigma_{k+1} + \sigma_k \sigma'_k) \right),$$

where $K = J/(kT)$, as we would use this for the partition function.

4.2.2 Long range order

Here $Z = \text{Tr}(T^M)$, and we will study long range order. For spin models this means the correlation of spins at two small areas centered at r_1 and r_2 . If spins at r_1 are all up, what is the distance $r = |r_2 - r_1|$ where spins are affected. Usually thermal fluctuations make large distance correlations negligible, but for certain systems with certain parameter values, long range order exists. We can study these problems with transfer matrices, by letting M be large.

For interpreting the various results of transfer matrix calculations, I find the presentation by Domb [12] very useful. Matrix T can be assumed to be symmetric. Denote the eigenvalues of T by $\lambda_1, \lambda_2, \dots, \lambda_t$ and the normalized, mutually orthogonal eigenvectors by $\xi_1, \xi_2, \dots, \xi_t$. Let e_k be the vector with a 1 at the k :th position and zero elsewhere. Then, assuming that the eigenvectors form a complete basis, we can expand

$$e_k = \sum_{i=1}^t \xi_i(k) \xi_i, \quad (4.34)$$

where $\xi_i(k)$ is the k :th component in vector ξ_i , and $t := 2^N$. Then $(v^T$ is the transpose of vector v)

$$\begin{aligned} (T^M)_{k,k} &= (e_k)^T \cdot T^M \cdot e_k = \left(\sum_{j=1}^t \xi_j(k) (\xi_j)^T \right) \left(\sum_{i=1}^t \lambda_i^M \xi_i(k) (\xi_i)^T \right) \\ &= \sum_{i=1}^t (\xi_i(k))^2 \lambda_i^M. \end{aligned} \quad (4.35)$$

Transfer matrix T was written for spin states on the rows of the lattice. There were 2^N such states (like $(1, -1, 1, 1)$ for $n = 4$, for example). The probability P of a given system being in state k ($k \in \{1, 2, \dots, 2^N\}$) is then

$$P(\text{system in state } k) = \frac{\sum_{i=1}^t (\xi_i(k))^2 \lambda_i^M}{\sum_{i=1}^t \lambda_i^M}. \quad (4.36)$$

For large M and simple eigenvalues, this reduces to $(\xi_1(k))^2$.

For analyzing correlation with the transfer functions, I will again follow Domb [12], with a simple generalization. I will change to the following, more modern Dirac's bracket-notation for the eigenvalues and -vectors of transfer matrix. This notation is commonly used in quantum mechanics:

$$T|\lambda_k\rangle = \lambda_k|\lambda_k\rangle, \quad k = 1, 2, \dots, t, \quad (4.37)$$

where λ_k and $|\lambda_k\rangle$ are the k :th eigenvalue and -vector, respectively. $\langle\lambda_j|\lambda_k\rangle$ is the inner product of states $|\lambda_j\rangle$ and $|\lambda_k\rangle$. Eigenvectors are assumed to be normalized and orthogonal, and to form a complete basis. The probability that we have state $|\alpha\rangle$ on row i and state $|\beta\rangle$ (both normalized) on row j is

$$P(\alpha \text{ row } i, \beta \text{ row } j) = \frac{1}{Z} \sum_{a=1}^t \langle\lambda_a|T^i|\alpha\rangle \langle\alpha|T^{j-i}|\beta\rangle \langle\beta|T^{M-j}|\lambda_a\rangle. \quad (4.38)$$

The partition function Z will be calculated below. Expanding in the basis of eigenstates

$$|\alpha\rangle = \sum_{k=1}^t \alpha_k |\lambda_k\rangle, \quad |\beta\rangle = \sum_{k=1}^t \beta_k |\lambda_k\rangle, \quad (4.39)$$

gives

$$\langle\lambda_a|T^i|\alpha\rangle = \alpha_a \lambda_a^i, \quad (4.40)$$

$$\langle\alpha|T^{j-i}|\beta\rangle = \sum_{k=1}^t \alpha_k^* \beta_k \lambda_k^{j-i}, \quad (4.41)$$

$$\langle\beta|T^{M-j}|\lambda_a\rangle = \beta_a^* \lambda_a^{M-j}, \quad (4.42)$$

$$P(\alpha \text{ row } i, \beta \text{ row } j) = \frac{1}{Z} \left(\sum_{a=1}^t \lambda_a^{M-j+i} \alpha_a \beta_a^* \right) \left(\sum_{k=1}^t \lambda_k^{j-i} \alpha_k^* \beta_k \right). \quad (4.43)$$

For the partition function we get

$$Z = \text{Tr}(T^M) = \lambda_1^M \left(1 + \left(\frac{\lambda_2}{\lambda_1}\right)^M + \left(\frac{\lambda_3}{\lambda_1}\right)^M + \dots + \left(\frac{\lambda_t}{\lambda_1}\right)^M \right). \quad (4.44)$$

Defining $r = j - i$, $a_k = \alpha_k^* \beta_k$, $k = 1, 2, \dots, t$ allows us to write (4.43) in form

$$\begin{aligned}
& P(\alpha \text{ row } i, \beta \text{ row } j) \\
&= \left(a_1 + a_2 \left(\frac{\lambda_2}{\lambda_1} \right)^{M-r} + a_3 \left(\frac{\lambda_3}{\lambda_1} \right)^{M-r} + \dots + a_t \left(\frac{\lambda_t}{\lambda_1} \right)^{M-r} \right) \\
&\cdot \left(a_1^* + a_2^* \left(\frac{\lambda_2}{\lambda_1} \right)^r + a_3^* \left(\frac{\lambda_3}{\lambda_1} \right)^r + \dots + a_t^* \left(\frac{\lambda_t}{\lambda_1} \right)^r \right) \\
&\cdot \left(1 + \left(\frac{\lambda_2}{\lambda_1} \right)^M + \left(\frac{\lambda_3}{\lambda_1} \right)^M + \dots + \left(\frac{\lambda_t}{\lambda_1} \right)^M \right)^{-1}. \tag{4.45}
\end{aligned}$$

Result (4.45) is usually studied at the limit $1 \ll r \ll M$, which allows an approximation of correlation length ξ :

$$P(\alpha \text{ row } i, \beta \text{ row } j) - |a_1|^2 \sim \left(\frac{\lambda_2}{\lambda_1} \right)^r \sim e^{-r/\xi}, \tag{4.46}$$

$$1/\xi = \ln \left(\frac{\lambda_1}{\lambda_2} \right), \tag{4.47}$$

a result often used. But we are actually interested in long range order, where $r \sim M$. Further, large eigenvalues may approach λ_1 very fast when N increases, and we should then take more than the first eigenvalue. And finally, this is not directly a result for the two-dimensional system at the continuum limit ($N, M \rightarrow \infty$, keeping the two-dimensional area invariant).

For shedding more light on these issues, I will do the following things, using the loop $O(n)$ models as the examples, in chapter 7. First, I study λ_2/λ_1 as a function of model parameters n, K . Then, since the correlation is related to degeneracy, I will study the behaviour $\sum_{k=2}^5 \lambda_k/\lambda_1$, also as a function of n and K (taking five eigenvalues is just a choice). Finally, I will do a direct numerical calculation of the correlation function.

4.2.3 Parafermionic observable

Parafermionic observable (section 3) is a function defined as a scaling limit of a discretely holomorphic (to be properly defined in chapter 5) function in a lattice. In section 8 I will calculate numerically the values for the parafermionic observable at some lattice points.

As will be shown in chapter 6, the discrete or lattice construction can be written using two transfer matrices T_1 and T_3 . A transfer matrix is written for transitions from states ϕ to ϕ' , and all these states belong to a set of vectors. The set of vectors V_1 for T_1 is quite different from the set of vectors V_3 for T_3 . Matrix $T_2(z)$, to be defined in chapter 6, is a connection matrix

from V_1 to V_3 so that parafermion endpoint is at $z = x + iy$, where x and y are real cartesian coordinates. The discrete construction will have form

$$\tilde{F}(z) = \frac{1}{Z} \langle \alpha | T_3^k T_2(x) T_1^{M-k} | \beta \rangle, \quad z \in \{1, 2, \dots, N\}. \quad (4.48)$$

where $\langle \alpha |$ is the transpose of a given state on the last row and $|\beta\rangle$ a given state on the first row. x determines the column and k determines the row, which is the y -coordinate.

Let V_0 be the set of possible end states $|\alpha\rangle$, and as will be explained, V_0 is a genuine subset of V_3 . In the numerator of (4.48), there is a sum over all graphs with a path and closed loops, and in the denominator, a sum over all graphs with loops (see chapters 3 and 6).

Now let the path for parafermion or correlation function start from the first row, state $|\beta\rangle$. Assuming normalized eigenvectors and completeness, it can be expanded in the eigenstates $\{|\lambda_j\rangle\}$ of T_1 :

$$\begin{aligned} T_1^{k_1} |\beta\rangle &= \sum_j^{t_1} \langle \lambda_j | \beta \rangle \cdot \lambda_j^{k_1} \cdot |\lambda_j\rangle, \\ T_1 |\lambda_j\rangle &= \lambda_j |\lambda_j\rangle, \quad j = 1, 2, \dots, t_1. \end{aligned} \quad (4.49)$$

For the end states, we have similarly

$$\begin{aligned} T_3^{k_2} |\alpha\rangle &= \sum_j^{t_3} \langle \nu_j | \alpha \rangle \cdot \nu_j^{k_2} \cdot |\nu_j\rangle, \\ T_3 |\nu_j\rangle &= \nu_j |\nu_j\rangle, \quad j = 1, 2, \dots, t_3. \end{aligned} \quad (4.50)$$

where $t_1 = |V_1|$, $t_3 = |V_3|$ and $\lambda_i \geq \lambda_{i+1}$, $\nu_i \geq \nu_{i+1}$ so that λ_1 and ν_1 are the largest eigenvalues for T_1 and T_3 , respectively. Plugging these into (4.48) gives

$$\tilde{F}(z) = \frac{1}{Z} \sum_{i=1}^{t_1} \sum_{j=1}^{t_3} \langle \lambda_i | T_2(x) | \nu_j \rangle \cdot \langle \alpha | \lambda_i \rangle \langle \nu_j | \beta \rangle \cdot \lambda_i^{k_1} \cdot \nu_j^{k_2}, \quad (4.51)$$

where T_2 is the $t_3 \times t_1$ -dimensional connection matrix.

Z is then the sum of all possible loop graphs from state $|\beta'\rangle$ to state $|\alpha\rangle$. I take $|\beta'\rangle$ to be the same state as $|\beta\rangle$, but with no starting parafermion path. This may be (but I think it is not, of course) an inaccurate approach for the parafermion, but for the correlation length the exact form of initial state $|\beta\rangle$ is not important. $\langle \alpha |$ is the configuration for the last row. I will often average over possible states $\langle \alpha$. Thus, if T_p is the transfer matrix for graphs with no parafermions, I will have

$$\begin{aligned} Z &= \langle \alpha | T_p^{M+1} | \beta \rangle, \\ T_p |\mu_s\rangle &= \mu_s |\mu_s\rangle, \quad s = 1, 2, \dots, t_p. \end{aligned} \quad (4.52)$$

Let us write ($k_1 + k_2 = M$)

$$F(z) = \frac{\lambda_1^{k_1} \nu_1^{k_2}}{Z} \langle \alpha | (T_1/\lambda_1)^{k_1} T_2(x) (T_3/\nu_1)^{k_2} | \beta \rangle, \quad z \in \{1, 2, \dots, N\},$$

$$Z = \sum_{i=1}^{t_p} \mu_i^{M+1} \langle \alpha | \mu_i \rangle \langle \mu_i | \beta \rangle. \quad (4.53)$$

Then, using (4.51) we get

$$\begin{aligned} & \langle \alpha | (T_1/\lambda_1)^{k_1} T_2(x) (T_3/\nu_1)^{k_2} | \beta \rangle \\ &= a_{11}(z) + a_{12}(z) \left(\frac{\nu_2}{\nu_1}\right)^{k_2} + a_{21}(z) \left(\frac{\lambda_2}{\lambda_1}\right)^{k_1} + a_{22}(z) \left(\frac{\lambda_2}{\lambda_1}\right)^{k_1} \left(\frac{\nu_2}{\nu_1}\right)^{k_2} + \\ &+ a_{13}(z) \left(\frac{\nu_3}{\nu_1}\right)^{k_2} + a_{31}(z) \left(\frac{\lambda_3}{\lambda_1}\right)^{k_1} + a_{23}(z) \left(\frac{\lambda_2}{\lambda_1}\right)^{k_1} \left(\frac{\nu_3}{\nu_1}\right)^{k_2} + \\ &+ a_{32}(z) \left(\frac{\lambda_3}{\lambda_1}\right)^{k_1} \left(\frac{\nu_2}{\nu_1}\right)^{k_2} + a_{33}(z) \left(\frac{\lambda_3}{\lambda_1}\right)^{k_1} \left(\frac{\nu_3}{\nu_1}\right)^{k_2} + \dots \end{aligned} \quad (4.54)$$

$$\begin{aligned} a_{11}(z) &:= \langle \alpha_1 | T_2(z) | \nu_1 \rangle \cdot \langle \alpha | \lambda_1 \rangle \langle \nu_1 | \beta \rangle, \\ a_{12}(z) &:= \langle \alpha_1 | T_2(z) | \nu_2 \rangle \cdot \langle \alpha | \lambda_1 \rangle \langle \nu_2 | \beta \rangle, \\ a_{21}(z) &:= \langle \alpha_2 | T_2(z) | \nu_1 \rangle \cdot \langle \alpha | \lambda_2 \rangle \langle \nu_1 | \beta \rangle, \\ a_{22}(z) &:= \langle \alpha_2 | T_2(z) | \nu_2 \rangle \cdot \langle \alpha | \lambda_2 \rangle \langle \nu_2 | \beta \rangle, \\ &\dots \end{aligned} \quad (4.55)$$

Following Domb, the condition for long range order or large correlation length is that the first eigenvalues become degenerate. From equations (4.54) - (4.55) we can see that with large gap between first and second eigenstates, the dependence on distance k_1 is $c_0 \lambda_1^{k_1} \nu_1^{M-k_1} / \mu_1^{M+1}$, with c_0 not depending on k_1 . Thus, for obtaining a function that is not constant in column direction, we should have degeneracy, which means long range order.

Chapter 5

Proving conformal invariance at the scaling limit

In chapter 3 we defined function $F(z)$ (2.35), and found that it is pre-holomorphic when $K = K_c(n)$. It is a reasonable expectation that, if $F(z)$ converges at the continuum limit, the limit will be a holomorphic function. Smirnov proved all this for the Ising or $O(1)$ -model [2]. As will be seen, proving the convergence is difficult.

As an introduction, let us examine figure 5.1 below. There we have a finite piece of hexagonal lattice, and we are interested in the values of $F(z)$, described as a path starting from point z_0 on the boundary below and ending at z . It is possible, with a simple calculation, to determine $F(z)$ when $z \in \partial\Omega$. Knowing the boundary values of a holomorphic function is important, as will be seen.

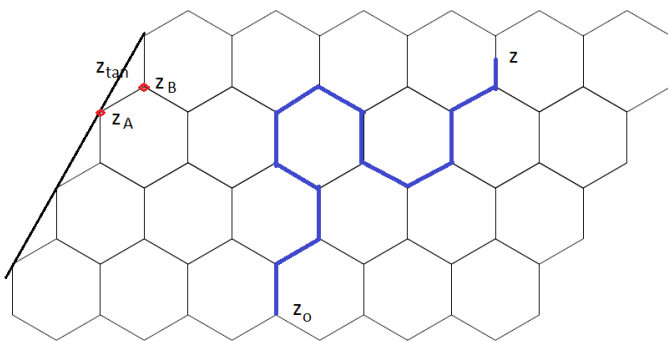


Figure 5.1: A parafermion path starting at $(1, 4)$ and ending at $z = (4, 5)$.

For a parafermion path in the hexagonal lattice, each turn to left gives

a factor $\lambda_l = e^{-is\pi/3}$, and each turn to right a factor $\lambda_r = e^{is\pi/3}$. Any path from z_0 to the points z_A or z_B can be completed to a loop by a path along the boundary, counterclock- or clockwise (see figure 5.1). A clockwise path to z_A along the boundary gives $(\lambda_r^4 \lambda_l^2 = \lambda_r^2)$, and counterclockwise λ_l^4 . Now $e^{i2\pi/3} = 1/2(-1+i\sqrt{3})$ and $e^{-i4\pi/3} = 1/2(-1+i\sqrt{3})$. A trigonometric calculation shows, that the tangent (see figure 5.1 is $z_t = 1/2(-1+i\sqrt{3})$. We get

$$\text{Im}(F(z_A)^{1/s} \cdot z_t) = 0. \quad (5.1)$$

So we have a preholomorphic function $F(z)$, and a boundary condition for function $F^{1/s}(z)$, all in the finite hexagonal lattice. For $s = 1/2$, Smirnov was able to prove that F converges (when the lattice constant $\epsilon \rightarrow 0$) to a holomorphic function, thus proving that the observables for the $O(1)$ model are conformally invariant at the scaling limit.

I will start from the basic results of complex analysis in \mathbb{C} , in section 5.1. Then I will turn to discrete complex analysis in section 5.2, and finally sketch the proof of holomorphicity of the $O(1)$ or Ising model in section 5.3.

5.1 Complex analysis in \mathbb{C}

Complex analysis is a rich and active field of mathematical research. The excerpt here is chosen for building corresponding things in lattice. I follow the fine lecture notes by Astala [13] and Ji [14].

A domain in complex plane \mathbb{C} is an open and connected subset of \mathbb{C} .

Definition 5.1.1. (*holomorphic function*)

Let $A \subset \mathbb{C}$ be nonempty. Let z_0 be an inner point of A . Function $f : A \rightarrow \mathbb{C}$ has a derivative $f'(z_0)$ at z_0 , if the following limit exists

$$\lim_{h \rightarrow 0} \frac{f(z_0 + h) - f(z_0)}{h} = f'(z_0). \quad (5.2)$$

f is holomorphic (analytic) at $z_0 \in A$, if there is an open disk $D(z_0, r) \subset A$, so that f has a complex derivative at every point $z \in D(z_0, r)$.

If A is a domain, f is holomorphic in A if it is holomorphic at every point $z \in A$.

It is important to note that h is a complex number. A complex number z can be written as $z = x + iy$, $x, y \in \mathbb{R}$. Any complex function can be written as $f = u + iv$, where u and v are real valued functions. These give the following form for holomorphicity

Theorem 5.1.1. *Function $f = u + iv$ has a complex derivative at z if and only if both u and v are differentiable at z , and*

$$u_x(z) = v_y(z), \quad u_y(z) = -v_x(z). \quad (\text{Cauchy-Riemann equations}) \quad (5.3)$$

Then $f'(z) = u_x(z) + iv_x(z) = v_y(z) - iv_y(z)$.

Function $g : \mathbb{R}^2 \rightarrow \mathbb{R}$ is *harmonic*, if $\Delta g = g_{xx} + g_{yy} = 0$. If $f = u + iv$ is holomorphic in A , it follows from (5.3) that u and v are harmonic functions in A .

Let $a, b \in \mathbb{R}$, $a < b$. A continuous function $\gamma : [a, b] \rightarrow \mathbb{C}$ is called a *path*. $\gamma(a)$ is the startpoint and $\gamma(b)$ the endpoint of γ . Let γ be differentiable at $t_0 \in [a, b]$. Then $\gamma'(t_0)$ is called a *tangent vector* of γ at t_0 . Angle $\phi = \arg \gamma'(t_0)$ is the directional angle of tangent at t_0 . If γ is differentiable at every point in $[a, b]$, it is called a *regular path* in $[a, b]$.

If function $f : A \rightarrow \mathbb{C}$ is holomorphic and $\gamma : [a, b] \rightarrow A$ a regular path in A , the tangent vector of $f \circ \gamma$ at $t_0 \in [a, b]$ is $(f \circ \gamma)'(t_0) = f'(\gamma(t_0))\gamma'(t_0)$, and directional angle is $\psi = \arg f'(\gamma(t_0)) + \phi$, where $\phi = \arg \gamma'(t_0)$.

Let two paths γ_1, γ_2 have directional angles ϕ_1 and ϕ_2 at $z_0 \in A$. Then $\psi_1 - \psi_2 = \phi_1 - \phi_2$. We say that a holomorphic f function conserves angles if $f'(z) \neq 0$. This is the idea of conformality.

Definition 5.1.2. (*pointwise conformality, conformal mapping*)

Let f be holomorphic in open set A . f is conformal at $z \in A$, if $f'(z) \neq 0$.

Conformal mappings are bijective functions $f : A \rightarrow A'$ such that $f'(z) \neq 0$ for all $z \in A$.

For integrals over paths in complex plane, we write

Definition 5.1.3. (*complex integral over path*)

Let $\gamma : [a, b] \rightarrow A$ be continuously differentiable (C^1) path in $A \subset \mathbb{C}$. If $f : A \rightarrow \mathbb{C}$ is continuous, path integral of f over path γ is

$$\int_{\gamma} f dz = \int_a^b f(\gamma(t)) \cdot \gamma'(t) dt. \quad (5.4)$$

A holomorphic function $F : A \rightarrow \mathbb{C}$ is the *integral function* of f , if $F'(z) = f(z)$ for all $z \in A$. This is related to holomorphicity by the following famous theorem

Theorem 5.1.2. (*Cauchy integral theorem*)

Let f be holomorphic in disk D . Then

i) f has an integral function

ii) For every closed path γ in D

$$\oint_{\gamma} f dz = 0. \quad (5.5)$$

The inverse theorem to 5.1.2 is another classical result.

Theorem 5.1.3. (*Morera's theorem*)

Let $f : A \rightarrow \mathbb{C}$ be continuous and $\oint_{\gamma} f dz = 0$ for every closed, piecewise C^1 path γ in A . Then f is holomorphic.

I will next give three integral reconstruction formulas for a holomorphic function f . They are all derived from the following cornerstone of calculus in complex variable. It says that the value of a holomorphic function f in any inner point of disk D can be calculated from the values at the boundary of the disk.

Theorem 5.1.4. (*Cauchy's integral formula, local form*)

Let f be holomorphic in A , and let $D = D(z_0, r)$ be a disc such that $\overline{D} \subset A$. Then

$$f(z) = \frac{1}{2\pi i} \oint_{\gamma} \frac{f(\xi)}{\xi - z} d\xi, \quad z \in D, \quad (5.6)$$

where integral path is along the boundary ∂D of D in counterclockwise direction.

Using parametrization $\theta \in [0, 2\pi)$ for the boundary of disc $D(z_0, r)$ gives

Theorem 5.1.5. (*Poisson integral formula for holomorphic functions*)

Let f be a continuous function on the closed disc $\overline{D}(z_0, r)$ and be holomorphic in $D(z_0, r)$. Then

$$f(z) = \frac{1}{2\pi} \int_0^{2\pi} f(z_0 + re^{i\theta}) \frac{r^2 - |z - z_0|^2}{|re^{i\theta} - (z - z_0)|^2} d\theta, \quad \forall z \in D(z_0, r). \quad (5.7)$$

Poisson integral formula can be written with the Poisson kernel $K(z_1, z_2)$.

$$f(z) = \frac{1}{2\pi} \int_0^{2\pi} f(re^{i\theta}) K(re^{i\theta} - z_0, z - z_0) d\theta \quad \forall z \in D(z_0, r), \quad (5.8)$$

$$K(z_1, z_2) := \frac{|z_1|^2 - |z_2|^2}{|z_1 - z_2|^2}. \quad (5.9)$$

Noticing that

$$K(z_1, z_2) = \operatorname{Re} \left(\frac{z_1 + z_2}{z_1 - z_2} \right), \quad (5.10)$$

we can write an integral representation for the real part u of $f = u + iv$:

$$u(z) = \frac{1}{2\pi} \int_0^{2\pi} u(re^{i\theta}) \operatorname{Re} \left(\frac{re^{i\theta} + z}{re^{i\theta} - z} \right) d\theta. \quad (5.11)$$

This gives another integral representation for f [14]:

Theorem 5.1.6. (*Schwarz' integral formula*)

Let f be a continuous function on the closed disc $\overline{D(z_0, r)}$ and be holomorphic in $D(z_0, r)$. Then

$$f(z) = \frac{1}{2\pi} \int_0^{2\pi} u(re^{i\theta}) \left(\frac{re^{i\theta} + z}{re^{i\theta} - z} \right) d\theta + i \cdot \text{Im}(f(0)). \quad (5.12)$$

The Riemann boundary value problem (BVP) is the problem of finding in domain Ω the holomorphic function that has a given behaviour at the boundary $\partial\Omega$. We are now trying to solve a particular form of so-called Riemann-Hilbert BVPs. These continuum problems can be stated as follows:

Definition 5.1.4. (*Riemann-Hilbert BVP*)

Find a continuous function $f : \Omega \rightarrow \mathbb{C}$ such that

$$f \text{ is holomorphic on } \Omega \text{ and } \text{Im}[f\bar{w}] = g \text{ on } \partial\Omega, \quad (5.13)$$

where w is a given complex-valued function and g a given real-valued function, both defined on boundary $\partial\Omega$.

Geometrically the boundary condition requires that every boundary value $f(z)$, $z \in \partial\Omega$ must lie on a straight straight line which is parallel to $w(z)$, considered as a vector in \mathbb{R}^2 .

5.2 Complex analysis in lattices

As noted in previous section, a holomorphic function f in domain Ω is determined by its behavior in boundary $\partial\Omega$. We have previously proved that $F(z)$ is preholomorphic in Ω_δ , when $K = K_c$, and we know the values of $F^2 \cdot z_{tan}$ in $\partial\Omega_\delta$. We would like to prove that the limit $\lim_{\delta \rightarrow 0} F(s)$ exists and find that it is holomorphic. For this purpose and related to the given information, I give here some general convergence results for preholomorphic and preharmonic functions, to be used in the next section. These are all from [2] or [15].

We start by proving that if f_δ is discretely holomorphic and $\lim_{\delta \rightarrow 0} f_\delta$ exists, the limit is a holomorphic function.

Lemma 5.2.1. *If the family $(f)_\delta$ of discrete holomorphic functions on Ω_δ converge uniformly on every compact subset of Ω to f , then f is holomorphic.*

Proof. As the convergence is uniform, f is continuous. As f_δ is preholomorphic, all closed contour integrals of f vanish. By Morera's theorem f is holomorphic. \square

Proving convergence needs much more work. In this section we prove the convergence of preharmonic functions.

Definition 5.2.1. (*preharmonic function*) Let Ω_δ be a square lattice with lattice constant δ and let $f : \Omega_\delta \rightarrow \mathbb{C}$. Define

$$\Delta_\delta f(u) = \frac{1}{4} \sum_{v \sim u} (f(v) - f(u)), \quad (5.14)$$

where the sum is over the four nearest neighbours to vertex u . A function $h : \Omega_\delta \rightarrow \mathbb{C}$ is preharmonic (resp. pre-superharmonic, pre-subharmonic) if $\Delta_\delta h(x) = 0$ (resp. $\leq 0, \geq 0$) for every $x \in \Omega_\delta$

Controlling a harmonic function allows to control its gradient. The same is true for the preharmonic functions. This and many other proofs in the field use the following relation of preharmonic functions and random walks:

Lemma 5.2.2. (*connection of preharmonic functions and random walks*)

Let (X_n) be a random walk in the lattice Ω_n , i.e. a Markov process of jumps to one of the nearest neighbours at each time step, with equal probability. For a graph Ω_δ , let τ be the hitting time of $\partial\Omega_\delta$.

A function $h : \Omega_\delta \rightarrow \mathbb{R}$ is discrete harmonic on $\Omega_\delta \setminus \partial\Omega_\delta$ if and only if for any $x \in \Omega_\delta \setminus \partial\Omega_\delta$, $h(X_{n \wedge \tau})$ is a martingale for the simple random walk starting from x .

Proof. Let $x \in \Omega_\delta \setminus \partial\Omega_\delta$ and (X_n) be the simple random walk starting from x . Then $\mathbb{E}[h(X_1)] = h(x)$ is equivalent to $\Delta_\delta h(x) = 0$. \square

Lemma 5.2.3. *There exists $C > 0$ such that, for any preharmonic function $h : \Omega_\delta \rightarrow \mathbb{C}$ and any two neighbouring sites $x, y \in \Omega_\delta$,*

$$|h(x) - h(y)| \leq C\delta \frac{\sup_{z \in \Omega_\delta} |h(z)|}{d(x, \Omega^c)} \quad (5.15)$$

Proof. See [2] or [15]. \square

The following lemma is central for proving the existence of continuum limits. Functions defined in Ω_δ are assumed to be extended to Ω , for example linearly like in the finite element method.

Lemma 5.2.4. *A family $(h_\delta)_{\delta > 0}$ of preharmonic functions on the graphs Ω_δ is precompact for the uniform topology on compact subsets of Ω if one of the following properties holds:*

- (1) $(h_\delta)_{\delta>0}$ is uniformly bounded on any subset of Ω ,
- (2) for any compact subset K of Ω , there exists $M = M(K) > 0$ such that for any $\delta > 0$

$$\delta^2 \sum_{x \in K_\delta} |h_\delta(x)|^2 \leq M.$$

Proof. Let K be a compact subset of Ω . Assume that $\delta_0 > 0$ is such that $K \subset \bar{\Omega}_{\delta_0}$. We study a family of continuous maps $h_\delta : K \rightarrow \mathbb{C}$ indexed by $\delta < \delta_0$. Let $2r = d(K, \Omega^c) > 0$.

Condition (1) We aim to apply Arzela-Ascoli theorem, which states that the set $\{h_\delta\}$ is precompact if it is uniformly bounded and uniformly equicontinuous. We have the uniform boundedness by assumption. For the latter condition, Lemma 5.2.3 gives that

$$|h_\delta(x) - h_\delta(y)| \leq C_K \delta,$$

$$C_K = C \frac{\sup_{\delta>0} \sup\{|h_\delta(z)| : z \in \Omega_\delta, \text{ with } d(z, K) \leq r\}}{2r},$$

so that $|h_\delta(x) - h_\delta(y)| \leq 2C_K|x - y|$ for any $x, y \in K_\delta$. Then, by Arzela-Ascoli, $(h_\delta)_{\delta>0}$ is precompact.

Condition (2) Assume now that (2) holds. We show that this implies (1) which finishes the proof. This means proving that $(h_\delta)_{\delta>0}$ is bounded on K . Let $U_\delta = (x + [-r, r]^2) \cap \delta\Omega$ and let $\Lambda_k^\delta = x + \delta\Lambda_k$. Let $x \in K_\delta$. Then

$$\frac{r}{2\delta} \min \left\{ \delta^2 \sum_{y \in \partial\Lambda_k^\delta} |h_\delta(y)|^2 : \frac{r}{2\delta} \leq k \leq \frac{r}{\delta} \right\} \leq \delta^2 \sum_{y \in U_\delta} |h_\delta(y)|^2.$$

Using the second hypothesis, there exists $k \in [\frac{r}{2\delta}, \frac{r}{\delta}]$ so that

$$h_\delta(x) = \sum_{y \in \partial\Lambda_k^\delta} |h_\delta(y)|^2 \leq 2M/r.$$

Harmonic function h_δ can be written as (see [15])

$$h_\delta(x) = \sum_{y \in \partial\Lambda_k^\delta} h_\delta(y) H_{\Lambda_k^\delta}(x, y),$$

where $H_{\Lambda_k^\delta}(x, y)$ is the probability that a random walk starting at x reaches $\partial\Lambda_k^\delta$ at y . As there is a $C > 0$ so that $H_{\Lambda_k^\delta}(x, y) \leq C\delta$, we get by using Cauchy-Schwartz inequality

$$h_\delta(x)^2 = \left(\sum_{y \in \partial\Lambda_k^\delta} h_\delta(y) H_{\Lambda_k^\delta}(x, y) \right)^2 \leq 2M/r \cdot C^2.$$

□

We are now able to prove a central convergence result [2], [15]. I follow the latter formulation, which uses Dobrushin domains. For the proof below, it is enough to say that these are connected domains with two marked points a and b on the boundary.

Theorem 5.2.1. *Let Ω be a simply connected domain with two marked points a and b on the boundary, and f a bounded continuous function on $\partial\Omega \setminus \{a, b\}$. Let $(\Omega_\delta, a_\delta, b_\delta)$ be Dobrushin domains converging to (Ω, a, b) in the Caratheodory sense.*

Let $f_\delta : \partial\Omega_\delta \rightarrow \mathbb{R}$ be a sequence of uniformly bounded functions converging uniformly away from a and b to f . Let h_δ be the unique preharmonic map on Ω_δ such that $(h_\delta)|_{\partial\Omega_\delta} = f_\delta$. Then

$$h_\delta \rightarrow h \quad \text{when } \delta \rightarrow 0$$

uniformly on compact subsets of Ω , where $h : \bar{\Omega} \setminus \{a, b\} \rightarrow \mathbb{R}$ is the unique continuous function which is harmonic on Ω and equal to f on $\partial\Omega \setminus \{a, b\}$.

Proof. We start the proof by noting the maximum and minimum principles for a discrete harmonic function h_δ :

$$\begin{aligned} \max\{h_\delta(x) : x \in \Omega_\delta\} &= \max\{h_\delta(x) : x \in \partial\Omega_\delta\}, \\ \min\{h_\delta(x) : x \in \Omega_\delta\} &= \min\{h_\delta(x) : x \in \partial\Omega_\delta\}, \end{aligned}$$

whose straightforward proof can be found in [15]. By assumption, $(f_\delta)_{\delta>0}$ is bounded by some constant M . Then by maximum and minimum principles $(h_\delta)_{\delta>0}$ is bounded by M . By Lemma 5.2.4 family $(h_\delta)_{\delta>0}$ is precompact and has a subsequential limit \tilde{h} .

We next prove that \tilde{h} can be continuously extended to the boundary. This proves that $\tilde{h} = h$. Let $x \in \partial\Omega \setminus \{a, b\}$ and $\epsilon > 0$. There exists $R > 0$ and small enough δ such that

$$|f_\delta(x') - f_\delta(x)| < \epsilon \quad \text{for every } x' \in \partial\Omega_\delta \cap Q(x, R),$$

where $Q(x, R) = x + [-R, R]^2$. Let X be a random walk starting at y and let τ be its hitting time of the boundary. For $r < R$ and $y \in Q(x, r)$, we have

$$|h_\delta(y) - f_\delta(x)| = \mathbf{E}[f_\delta(X_\tau) - f_\delta(x)].$$

Decomposing between walks exiting the domain inside $Q(x, R)$ and others, we find

$$|h_\delta(y) - f_\delta(x)| \leq \epsilon + 2M\mathbf{P}[X_\tau \notin Q(x, R)].$$

By the weak Beurling's estimate (see [15]) we have $\mathbf{P}[X_\tau \notin Q(x, R)] \leq (r/R)^\alpha$ for some independent constant $\alpha > 0$. Taking $r = R(\epsilon/2M)^{1/\alpha}$ and letting $\delta \rightarrow 0$, we obtain $|\tilde{h}_\delta(y) - f_\delta(x)| \leq 2\epsilon$ for every $y \in Q(x, r)$. \square

5.3 Proofs and proof ideas of conformal invariance

In Theorem 5.2.1 it was proven that, for a discretely harmonic function $f_\delta(z)$ in a domain Ω_δ with a known and good behaviour at the boundary, there exists a limit $\lim_{\delta \rightarrow 0} f_\delta(z)$ and this limit is a harmonic function. δ is the lattice constant, the smallest distance between lattice points.

For the parafermion $F(z)$ we have preholomorphicity when $K = K_c$, and have shown in Lemma 5.2.1 that if the limit $\lim_{\delta \rightarrow 0} F_\delta(z)$ exists, it is a holomorphic function. Proving the convergence is difficult, and has been done only for Ising model in square lattice.

One difficulty is that the boundary condition is not given for function $F(z)$, but for $Im(F(z)^2 dz)$. In the continuum, if f is holomorphic, function $H = Im(\int^z f^2)$ is a harmonic function that can be determined from its behaviour on the boundary. For example, in continuum $f_1(z) = z$, $f_2(z) = z^2$ and $f_3(z) = z^3$ are holomorphic, but when discretized to a square lattice, only f_1 and f_2 are preholomorphic. F^2 may not be preholomorphic, although F is.

But we need to construct a discrete primitive for $Im[\int F^{1/s} dz]$. By this I mean a function $H_\delta : \Omega_\delta \rightarrow \mathbb{C}$ whose continuum limit is $Im[\int F^{1/s} dz]$. Smirnov did this for the $O(1)$ or Ising model, in square lattice. The parafermion spin must then have value $s = 1/2$. Smirnov found that for the existence of the discrete primitive above, the discrete function F should be s -holomorphic (which implies preholomorphicity). The constructed H is not discretely harmonic, but its continuum limit is found to be harmonic. Using the discrete relation between H and F , it is possible to show the holomorphicity of the latter. Finding a holomorphic observable is a proof of conformal invariance [2].

5.3.1 $O(1)$ is conformally invariant at the scaling limit

I will give the main steps in proving conformal invariance of the $O(1)$ model. We will study its scaling limit at $K_c = 1/\sqrt{3}$ with the parafermionic observable with spin $s = 1/2$. I will not produce the copy of the whole story, which is written in [2] and [15], for example. I will instead concentrate on the construction of the discrete primitive H . The following steps in the proof that F holomorphic, are explained without detailed proofs, which can be found in [2] and [15]. I will start with some definitions.

We will use the square lattice with lattice points $\mathbb{Z}_\delta^2 = \{(n, m) : n, m \in \mathbb{Z}\}$ in the infinite case. For a finite continuous domain $\Omega \subset \mathbb{Z}^2$, we set $\Omega_\delta = \Omega \cap \mathbb{Z}_\delta^2$.

We will work with Ω_δ letting $\delta \rightarrow 0$.

Two other related lattices are needed. The points in the medial lattice are the midpoints of edges of the original lattice (and the edges in the original lattice are the straight lines between nearest neighbour -points). Symbol for the finite medial lattice is Ω_δ° . Third necessary lattice is called dual lattice, and its lattice points (or vertices) are $\mathbb{Z}_{\delta^*}^2 = (1/2, 1/2) + \mathbb{Z}_\delta^2$. Symbol for the finite dual lattice is Ω_δ^* .

Operator $\bar{\partial} = 1/2(\partial_x + i\partial_y)$ can be discretized in the following way in the square lattice. Let $f : \Omega_\delta^\circ \rightarrow \mathbb{C}$ and $x \in \Omega_\delta \cup \Omega_\delta^*$. Then

$$\bar{\partial}_\delta := \frac{1}{2} [f(E) - f(W)] + \frac{i}{2} [f(N) - f(S)], \quad (5.16)$$

where S, E, N and W denote the four vertices (N up, E right, S down, W left) of Ω_δ° adjacent to the medial vertex x . Smirnov [2] then defines discrete holomorphic functions in the following way

Definition 5.3.1. (*discrete holomorphic function*)

Function $f : \Omega_\delta^\circ \rightarrow \mathbb{C}$ is discrete holomorphic if $\bar{\partial}_\delta f = 0$ for every $x \in \Omega_\delta \cup \Omega_\delta^*$. Equation $\bar{\partial}_\delta f = 0$ is called the discrete Cauchy-Riemann equation at x .

If $\bar{\partial}_\delta f = 0$, the discrete contour integrals of f vanish, which was the previously given (chapter 3) definition for a discretely holomorphic function. Then by Lemma 5.2.1, if family $(f)_\delta$ converges uniformly to f , then f is holomorphic.

A function $f : \Omega_\delta^\circ \rightarrow \mathbb{C}$ is a discrete holomorphic solution to the Dirichlet BVP on $\Omega_\delta \cup \Omega_\delta^*$ with boundary conditions $g : \partial\Omega_\delta \rightarrow \mathbb{C}$ if f is discrete holomorphic and $f = g$ on $\partial\Omega_\delta$. There is a existence and uniqueness result for this problem (for proof, see [15]):

Lemma 5.3.1. *Let Ω_δ be a discrete domain. For any $g : \partial\Omega_\delta \rightarrow \mathbb{C}$, there exists a solution f to the Dirichlet BVP on $\Omega_\delta \cup \Omega_\delta^*$. The solution is unique up to the addition of a constant to $f|_{\Omega_\delta^*}$.*

The next issue is the construction of a primitive H for $Im(f f^2 dz)$, with $f : \Omega_\delta^\circ \rightarrow \mathbb{C}$ a discretely holomorphic function. A natural starting point is

$$H(b_1) - H(b_2) = Im [f(v)^2 \cdot (b_1 - b_2)], \quad (5.17)$$

where b_1 and b_2 are vertices in the Ω_δ , and v is the vertex in medial lattice between b_1 and b_2 (see figure 5.2 below).

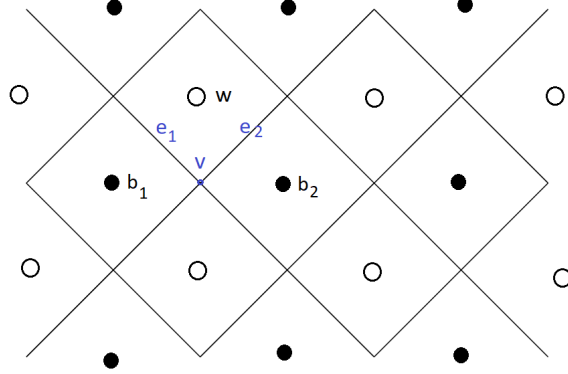


Figure 5.2: Square lattice (dark spheres), and its dual (white spheres) and medial lattices (lines are edges in medial lattice).

A candidate construction for $H(z)$, $z \in \Omega_\delta$ is the following. Set $H(z_0) = c$ at some given point $z_0 \in \Omega_\delta$ and some given value $c \in \mathbb{C}$. Then take a path γ from z_0 to z and set

$$H(z) = c + \sum_{k \in \gamma} \text{Im} [f(v_k)^2 \cdot (b_k - b_{k+1})], \quad (5.18)$$

where b_k is the k :th point in path γ and $v_k \in \Omega_\delta^\circ$ is between b_k and b_{k+1} . To be well defined, the result must be independent of path γ from z_0 to z .

To formulate this condition for f , Smirnov and Duminil-Couperin [2], [15] rewrite (5.18) as

$$\begin{aligned} H(b_1) - H(b_2) &= \frac{1}{2} \left[\left(\sqrt{e_1} f(v) + \overline{\sqrt{e_1} f(v)^2} \right)^2 - \left(\sqrt{e_2} f(v) + \overline{\sqrt{e_2} f(v)^2} \right)^2 \right] \\ &= \sqrt{2} \delta \left[|P_{l(e_1)}[f(v)]|^2 - |P_{l(e_2)}[f(v)]|^2 \right], \end{aligned} \quad (5.19)$$

where e_1 and e_2 are medial edges bordered by b_1 and w , and b_2 and w respectively, and $w \in \Omega_\delta^*$ is adjacent to both b_1 and b_2 (see figure 5.3 below).

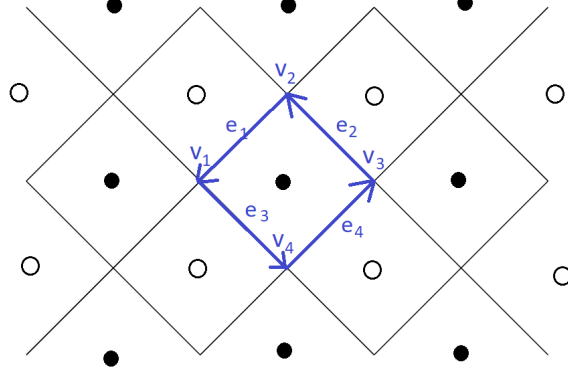


Figure 5.3: Square lattice (dark spheres), and its dual (white spheres) and medial lattices. Complex vectors e_1, e_2, e_3, e_4 are vectors along edges in medial lattice.

Function

$$P_l[x] := \alpha \operatorname{Re}(\bar{\alpha}x) = \frac{1}{2}(x + \alpha^2 \bar{x}), \quad (5.20)$$

where α is any unit vector collinear to l , is a projection to the direction of l . In (5.20) $l(e)$ is a real line to the direction of \sqrt{e} .

For proving that (5.18) is independent of path, let us calculate

$$\begin{aligned} e_1 = e^{i\pi/4}, \quad \sqrt{e_1} = e^{i\pi/8}, \quad e_2 = e^{i3\pi/4}, \quad \sqrt{e_2} = e^{i3\pi/8}, \\ e_3 = e^{i5\pi/4}, \quad \sqrt{e_3} = e^{i5\pi/8}, \quad e_4 = e^{i7\pi/4}, \quad \sqrt{e_4} = e^{i7\pi/8}, \end{aligned}$$

so that $\sqrt{e_1}, \sqrt{e_3}$ and $\sqrt{e_2}, \sqrt{e_4}$ are orthogonal. Thus

$$|P_{l(e_1)}[f(v)]|^2 + |P_{l(e_3)}[f(v)]|^2 - |P_{l(e_2)}[f(v)]|^2 - |P_{l(e_4)}[f(v)]|^2 = 0, \quad (5.21)$$

which is understood [15] to prove that a closed loop path gives a zero contribution, which means that (5.19) is independent of path. We therefore have a well defined primitive (discretization) for $\operatorname{Im}(f^2 dz)$.

To prove that f converges at $\delta \rightarrow 0$, we would like the function H to be harmonic at the limit $\delta \rightarrow 0$. And we would like to present the sufficient conditions as properties of f and the lattice. The key property of f is the s -holomorphicity:

Definition 5.3.2. (*s-holomorphicity*)

A function $f : \Omega_\delta^\circ \rightarrow \mathbb{C}$ is s -holomorphic, if for any edge $e = [xy]$ of Ω_δ° , we have

$$P_{l(e)}[f(x)] = P_{l(e)}[f(y)]$$

It is useful to define H in lattice $\Omega_\delta \cup \Omega_\delta^\circ$. Using the ideas above, the following theorem can be proved (see [15])

Theorem 5.3.1. *Let $f : \Omega_\delta^\circ \rightarrow \mathbb{C}$ be an s -holomorphic function on Ω_δ° . Then there exists a unique (up to an additive constant) function $H : \Omega_\delta \cup \Omega_\delta^\circ \rightarrow \mathbb{C}$ such that*

$$H(b) - H(w) = \sqrt{2}\delta |P_{l(e)}[f(x)]|^2$$

for every edge $e = [xy]$ of Ω_δ° bordered by $b \in \Omega_\delta$ and $w \in \Omega_\delta^\circ$. Furthermore, for two neighbouring vertices $b_1, b_2 \in \Omega_\delta$, with v being the medial vertex at the center of $[b_1b_2]$,

$$H(b_1) - H(b_2) = \text{Im} [f(v)^2 \cdot (b_1 - b_2)], \quad (5.22)$$

the same relation holding for vertices of Ω_δ° .

By the next lemma, function H has the required properties if f is s -holomorphic. Let H^\bullet and H° be the restrictions of $H : \Omega_\delta \cup \Omega_\delta^\circ \rightarrow \mathbb{C}$ to Ω_δ and Ω_δ° respectively.

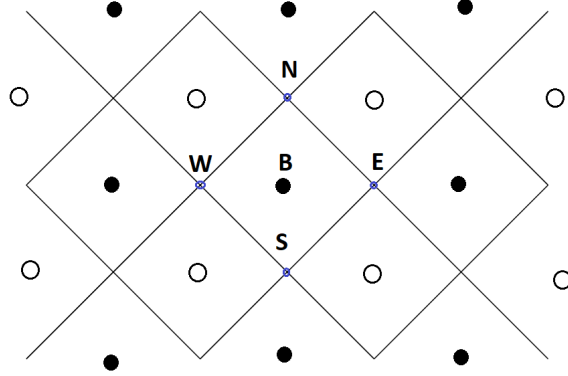


Figure 5.4: Square lattice (dark spheres), and its dual (white spheres) and medial lattices (lines are edges in medial lattice).

Lemma 5.3.2. *Let $f : \Omega_\delta^\circ \rightarrow \mathbb{C}$ be s -holomorphic. Let Δ^\bullet and Δ° be the nearest neighbour discrete Laplacian for functions on Ω_δ and Ω_δ° respectively. Using the notation in figure 5.4 above*

$$\Delta^\bullet H^\bullet(B) = \frac{\delta}{4} \text{Im} [f(E)^2 - if(S)^2 - f(W)^2 + if(N)^2] \quad (5.23)$$

Then H^\bullet is subharmonic for Δ^\bullet on $\Omega_\delta \setminus \partial\Omega_\delta$, and H° is superharmonic for Δ° on $\Omega_\delta^\circ \setminus \partial\Omega_\delta^\circ$.

Proof. Let B, N, E, S, W be as in figure 5.4 above. Using s-holomorphicity, we can set

$$\begin{aligned} a &= e^{i\frac{\pi}{8}} P_{l([ES])}[f(E)] = e^{i\frac{\pi}{8}} P_{l([ES])}[f(S)], \\ b &= e^{i\frac{\pi}{8}} P_{l([SW])}[f(S)] = e^{i\frac{\pi}{8}} P_{l([SW])}[f(W)], \\ c &= e^{i\frac{\pi}{8}} P_{l([WN])}[f(W)] = e^{i\frac{\pi}{8}} P_{l([WN])}[f(N)], \\ d &= e^{i\frac{\pi}{8}} P_{l([NE])}[f(N)] = e^{i\frac{\pi}{8}} P_{l([NE])}[f(E)]. \end{aligned}$$

Using orthogonality as above in (5.21), we get

$$\begin{aligned} f(E) &= \sqrt{2}i(e^{-3i\pi/8}d + e^{-i\pi/8}a), \\ f(S) &= \sqrt{2}i(e^{3i\pi/8}a - e^{5i\pi/8}b), \\ f(W) &= \sqrt{2}i(e^{i\pi/8}b - e^{3i\pi/8}c), \\ f(N) &= \sqrt{2}i(e^{-i\pi/8}c - e^{i\pi/8}d), \end{aligned}$$

Plugging these in to (5.23) gives

$$\Delta^\bullet H^\bullet(B) = \delta[a^2 + b^2 + c^2 + d^2 - \sqrt{2}(ab + bc + cd - ad)].$$

As

$$\begin{aligned} &|f(E) - f(S)|^2 + |f(W) - f(N)|^2 \\ &= 4[a^2 + b^2 + c^2 + d^2 - \sqrt{2}(ab + bc + cd - ad)] \geq 0, \end{aligned}$$

we get $\Delta^\bullet H^\bullet(B) \geq 0$. Similar proof gives that $\Delta^\circ H^\circ(B) \geq 0$. \square

The next task is to prove compactness for (f_δ) , since then there exists a convergent subsequence. The complete, somewhat difficult proof of the following theorem can be found in [15]. Here I will only give its first part, showing the role of s-holomorphicity.

Theorem 5.3.2. (*Precompactness for s-holomorphic maps.*)

Let $(f_\delta)_{\delta>0}$ be a family of s-holomorphic maps on Ω_δ° and $(H_\delta)_{\delta>0}$ be the corresponding functions defined in Theorem 5.3.1. Let $Q \subset \Omega$ such that $9Q \subset \Omega$. If $(H_\delta)_{\delta>0}$ is uniformly bounded on $9Q$, then $(f_\delta)_{\delta>0}$ is a precompact family of functions on Q .

Proof. Color the vertices of $(\delta\mathbb{Z}^2)^\circ$ of the medial lattice like a chessboard. Denote the sets of black vertices by $(\delta\mathbb{Z}^2)^\bullet$ and the white vertices by $(\delta\mathbb{Z}^2)^\circ$. Since f_δ is s-holomorphic, it is also holomorphic and therefore harmonic for the modified Laplacian on Ω_δ° , which corresponds to the standard Laplacian on $(\delta\mathbb{Z}^2)^\circ$.

Assume that (f_δ) satisfies the second property of Lemma 5.2.4. Then Lemma 5.2.4 implies that the restrictions f_δ^\bullet of functions f_δ to $\Omega_\delta^\circ \cap (\delta\mathbb{Z}^2)^\circ$ form a precompact family of functions.

s-holomorphicity then implies that $(f_\delta)_{\delta>0}$ itself is precompact. Let $x \in \Omega_\delta^\circ \cap (\delta\mathbb{Z}^2)^\circ$. Denote the north-east and south-west neighbouring vertices of x in $(\delta\mathbb{Z}^2)^\circ$ by y and z . s-holomorphicity and orthogonality of $l(xy)$ and $l(xz)$ then gives

$$\begin{aligned} f_\delta(x) &= P_{l(xy)}(f_\delta(x)) + P_{l(xz)}(f_\delta(x)) \\ &= P_{l(xy)}(f_\delta(y)) + P_{l(xz)}(f_\delta(z)) \\ &= f_\delta(y) - P_{l(xz)}(f_\delta(y)) + P_{l(xz)}(f_\delta(z)) \\ &= f_\delta(y) + O(f_\delta(z) - f_\delta(y)). \end{aligned} \tag{5.24}$$

By the assumption above, and Lemma 5.2.4, we may extract a subsequence $(f_{\delta_n}^\bullet)_n$ converging uniformly on every compact subset of Ω when seen as a function of $\Omega_\delta^\circ \cap (\delta\mathbb{Z}^2)^\circ$. Result (5.24) then implies that $(f_{\delta_n})_n$ itself converges uniformly on every compact subset of Ω .

The second part of the proof in [15] then proves the second property of Lemma 5.2.4. \square

Proving the conformal invariance of the Ising model then uses the results above. The proof advances in the following steps [2]:

- prove that $F_\delta(z)$ is s-holomorphic,
- prove the convergence of H_δ ,
- prove that $F_\delta(z)/\sqrt{2\delta}$ converges to $\sqrt{\phi'}$, where ϕ is a conformal map.

The theorem of the conformal invariance of the Ising model is [2]

Theorem 5.3.3. *Let (Ω, a, b) be a simply connected domain with two marked points on the boundary. Let F_δ be the vertex fermionic observable in (Ω°, a, b) . Then*

$$\frac{1}{\sqrt{2\delta}}F_\delta(z) \rightarrow \sqrt{\phi'(z)} \quad \text{when } \delta \rightarrow 0 \tag{5.25}$$

uniformly on any compact subset of Ω , where ϕ is any conformal map from Ω to the strip $\mathbb{R} \times (0, 1)$ mapping a to $-\infty$ and b to ∞ .

Proof. (Idea, see [2] or [15] for the actual proof)

After showing that F_δ is s-holomorphic, the family $(F_\delta/(\sqrt{2\delta}))$ is proved to be a precompact family for the uniform convergence on compact subsets of Ω , using Theorem 5.3.2. Then the possible subsequential limits are identified using H_δ . \square

5.3.2 Studying conformal invariance with transfer matrices

Thus, we have a proof of conformal invariance for the $O(n)$ model in the square lattice with parameter values $n = 1$, $K = 1/\sqrt{3}$, $s = 1/2$, where s is the parafermion (or fractional) spin (and thus not a model parameter). In the next section, I will form a transfer matrix for $O(n)$ model in a hexagonal lattice. This construction will lead to values of the parafermionic function F at the vertices of a parallelogram lattice, with the geometry shown in figure 5.5 below.

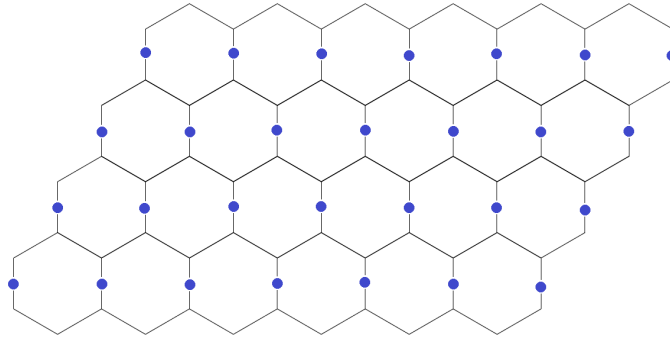


Figure 5.5: The blue points form a lattice (its vertices). Transfer matrix calculations in chapter 8 determine $F(z)$ at these points.

Let the coordinates in this lattice be $z = x + iy$, where x is the column number and y is the row number. As will be shown in the next section, in a finite slab with N rows and M columns with the lattice geometry as in figure 5.1 above, function F (defined in 3.1.1) can be written as

$$F(x + iy) = \langle \Psi_b | T_3^{N-y-1} \cdot T_2(x) \cdot T_1^{y-1} | \Psi_a \rangle, \quad (5.26)$$

where $|\Psi_a\rangle$ and $|\Psi_b\rangle$ are chosen states in the first and last row, respectively.

The purpose is to test, if F such defined is s-holomorphic in finite lattices. For that purpose, choose a coordinate system like in figure 5.6 below, so that its origin is at the center of the parallelogram. Then the vectors to the middle points of the edges (corners in parallelogram) are (all lengths in δ)

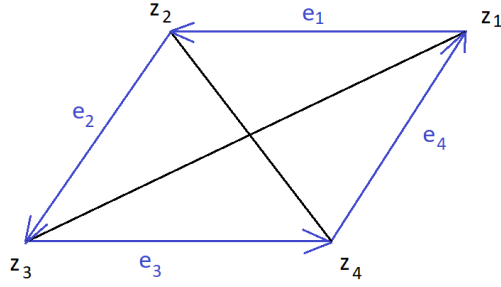


Figure 5.6: Unit cell in the for the medial lattice from Figure 9. Transfer matrix calculations in chapter 8 determine $F(z)$ at points z_1, z_2, z_3, z_4 .

$$z_1 = \frac{3}{2} \cdot e^{i\pi/4}, \quad z_2 = \frac{3}{2} \cdot e^{i3\pi/4}, \quad z_3 = \frac{3}{2} \cdot e^{i5\pi/4}, \quad z_4 = \frac{3}{2} \cdot e^{i7\pi/4}, \quad (5.27)$$

and the directions of vectors $e_k, k = 1, 2, 3, 4$ are

$$e_1 = -1, \quad e_2 = e^{i4\pi/3}, \quad e_3 = 1, \quad e_4 = e^{i\pi/3}. \quad (5.28)$$

By definitions 5.3.2 and (5.20), the condition of s-holomorphicity is now

$$\begin{aligned} (e_1): \quad & F(z_1) + \bar{e}_1^{2s} \overline{F(z_1)} = F(z_2) + \bar{e}_1^{2s} \overline{F(z_2)}, \\ (e_2): \quad & F(z_2) + \bar{e}_2^{2s} \overline{F(z_2)} = F(z_3) + \bar{e}_2^{2s} \overline{F(z_3)}, \\ (e_3): \quad & F(z_3) + \bar{e}_3^{2s} \overline{F(z_3)} = F(z_4) + \bar{e}_3^{2s} \overline{F(z_4)}, \\ (e_4): \quad & F(z_4) + \bar{e}_4^{2s} \overline{F(z_4)} = F(z_1) + \bar{e}_4^{2s} \overline{F(z_1)}, \end{aligned} \quad (5.29)$$

where

$$\bar{e}_1 = -1, \quad \bar{e}_2 = e^{-i4\pi/3}, \quad \bar{e}_3 = 1, \quad \bar{e}_4 = e^{-i\pi/3}. \quad (5.30)$$

In section 8 I will test these relations with some finite lattices.

Chapter 6

Constructing the transfer matrices for the loop $O(n)$ model

Transfer matrix is a versatile tool for lattice calculations. For the Ising model the transfer matrix elements can be assembled for any lattice size, and the resulting matrix can be used for an algebraic solution. For the $O(n)$ loop model, forming the matrix elements is more difficult, and the calculations are usually done with only a few columns. Reason for this is that, although there is a weight model formulation for the $O(n)$ loop model, the lines/weights in the following row must be chosen so that an allowed pattern is formed.

A general introduction to transfer matrices was given in chapter 4. Here I start with a short representation of a $O(n)$ -model transfer matrix construction by Blöte and Nienhuis [16]. Then I will continue with my construction by representing the lattice geometry it is based on. This construction is can be easily varied for calculating correlation functions or expectation values for the parafermionic observable.

6.1 Transfer matrix for the $O(n)$ loop model, the Blöte-Nienhuis -construction

Recall that

$$Z = \sum_{\mathcal{G}} K^{\epsilon} \cdot n^L, \quad (6.1)$$

where ϵ is the number of edges, L is the number of loops. Blöte and Nienhuis [16] start by writing the partition function as

$$Z = \sum_{\mathcal{G}} K^{N_v} n^L \quad (6.2)$$

where N_v is the number of occupied vertices, and the vertex weight w is one if vertex is not occupied (by a loop) and K if vertex is occupied.

If lines k and m are in the same loop, they are called connected. Connectivity of lines can be given as a sequence of positive integers (i_1, i_2, \dots, i_M) such that $i_k = i_l$, if lines k and l are connected. If not connected, the integer is zero. For a strip of width M , the idea is to write the partition function as

$$Z_\alpha^{N+1} = \sum_\beta T_{\alpha\beta} Z_\beta^N, \quad (6.3)$$

where sum is over connectivities, and Z_α^{N+1} is the partition function for a lattice with $N+1$ rows, M columns and connectivity α . $T_{\alpha\beta}$ is the transform matrix.

Let us calculate the number of possible connections for two cases. Let n_d be the number of lines that start from the first row and are not restricted to be in any loop (like the spin-spin -correlation functions).

Let c_m be the number of dense $2m$ connectivities. Let a_M be the number of $n_d = 0$ (or non-magnetic) connectivities. Let $[M/2]$ be the integer part of $M/2$. Then [16]

$$a_M = \sum_{j=0}^{[M/2]} \frac{M!}{j!(j+1)!(M-2j)!}. \quad (6.4)$$

Let b_M be the number of $n_d = 1$ (non-magnetic) connectivities. Then [16]

$$b_M = M a_{M-1}. \quad (6.5)$$

The partition function for row N can be written as

$$Z^{(N)} = \sum_\beta Z_\beta^N. \quad (6.6)$$

Let N_v be the number of occupied vertices and N_l the number of finished loops in row N . For the next row $N+1$, let these be N'_v and N'_l . Further define n_v and n_l by

$$N'_v = N_v + n_v, \quad N'_l = N_l + n_l. \quad (6.7)$$

n_l is the number of loops closed at level $N+1$. n_v is the number of occupied vertices at level $N+1$.

Let $S(N+1) \in \mathcal{G}_{N+1}$. S is a graph with loops and lines. Let $\phi_{N+1}(S(N+1))$ be the connectivity of line $N+1$. Let $\phi_N(S(N+1))$ be the connectivity of line N . Then we can write

$$Z_\alpha^{(N+1)} = \sum_{S(N+1) \in \mathcal{G}_{N+1}} \delta_{\alpha, \phi(S(N+1))} K^{N'_v} n^{N'_l} \quad (6.8)$$

where the sum is over all loop and line configurations. The delta function causes that only those graphs in \mathcal{G}_{N+1} that have given connectivity α on row $N + 1$, are actually counted.

Let g_{N+1} be row $N + 1$ in graph $S(N + 1)$. Then

$$Z_\alpha^{(N+1)} = \sum_{S(N) \in \mathcal{G}_N} K^{N_v} n^{N_l} \left(\sum_{g_{N+1}|S(N)} \delta_{\alpha, \phi(S(N+1))} K^{n_v} n^{n_l} \right), \quad (6.9)$$

where the latter sum is over those graphs on line $N + 1$ that match to graph $S(N) \in \mathcal{G}_N$.

$\phi(S(N + 1))$ is the connectivity of graph $S(N + 1) \in \mathcal{G}_{N+1}$. However, this depends on the connectivity of the same graph up to N , or $\phi(S(N))$ and the graph on line $N + 1$. Writing this dependence as function $\psi(\phi(S(N)), g_{N+1}) = \phi(S(N + 1))$ we get

$$Z_\alpha^{(N+1)} = \sum_{\beta} \sum_{S(N) \in \mathcal{G}_N} \delta_{\beta, \phi(S(N))} K^{N_v} n^{N_l} \left(\sum_{g_{N+1}|\beta} \delta_{\alpha, \psi(\beta, g_{N+1})} K^{n_v} n^{n_l} \right), \quad (6.10)$$

or

$$Z_\alpha^{(N+1)} = \sum_{\beta} T_{\alpha\beta} Z_\beta^{(N)}, \quad (6.11)$$

$$T_{\alpha\beta} = \sum_{g_{N+1}|\beta} \delta_{\alpha, \psi(\beta, g_{N+1})} K^{n_v} n^{n_l}. \quad (6.12)$$

To conclude, α is the connectivity in row $N + 1$ and β is the connectivity in row N . Sum over $g_{N+1}|\beta$ is a sum over graphs on line $N + 1$ that match the connectivity β . $\psi(\beta, g_{N+1})$ is the connectivity that results when adding a row g_{N+1} to a graph with connectivity β .

6.2 Transfer matrix for the $O(n)$ loop model, the $|-$ row V -row construction

I give my construction as a series of algorithms, one for each partial task. I use the same notation as before, calling the edges occupied by a loop bonds. The rule that there may be zero or two bonds from (or to) each vertex, will be applied many times. This new method of constructing the T -matrix for loop models should be applicable to any lattice, not just hexagonal.

Let us orient the hexagonal lattice as in figure 6.1 below.

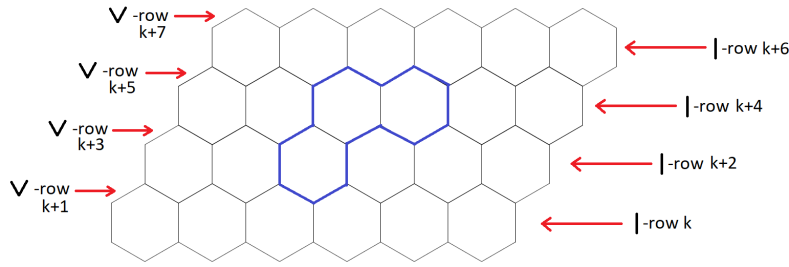


Figure 6.1: Orientation of the hexagonal lattice for constructing the transfer matrix. $|-$ -rows and V -rows.

Then there are consecutive rows of $|-$ s and V -s, as noted in figure 6.1 above. Let us draw a loop in this lattice. I call edges belonging to loops for bonds. The main idea with this construction is that for a loop there must be two vertical bonds in each $|-$ -row, a left and a right $|-$ -line.

Let there be M $|-$ -lines on a row. I form a M -dimensional vector W describing the state of a $|-$ -row in the following way. Let the k :th element $W(k)$ in this vector correspond to the k :th $|-$ -line. If the k :th $|-$ -line $k \in \{1, 2, \dots, M\}$ is not occupied by a bond, I put $W(k) = 0$. If there is only one loop going through the $|-$ -row, with left arm at bond i_1 and right arm at bond i_2 , I put $W(i_1) = -2$ and $W(i_2) = 2$. If there are n loops going through a $|-$ -row, I mark the positions of the corresponding bond pairs by $(-2, 2)$, $(-3, 3)$, \dots , $(-n, n)$, so that I know the positions of both arms for each loop. I will call such M -vectors for states.

Example 6.2.1. *The state on row 3 in figure 6.2 below is $(0 -2 0 -3 3 2 0)$.*

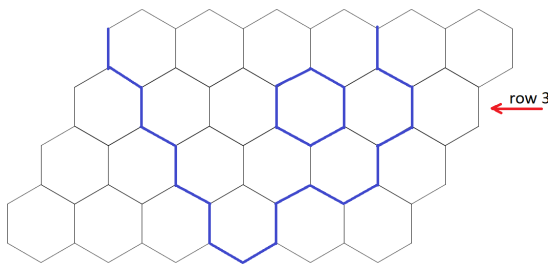


Figure 6.2: The state on row 3 is $(0 -2 0 -3 3 2 0)$.

The next task is to form all possible states, for some given M (M is the number of $|-$ -lines in a row). Loops may not intersect, so $(0 0 -2 -3 0 2 0 3 0)$ is not an allowed state, for example. Further, for not to count same state

multiple times, -2 must always be on the left of -3 , if there are two loops going through the $|$ -row. Generally, for loops $(-k, k)$, $(-p, p)$, $0 < k < p$, $-k$ must be to the left of $-p$. It is now straightforward to write a computer program that forms all these vectors. Let V_1 denote the resulting set of vectors. In Appendix A I have written a formal algorithm for forming all one- and two-loop vectors W_N .

The next row, say $N+1$:th, is a V -row, and the task is to form all possible configurations or states for this row, for a given vector W_N of $|$:s for row N . Let us consider what can happen to bonds. As can be seen from figure 6.2, for example, if there is a bond on the first $|$ -line, it can only turn to the right. The other $|$ -bonds have two alternatives: turn to the right or turn to the left. Then there are free V :s, with no incoming $|$ -line. These free V :s may be chosen to be either occupied 11 or unoccupied 00.

Choosing a direction for each bond and either 00 or 11 for free V :s results to what I call an *intermediate V -state* \tilde{V} .

Example 6.2.2.

For state

$$W_N = (0, 0, -2, 0, -3, 0, 3, 0, 0, 2, 0, 0),$$

the possibilities for each $|$ are

0	0	-2	0	-3	0	3	0	0	2	0	0
0	00	0-2	00	0-3	00	03	00	00	02	00	00
0	11	-20	11	-30	11	30	11	11	20	11	11

one possible intermediate V -state is then

$$\tilde{V}_{N+1} = (0, 1, 1, -2, 0, 1, 1, 0, -3, 1, 1, 3, 0, 1, 1, 1, 1, 2, 0, 0, 0, 1, 1),$$

so that $-2, -3, 3, 2$ have turned to left, right, left, left, respectively. Now $\epsilon_1 = 16$.

It is easy to count the number of new bonds ϵ_1 on the \tilde{V} -line. Example 6.2 above may be a good clarification of these ideas.

Each such intermediate state \tilde{V} determines a final V -state. This process is essentially interpreting the intermediate state \tilde{V} as unfinished loops continuing upwards, new loops initiated from this V -row, and finally finished loops, thus determining the number of new finished loops L . This means that each sequence of $1 : s$, if attached to a loop or loops, must be connected to them in the correct way. If not connected, a new loop starts.

The last step is to construct the next line of vertical bonds, $W_{N+2} \in \mathbb{Z}^M$. This means that each sequence of $1 : s$, if attached to a loop or loops, must be connected to them in the correct way. If not connected, a new loop starts. I call this the formation of final V -state from an intermediate V -state.

Vector W_{N+2} of vertical edges can be directly read from the resulting V -state vector V_{N+1} . Formally: let there be M elements in W_{N+2} . Then there are $2M - 1$ elements in V_{N+1} . For $1 \leq k \leq M - 1$, if $|V_{N+1}(2k - 1)| \geq |V_{N+1}(2k)|$, then set $W_{N+2} = V_{N+1}(2k - 1)$. For $1 \leq k \leq M - 1$, if $|V_{N+1}(2k - 1)| \leq |V_{N+1}(2k)|$, then set $W_{N+2} = V_{N+1}(2k)$. Finally, set $W_{N+2}(M) = V_{N+1}(2M - 1)$. The resulting numbers $W_{N+2}(k)$, $k \in \{1, 2, \dots, M\}$ may not be in standard order (where negative numbers are in descending order), so the the last step in the process is transforming to this order. Let us continue with the example above.

Example 6.2.3.

$$W_N = (0, 0, -2, 0, -3, 0, 3, 0, 0, 2, 0, 0)$$

$$\tilde{V}_{N+1} = (0, 1, 1, -2, 0, 1, 1, 0, -3, 1, 1, 3, 0, 1, 1, 1, 1, 2, 0, 0, 0, 1, 1),$$

transformed to

$$V_{N+1} = (0, -2, 0, 0, 0, -4, 4, 0, 0, 0, 0, 0, 0, 2, 0, 0, 0, 0, 0, 0, -5, 5)$$

transformed to

$$V_{N+1} = (0, -2, 0, 0, 0, -3, 3, 0, 0, 0, 0, 0, 0, 2, 0, 0, 0, 0, 0, 0, -4, 4)$$

transformed to

$$W_{N+2} = (-2, 0, -3, 3, 0, 0, 2, 0, 0, 0, -4, 4),$$

and one loop was formed, so $L = 1$. The number of new bonds on row $N+2$ is $\epsilon_2 = 6$.

For a given $\alpha := W_N$ and $\beta := W_{N+2}$, the matrix element $T_{\alpha\beta}$ is $K^{\epsilon n^L}$, where ϵ is the number of new bonds and L the number of new loops. L is determined in the process described above. ϵ is the sum of the number of bonds in the V -line \tilde{W}_{N+1} , and the number of bonds in line W_{N+2} . Number of bonds ϵ_1 in the V -line can be calculated to be $k + 2 \cdot v$, where k is the number of bonds in line W_N and v is the number of bonded V :s in line \tilde{W}_{N+1} . Number of bonds ϵ_2 in line $\beta := W_{N+2}$ is determined in the process described above.

Continuing with the example above, we finally get the transfer matrix element:

Example 6.2.4.

$$\begin{aligned}\alpha &= W_N = (0, 0, -2, 0, -3, 0, 3, 0, 0, 2, 0, 0) \\ \beta &= (-2, 0, -3, 3, 0, 0, 2, 0, 0, 0, -4, 4), \\ \epsilon &= \epsilon_1 + \epsilon_2 = 16 + 6 = 22, \quad L = 1, \\ T_{\alpha\beta} &= K^{22}n.\end{aligned}$$

6.3 Transfer matrix for the $O(n)$ loop model with a parafermionic observable

Here we have a parafermion which starts from the bottom row and ends at point z . To describe states on $|\cdot$ -lines three sets of states V_1 , V_2 , and V_3 will be needed.

Below z , there will be one parafermion line which starts from the first or bottom line. On the left and right side of a single parafermion line there may loops which further may combine to the parafermion. I denote the set of possible states of vertical lines for this part of the lattice V_1 . I use number -23 for the end point of the parafermion path that starts from the first row. An example of possible state of vertical lines in V_1 is

Example 6.3.1.

$$W_N^1 = (0, 0, -2, -3, 0, 3, 0, 2, 0, -23, 0, -4, 0, 4)$$

A typical parafermion path in V_1 is given in Figure 6.3 below.

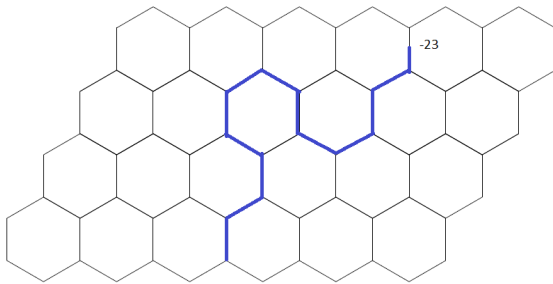


Figure 6.3: Typical situation in space V_1 . A parafermion path starts at $m = 4$. On the 4:th V -row it combines with a loop.

The first or V_1 -part ends at height where the parafermion has its endpoint z . There the parafermion may hit the point z , whence it ends, and in the

upper row there is no parafermion. Then, above z -level, there will be no parafermion lines, only loops. I call V_3 the set of states with no parafermion lines.

If the parafermion from V_1 does not hit the given point z , we have two loose ends for the parafermion, until they combine. These are the old -23 from the first row and a new parafermion line 23 ending at point z . Thus, I use number 23 for the parafermion path that ends at z . I call the set of possible states of vertical lines for this area V_2 . An example of possible state of vertical lines is

Example 6.3.2.

$$W_N^2 = (-2, 0, 2, -23, 0, -3, 0, 23, 0, 3, 0, -4, 0, 4)$$

A typical parafermion path ending at states in V_2 is given in Figure 6.4 below. The corresponding state vector expression $(-23, 0, 0, 23, -2, 2, 0)$ for row 4 is explained in subsection 6.2.

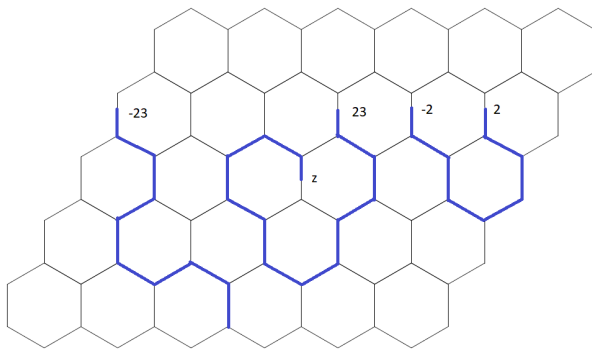


Figure 6.4: A typical situation in space V_2 . A parafermion path starts at $m = 4$ on the first row. Parafermion ends at point $z = 4$ on row 3.

Note that the endpoint z (marked by 23) may be inside an open loop like $-3, 3$ in the example. $-3, 3$ must combine to 23 at some height. These structures will determine the winding number for the parafermion.

After the parafermion has found its way to z , there will be no parafermion in the states of vertical lines. These states are defined in subsection 6.2. I call the set of possible states of vertical lines for this area V_3 . An example of possible state of vertical lines in V_3 is

Example 6.3.3.

$$W_N^3 = (0, 0, -2, -3, 0, 3, 0, 2, 0, 0, 0, -4, 0, 4)$$

The states within sets V_1 , V_2 and V_3 are connected in a similar way as in the previous section. For a state of vertical lines in row N , there are many possible states of V :s in row $N + 1$. Each such V -state gives a state of vertical lines for row $N + 2$. In this process, there may be new bonds, new loops completed and winding angles produced. This information will determine the matrix element from row N to row $N + 2$.

Let us first determine, how the winding angle of a parafermion may change, from a row of vertical lines (row N) to next row of vertical lines (row $N + 2$). In V_1 the parafermion path -23 may combine to unfinished, open loops. Then the winding angle does not change. Winding angle does neither change when parafermion -23 moves without combinations from row N to row $N + 2$.

At height z , if the parafermion -23 hits the point z , winding angle is zero. In the rows above, there will then be no parafermion lines. If the parafermion -23 -line does not hit point z , I will start another parafermion path 23 from point z . The direction of 23 -path is such that it ends at point z . As mentioned above, there may now be unfinished loops such that the negative part is on the left side of 23 and positive part on the right side (like $-3 \ 23 \ 3$). If 23 connects to -3 (at the next V -line) so that at 3 we put 23 , there must be six turns to left, or winding angle $6 \cdot \pi/3$. If 23 is connected to 3 , there are six turns to right and winding angle is $-6 \cdot \pi/3$. Otherwise, if 23 is connected to an open loop completely on its right or left side, there is no phase change.

When the two parafermion lines are connected in order $23 \ -23$, there are three left turns so that the winding angle is $-3 \cdot \pi/3$. When the two parafermion lines are connected in order $-23 \ 23$, there are three right turns so that the winding angle is $3 \cdot \pi/3$.

The purpose is to construct a transfer matrix T , whose element (i, j) is the weight for the transition from state j on row N to state i on row $N + 2$. Weight is determined by the number of new bonds ϵ , loops completed L , and left and right turns of the parafermion path t_l , t_r , counted from row N of vertical lines to row $N + 2$ of vertical lines:

$$T_{ij} = \lambda^{t_r - t_l} \cdot n^L \cdot K^\epsilon, \quad (6.13)$$

where $\lambda = e^{is\pi/3}$. As noted above, $t_r - t_l$ can in this case have values -6 , -3 , 3 or 6 .

Example 6.3.4. *Let there be five hexagons on a row. Let the states i (N :th row) and j ($N+2$:th row) be*

$$i = (0 \ 0 \ -23 \ 0 \ -2 \ 2 \ 0), \quad j = (-2 \ 2 \ -23 \ 0 \ 0 \ 0 \ 0).$$

As shown in Figure 6.5 below, this means that there are $\epsilon = 4 + 2 + 2 = 8$ new bonds, $L = 1$ new loops and parafermion turns $t_l = t_r = 1$ between the states. Therefore

$$T_{ij} = n \cdot K^8.$$

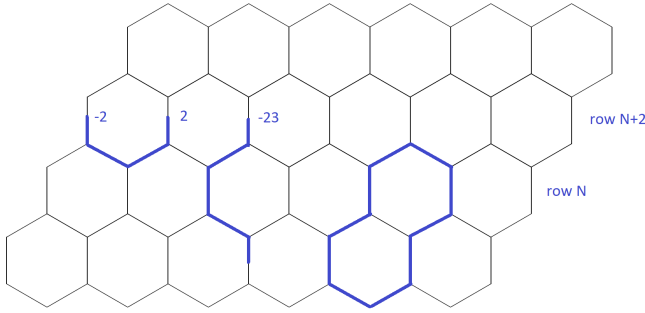


Figure 6.5: A typical situation in space V_1 . A parafermion path starts at $m = 4$.

As explained in section 6.2, a state on row N can give many states on row $N + 2$. Calculating all possible configurations and corresponding weights is again done with a Matlab program.

Transfer matrix is then constructed between the three sets of states, V_1 , V_2 and V_3 . Let there be n_1 , n_2 and n_3 states in these sets. Below the z -row, there are transitions within set V_1 , so the first matrix T_1 has dimension $n_1 \times n_1$. At row z , the parafermion may end at z or there may be two loose ends -23 and 23 for the parafermion. Thus there is a matrix T_2 from set V_1 to set $V_2 \cup V_3$, which is of dimension $(n_2 + n_3) \times n_1$. Above row z , there is a matrix T_3 from set $V_2 \cup V_3$ to set $V_2 \cup V_3$, of dimension $(n_2 + n_3) \times (n_2 + n_3)$. It is useful to rewrite the matrices in $V_1 \cup V_2 \cup V_3$:

$$T_1 = \begin{pmatrix} T_1^a & 0 & 0 \\ 0 & 0 & 0 \\ 0 & 0 & 0 \end{pmatrix}, \quad \tilde{T}_2 = \begin{pmatrix} 0 & 0 & 0 \\ T_2^a & 0 & 0 \\ T_2^b & 0 & 0 \end{pmatrix}, \quad T_3 = \begin{pmatrix} 0 & 0 & 0 \\ 0 & T_3^a & 0 \\ 0 & T_3^b & T_3^c \end{pmatrix}. \quad (6.14)$$

Element (i, j) in these matrices is the weight for transition from state i to state j .

Take now a hexagonal strip with N rows and M columns. Let the state on the first row be $|\beta\rangle$ and the state on the last or N :th row be $|\alpha\rangle$. As the transfer matrices calculate the contributions from all possible states in the lattice, we have the following expression for the expectation value of the

parafermionic observable, $F(k, m) = \langle O(\gamma) \rangle$ (see chapter 3):

$$F(k, m) = \frac{1}{Z} \langle \alpha | T_3^{N-k-1} T_2(m) T_1^k | \beta \rangle, \quad (6.15)$$

where (k, m) is the given end point z of the parafermion path ($k \in \{1, 2, \dots, N\}$, $m \in \{1, 2, \dots, M\}$). In the numerical calculations I usually sum over possible final states $|\alpha\rangle$.

Chapter 7

Loop $O(n)$ model transfer matrix calculations I: the long range order

Transfer matrix T for the loop $O(n)$ model in a hexagonal lattice like in figure 6.2 was constructed in the way explained in section 6.2. I wrote the program for five loops, which means that there could be eleven vertical lines or ten hexagons, in a row (see figure 6.2). But my old PC was able to do calculations with no more than $M = 10$ vertical lines in a row.

The quotient λ_2/λ_1 of the first two eigenvalues of the transfer matrix T should be near one at the critical points. With the transfer matrix $M = 10$ vertical lines, I calculated first two large scale pictures: in Figure 7.1 we have λ_2/λ_1 as a function of temperature dependent coupling constant K , with four values for the dimension n . There should be two critical values K_c for each $n \in [1, 2)$ and one for $n = 2$. For $n < 1$ or $n > 2$, there are no critical points. For the values of K_{c1} , K_{c2} for a given value for n , see section 3.2.

When $K \geq 1$, the loop model is not well defined, so the corresponding results are unimportant. In Figure 7.2 we have $\sum_{k=2}^7 \lambda_k/\lambda_1$ as a function of K .

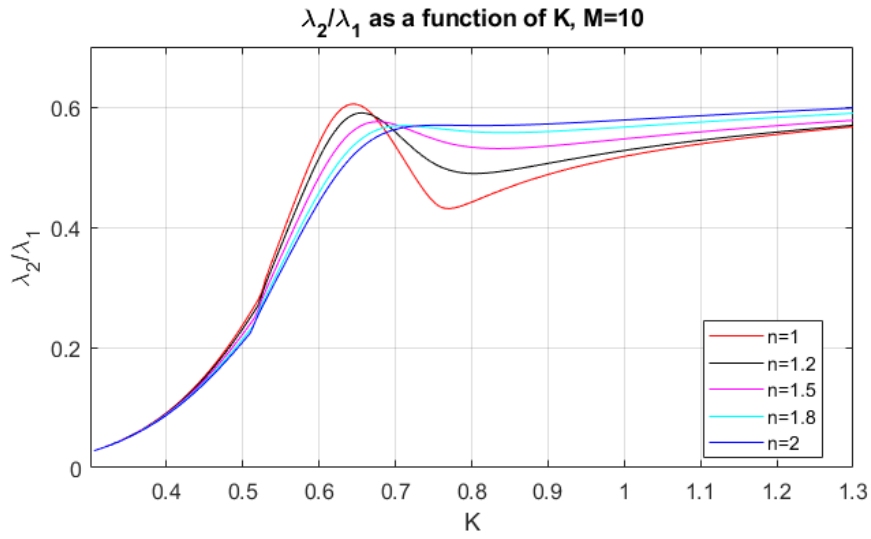


Figure 7.1: Quotient of two first eigenvalues λ_2/λ_1 of transfer matrix T , as a function of coupling constant K . Five values for the parameter n .

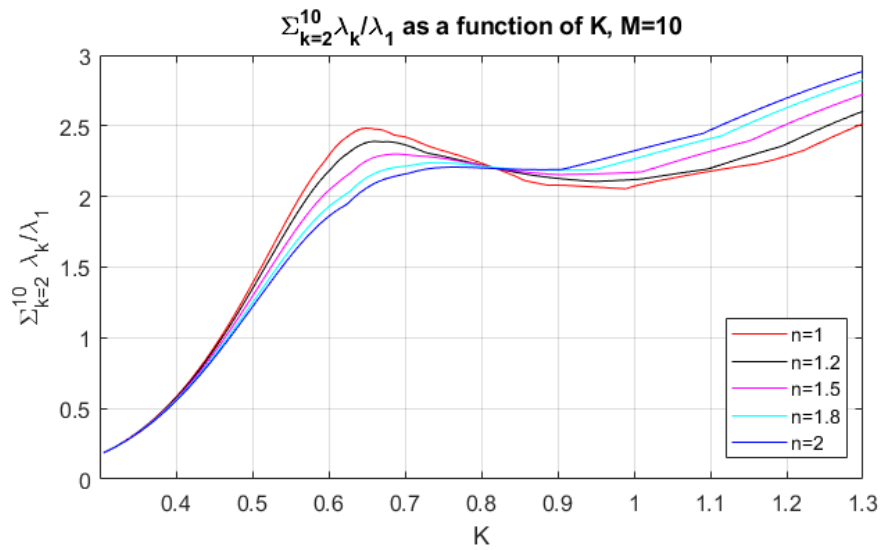


Figure 7.2: Quotient of two first eigenvalues $\sum_{k=2}^7 \lambda_k/\lambda_1$ of transfer matrix T , as a function of the coupling constant K . Five values for parameter n .

Figures 7.1 and 7.2 tell us that the system is delicate to parameter changes between the critical points. Next I study what happens near the critical

points, when the number of columns M in the lattice is varied. It is expected that at the critical points (so that we have $K = K_c$) we have (chapter 4), [16]

$$\xi^{-1}(M) \propto \ln\left(\frac{\lambda_1(M)}{\lambda_2(M)}\right), \quad \frac{1}{X} \propto \frac{\xi_c(M)}{M}, \quad (7.1)$$

where M is the number of columns and c_0 a constant, and X is the scaled gap [16].

I calculated $\ln\left(\frac{\lambda_1(M)}{\lambda_2(M)}\right)$ as a function of K for $M = 7, 8, 9, 10$, for $n = 1.2$ and $n = 1.8$. The results of this are given in the figures 7.3 and 7.4 below. The critical points K_{c1} and K_{c2} are marked as balls: blue for the smaller and red for the larger critical point.

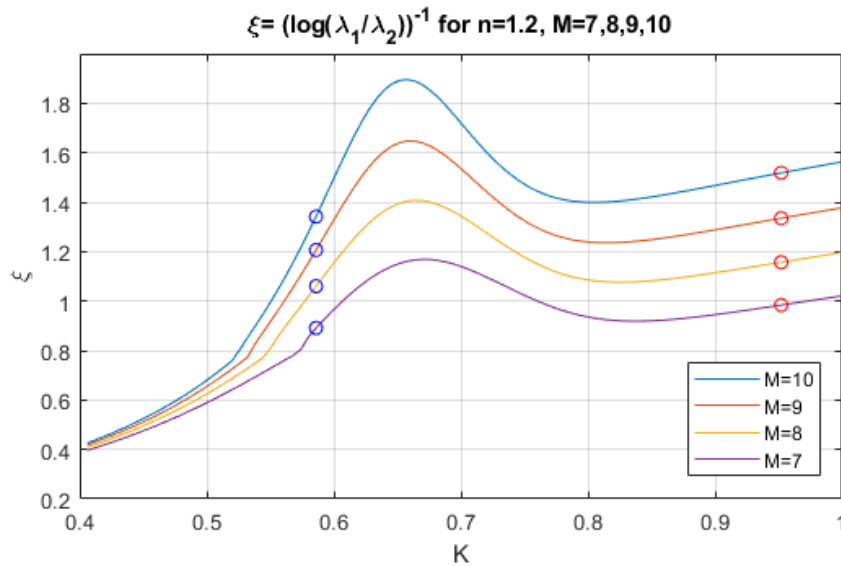


Figure 7.3: Quotient of two first eigenvalues λ_2/λ_1 of transfer matrix T , as a function of the coupling constant K . Five values for the number of columns M .

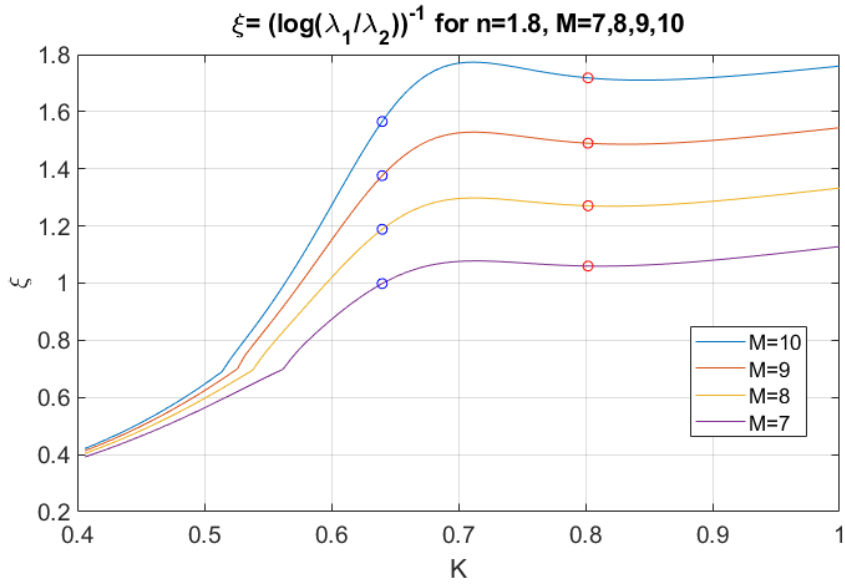


Figure 7.4: Quotient λ_2/λ_1 of eigenvalues of transfer matrix T , as a function of the coupling constant K . Five values for the number of columns M .

I then calculated an approximation for the inverse of scaled gap $1/X$, at the critical points. The results of this calculation are given in figures 7.5 and 7.6 below.

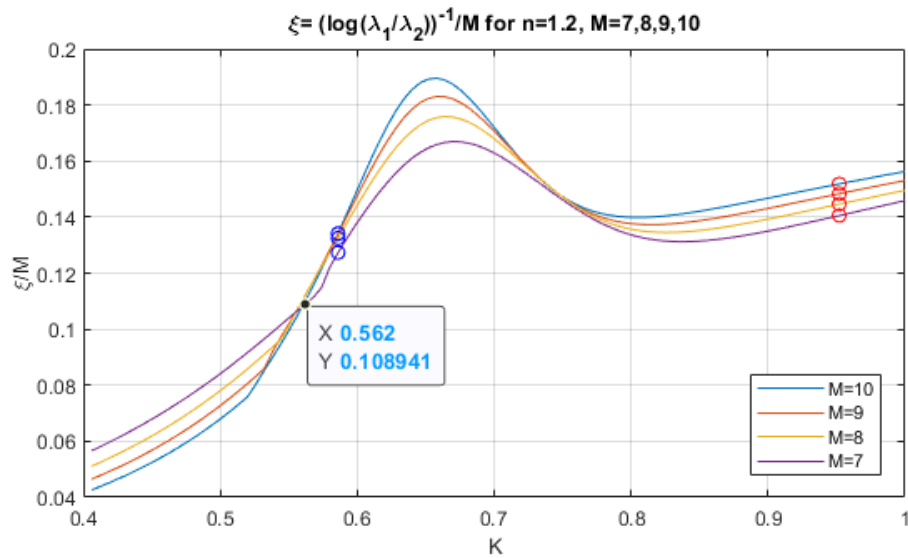


Figure 7.5: $\frac{1}{M} \ln\left(\frac{\lambda_1(M)}{\lambda_2(M)}\right)$ as a function of the coupling constant K . Five values for the number of columns M . $n = 1.2$

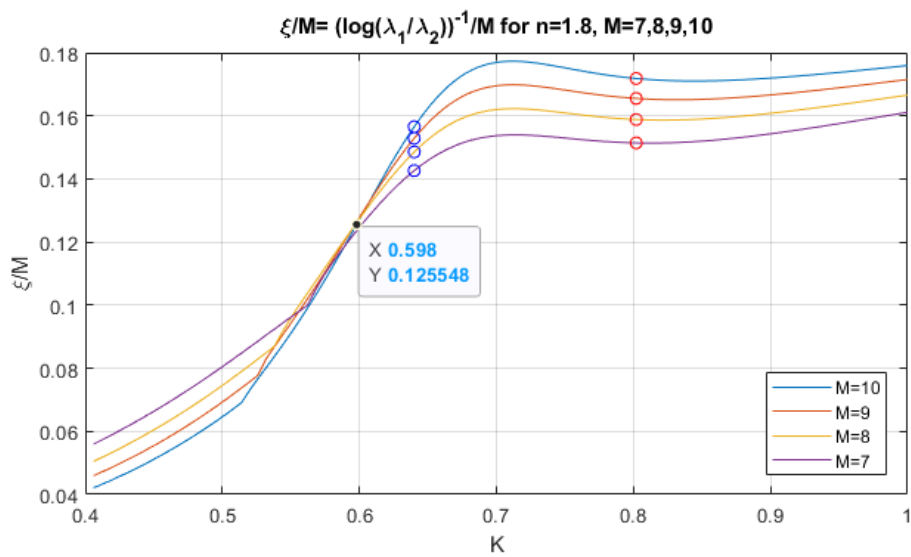


Figure 7.6: $\frac{1}{M} \ln\left(\frac{\lambda_1(M)}{\lambda_2(M)}\right)$ as a function of the coupling constant K . Five values for the number of columns M . $n = 1.8$

The results above make sense, but are not really that good. I think the next ones are more revealing. For the $O(n)$ loop models it is possible to

study correlation lengths directly with the transfer matrix. By this I mean the numerical approach, where we, using the transfer matrix composed as explained in section 6, calculate the following expectation as a function of distance k :

$$F(k, m) = \frac{1}{Z} \langle \alpha | T_3^{M-k} T_2(m) T_1^k | \beta \rangle, \quad m \in \{1, 2, \dots, M\}, \quad (7.2)$$

where $|\beta\rangle$ is an initial state, a state in row one, and is of form $(0, 0, \dots, 0, -23, 0, \dots, 0)$, where element -23 is at the point where the correlation function starts. I chose $m = 4$ for the starting point for the path of the correlation function. Correlation function path ends on row k , at column m . The finite two-dimensional lattice has N rows and M columns. If $N - k > 10$, I found that the state at last row will be one of the states in set V_3 (see section 6.3), as the probability of states in V_2 becomes very small on the rows far above the k :the row. We can either set $|\alpha\rangle = (0, 0, \dots, 0)$, or calculate the average value over all end states. I chose the latter in my calculations.

What kind of results should we expect from such a calculation? For small K , there are many graphs that give a relevant contribution in the numerator. But the difference in numbers of loop configurations for having a correlation path in the middle or not, is also large. Thus, for small $K \simeq 0.1$, I expect larger values for the correlation function (7.2) for small m , with fast decrease fast as m increases. An vice versa for large $K \simeq 1$: the overall values are small, but they do not decrease fast, as m is increased.

I will now study these questions, and more importantly, the change in the functional form of the correlation function (7.2), if it is exponentially decreasing, and how it behaves as a function of M and K . I did my calculations with a lattice of 50 rows and $M \in \{7, 8, 9\}$ columns. It is numerical accuracy that limits the number of rows to 50: $F(m, k)$, $k > 50$ is so small, that the Matlab routines do not work correctly.

I used $m = 4$ and, for the figures below, normalized $F(4, 10) = 1$, so that the correlation functions in the figures start from the same point. This is because I study, for different values of K and M , if these functions decrease exponentially and compare the behaviour for different values of K .

In the first set of three figures where $n = 1.1$, each figure gives $F(m)$ for seventeen different values of K . There are fifteen equally spaced values for the interval $[0.2, 1]$. As $F(4, k)$ is calculated for 41 integer values values $k \in [10, 50]$, we have fifteen sets of 41 points, which are the centers for the red balls in the figures. To each set of 41 points, I fitted an exponential curve by the method of least squares, resulting in the blue curves in the figures. They do not always fit well to the 41 points, which I will try to quantise below, in a different calculation. For $n = 1.1$, there are two critical values for K :

$K_{c1} \simeq 0.5824$ and $K_{c2} \simeq 0.9753$. Again I calculated the 41 values for $F(4, k)$, but now use colours blue for the balls, and red for the fitted exponential function.

Figure 7.7 is for $M = 7$, figure 7.8 for $M = 8$ and figure 7.9 for $M = 9$, and as noted above, $n = 1.1$. The main result of this work is how the blue curves behave, related to the critical red curves, as M increases. It is clear, that the distance of blue curves from the red K_{c1} curve increase, as M increases. The distance of blue curves from the red K_{c2} curve increase, as M increases.

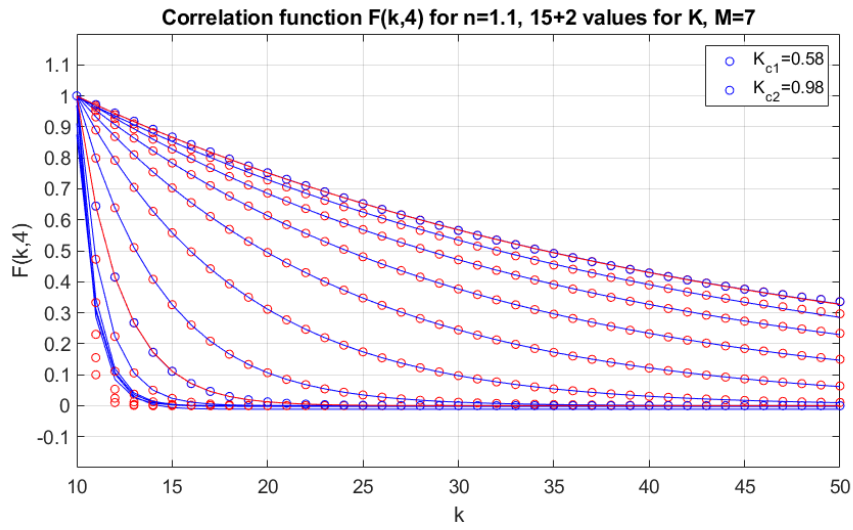


Figure 7.7: Correlation function $F(k, 4)$ as a function of height k . $M = 7$, $n = 1.1$.

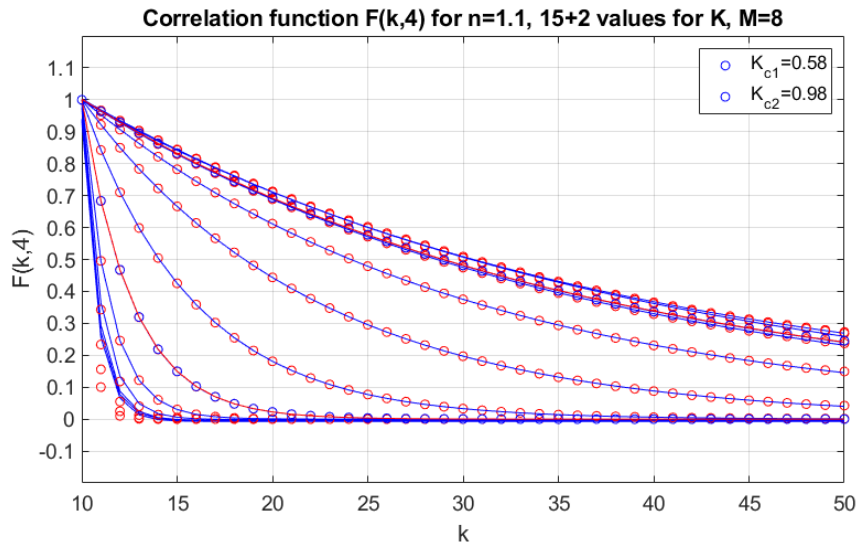


Figure 7.8: Correlation function $F(k,4)$ as a function of height k . $M = 8$, $n = 1.1$.

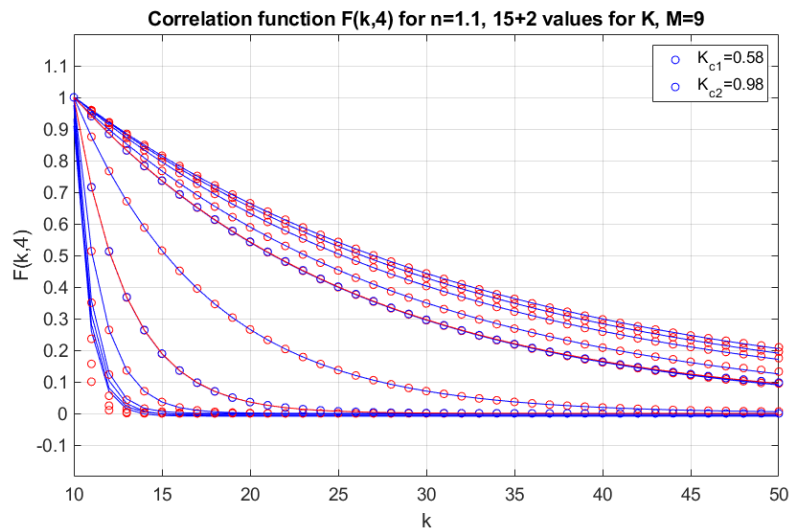


Figure 7.9: Correlation function $F(k,4)$ as a function of height k . $M = 9$, $n = 1.1$.

Then I performed similar calculations with $n = 1.9$, keeping all other parameters the same. The results described in figures 7.10 ($M = 7$), 7.11 ($M = 8$) and 7.12 ($M = 9$) confirm the conclusions given above.

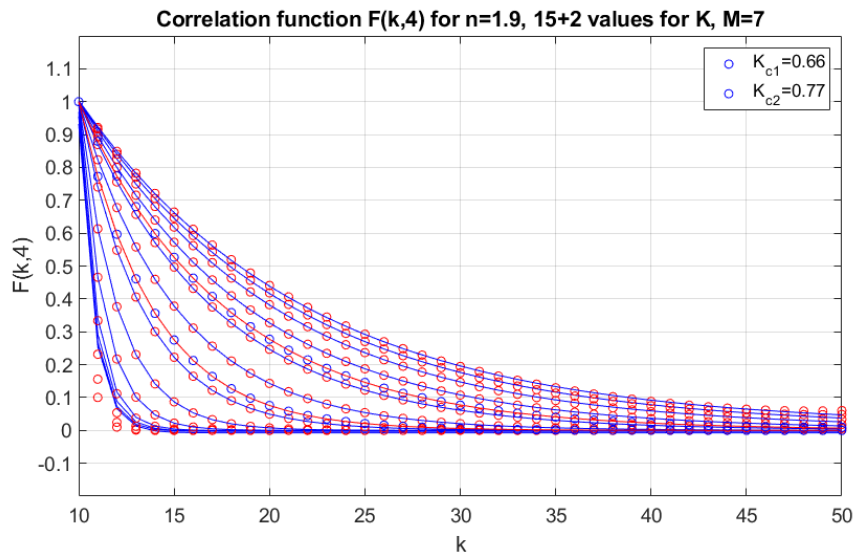


Figure 7.10: Correlation function $F(k,4)$ as a function of height k . $M = 7$, $n = 1.9$.

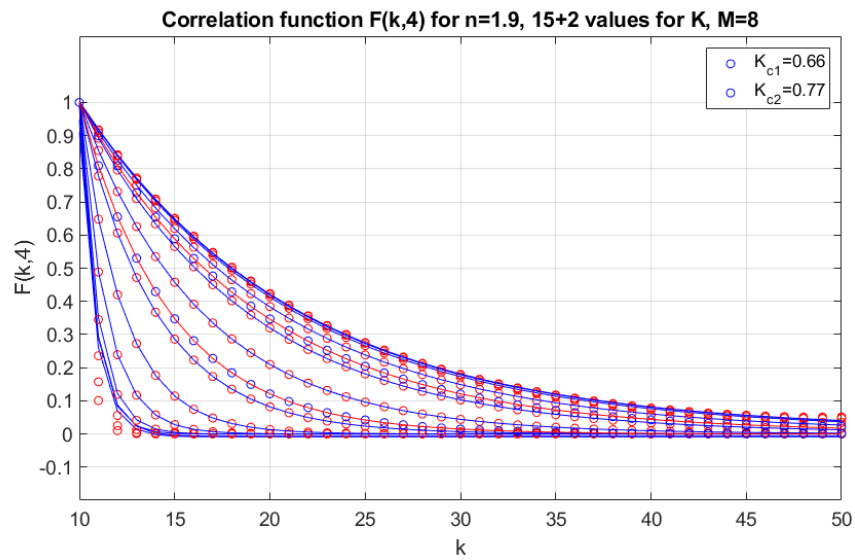


Figure 7.11: Correlation function $F(k,4)$ as a function of height k . $M = 8$, $n = 1.9$.

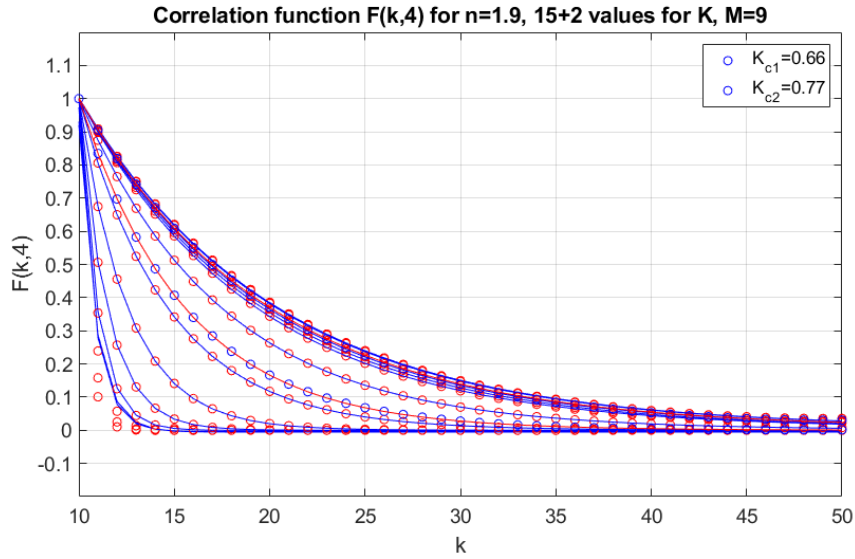


Figure 7.12: Correlation function $F(k, 4)$ as a function of height k . $M = 9$, $n = 1.9$.

It is important to understand that I have normalized all correlation functions by dividing them by $F(10, 4)$. Values $F(10, 4)$ depend strongly on K .

These result result can be expressed in another way, showing the change in $\xi(K)$ as a function of M . For that purpose I calculated the pointwise distance of normalized correlation functions to the normalized critical correlation functions. By the pointwise distance $D(K, K_c, M)$ I mean the following. Take a calculated point p from the critical correlation function $F(k, 4)_{K_c}$. Then draw the normal from point p to the normalized correlation function $F(k, 4)_K$. Let this intersection point be q . Then $D(K, K_c, M) := |p - q|$.

Figure 7.13 below shows how the distance to $D(K, K_{c1}, M)$ changes as M increases. Figure 7.14 is a part of 7.13, giving a closer view of $D(M) \in [0, 0.05]$. These results show that the distance $D(K, K_{c1}, M)$ increases as M increases.

Figure 7.15 below shows how the distance to $D(K, K_{c2}, M)$ changes as M increases. The distance $D(K, K_{c2}, M)$ decreases as M increases.

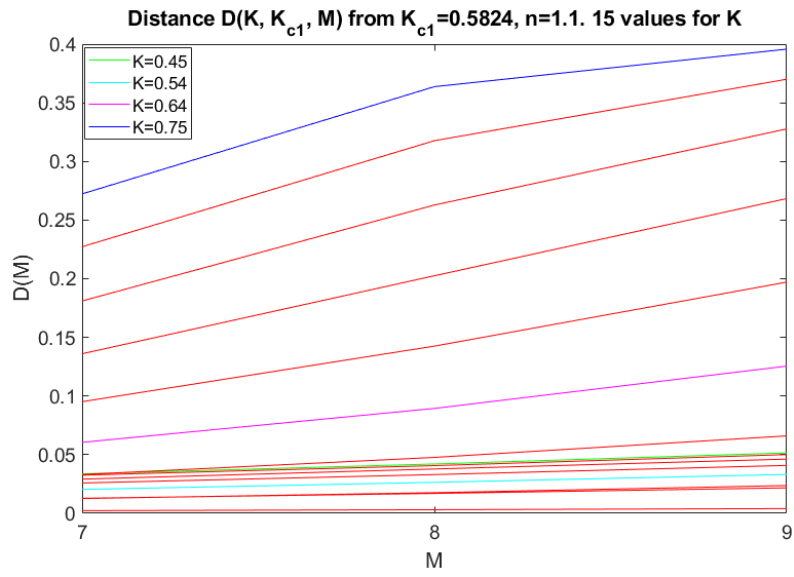


Figure 7.13: Distance $D(K, K_{c1}, M)$ as a function of M . $n = 1.1$.

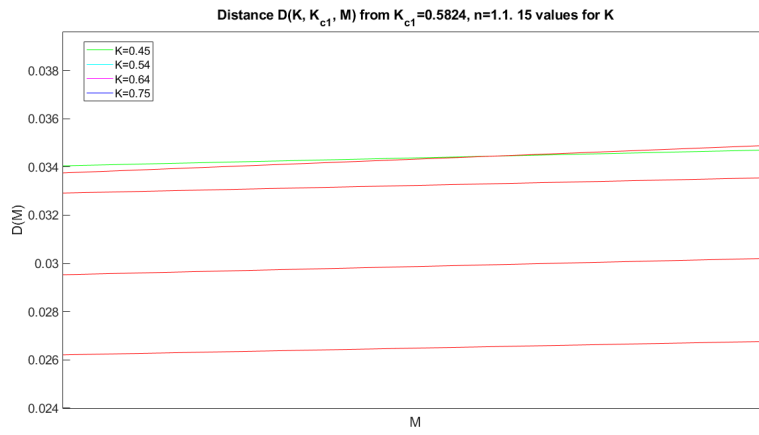


Figure 7.14: Distance $D(K, K_{c1}, M)$ as a function of M . $n = 1.1$.

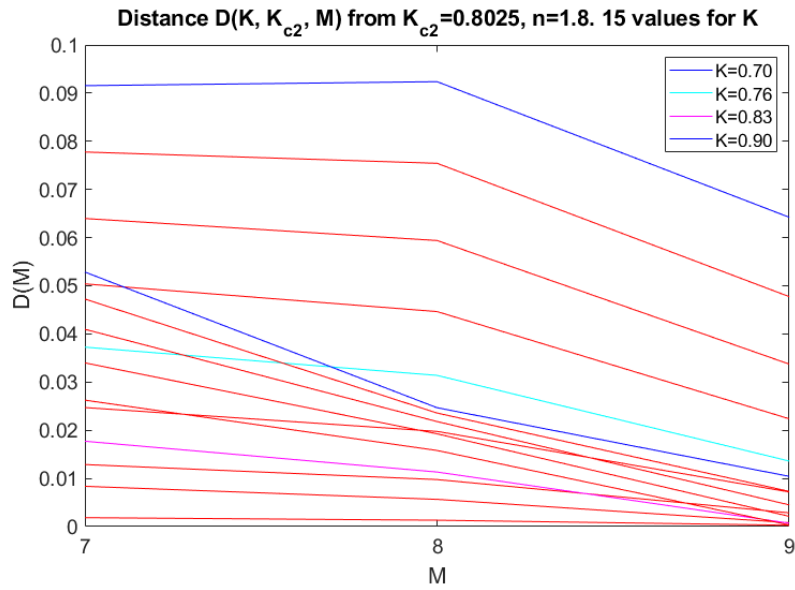


Figure 7.15: Distance $D(K, K_{c2}, M)$ as a function of M . $n = 1.8$.

These results, given in figures 7.13-7.15 confirm the RG-result given in figure 4.2. This approach is new, and seems to be better than the previous approaches, like the comparison of eigenvalues or correlation lengths.

Chapter 8

Loop $O(n)$ model transfer matrix calculations II: testing the s -holomorphicity of the parafermionic observable

In chapter 5 we found the following conditions for the s -holomorphicity

$$\begin{aligned}(e_1): \quad & F(z_1) + \bar{e}_1^{2s} \overline{F(z_1)} = F(z_2) + \bar{e}_1^{2s} \overline{F(z_2)}, \\(e_2): \quad & F(z_2) + \bar{e}_2^{2s} \overline{F(z_2)} = F(z_3) + \bar{e}_2^{2s} \overline{F(z_3)}, \\(e_3): \quad & F(z_3) + \bar{e}_3^{2s} \overline{F(z_3)} = F(z_4) + \bar{e}_3^{2s} \overline{F(z_4)}, \\(e_4): \quad & F(z_4) + \bar{e}_4^{2s} \overline{F(z_4)} = F(z_1) + \bar{e}_4^{2s} \overline{F(z_1)},\end{aligned}\tag{8.1}$$

where

$$e_1 = -1, \quad e_2 = e^{i4\pi/3}, \quad e_3 = 1, \quad e_4 = e^{i\pi/3}.\tag{8.2}$$

$$\bar{e}_1 = -1, \quad \bar{e}_2 = e^{-i4\pi/3}, \quad \bar{e}_3 = 1, \quad \bar{e}_4 = e^{-i\pi/3}.\tag{8.3}$$

These equations and the related geometry in figure 8.1 below were explained in chapter 5.

Function F is here formed with the transfer matrix method, numerically. $F(k, m)$ was defined and explained in chapter 6, so that

$$F(k, m) = \frac{1}{Z} \langle \alpha | T_3^{M-k} T_2(m) T_1^k | \beta \rangle, \quad m \in \{1, 2, \dots, M\}.\tag{8.4}$$

As the initial state $|\beta\rangle$, I chose $(0, 0, 0, -23, 0, 0, 0)$, and I averaged over all possible final states $|\alpha\rangle$.

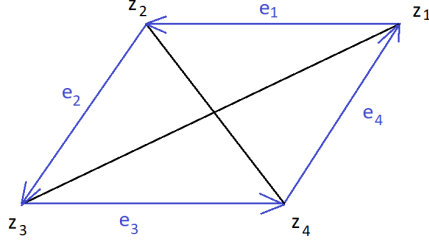


Figure 8.1: Unit cell in the medial lattice from Figure 5.5. Numerical transfer matrix calculations determine $F(z)$ at points z_1, z_2, z_3, z_4 .

I will test relations (8.1) with lattices of $N \times M$ hexagons, with $N = 50$ and $M \in \{7, 8\}$. For the points z_1, z_2, z_3, z_4 I will use sets (expressing z as *(row, column)*)

$$\text{set 1: } \quad z_3 = (25, 4), \quad z_4 = (25, 5), \quad z_2 = (26, 4), \quad z_1 = (26, 5), \quad (8.5)$$

$$\text{set 2: } \quad z_3 = (20, 4), \quad z_4 = (20, 5), \quad z_2 = (21, 4), \quad z_1 = (21, 5), \quad (8.6)$$

$$\text{set 3: } \quad z_3 = (25, 2), \quad z_4 = (25, 3), \quad z_2 = (26, 2), \quad z_1 = (26, 3), \quad (8.7)$$

To have a reasonable number of figures in the text, I will give results for only the set 1 in this chapter. Some results for sets 2 and 3 are given in appendix B.

I use the parameter expressions by Cardy [5], explained in chapter 3:

$$\begin{aligned} n &= -2 \cos(4\pi/\alpha), \\ s &= (6 - \alpha)/2\alpha, \\ K &= \left(2 \pm \sqrt{2 - n}\right)^{-1/2}. \end{aligned} \quad (8.8)$$

For values $n \in (0, 2]$, we should have $\alpha \in (-8, -8/3) \cup (8/3, 8)$. Each value for α determines the value for s, n, K_1 and K_2 . I call the values related to $\alpha \in (-8, -8/3)$ and $\alpha \in (8/3, 8)$ branches 1 and 2, respectively. Figure 8.2 below shows the possible sets of parameter values.

I tested s-holomorphicity by calculating errors $\epsilon_k, k = 1, 2, 3, 4$:

$$\begin{aligned} \epsilon_1 &:= \left| F(z_1) + \bar{e}_1^{-2s} \overline{F(z_1)} - F(z_2) - \bar{e}_1^{-2s} \overline{F(z_2)} \right|, \\ \epsilon_2 &:= \left| F(z_2) + \bar{e}_2^{-2s} \overline{F(z_2)} - F(z_3) - \bar{e}_2^{-2s} \overline{F(z_3)} \right|, \\ \epsilon_3 &:= \left| F(z_3) + \bar{e}_3^{-2s} \overline{F(z_3)} - F(z_4) - \bar{e}_3^{-2s} \overline{F(z_4)} \right|, \\ \epsilon_4 &:= \left| F(z_4) + \bar{e}_4^{-2s} \overline{F(z_4)} - F(z_1) - \bar{e}_4^{-2s} \overline{F(z_1)} \right|, \end{aligned} \quad (8.9)$$

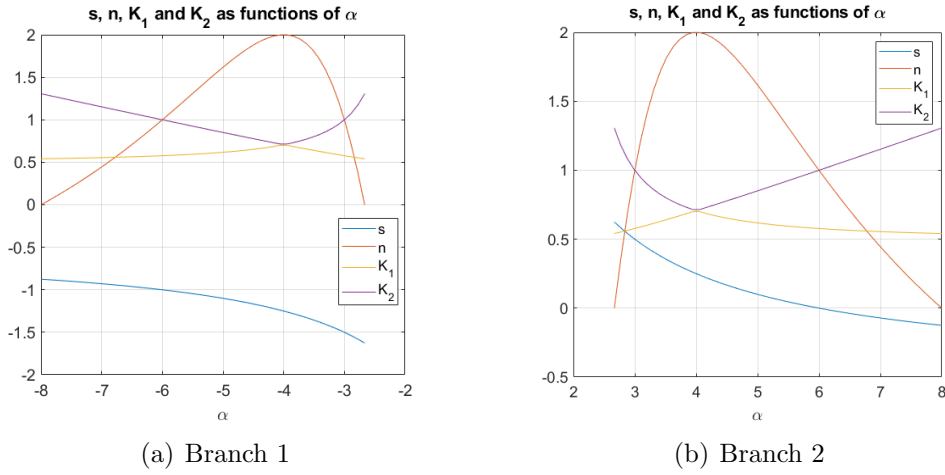


Figure 8.2: s , n , K_1 and K_2 for branches 1 ($\alpha \in (-8, -8/3)$) and 2 ($\alpha \in (8/3, 8)$).

In the numerical studies of s -holomorphicity, I calculated errors $\epsilon_1, \epsilon_2, \epsilon_3, \epsilon_4$ as a function of α , for the two branches and the two values for K , and for two values for M , $M = 7$ and $M = 8$. Thus there would be 8 figures representing the results. I will only show here the figures for branch 2, $K = K_2$, $M = 7$ (Figure 8.3 below) and branch 2, $K = K_2$, $M = 8$ (Figure 8.4 below), which is the most promising case. The other 6 figures can be found in Appendix B.

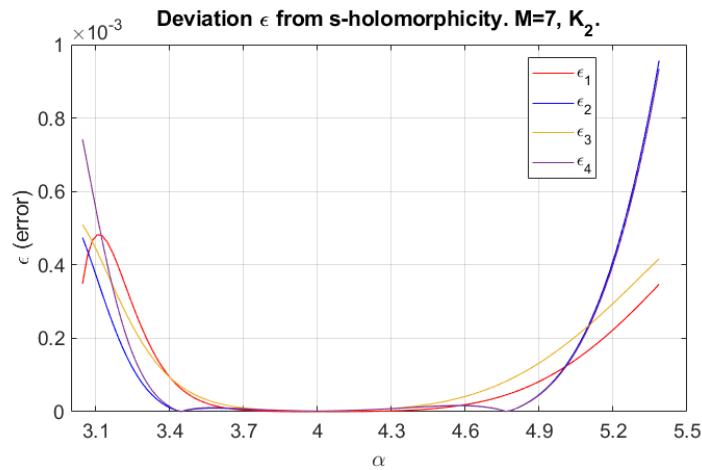


Figure 8.3: Deviation ϵ from s -holomorphicity in the four directions of the unit cell in figure 8.1, $M=7$, $K = K_2$, branch 2.

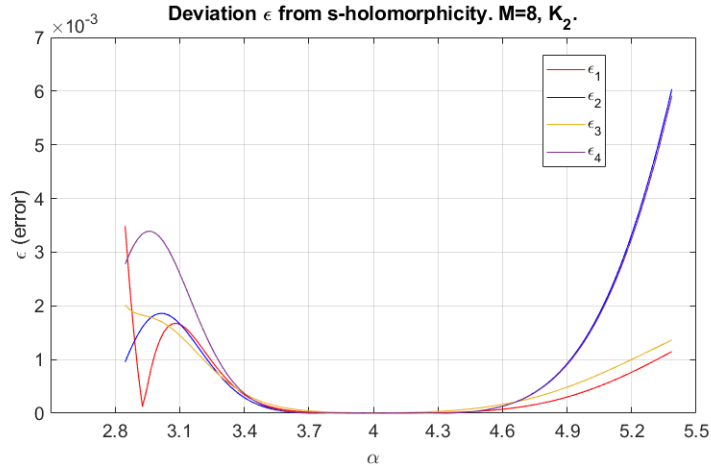


Figure 8.4: Deviation ϵ from s-holomorphicity in the four directions of the unit cell in figure 8.1, $M = 8$, $K = K_2$, branch 2.

Thus, at $\alpha = 4$, $n = 2$, $K = 1/\sqrt{2}$, we might experience s-holomorphicity. However, a closer inspection around $\alpha = 4$, given in figures 8.5 and 8.6 below contradicts this, although the discrepancy seems small.

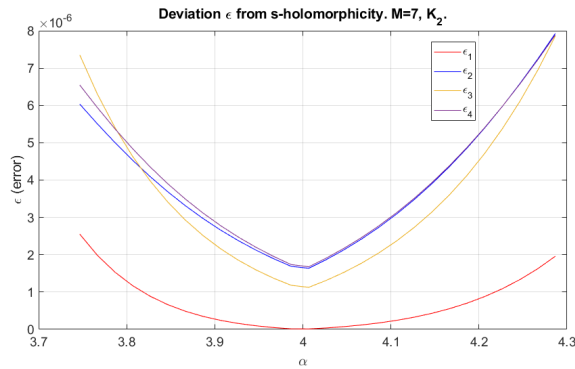


Figure 8.5: Deviation ϵ from s-holomorphicity in the four directions of the unit cell in figure 8.1, $M = 7$, $K = K_2$, branch 2.

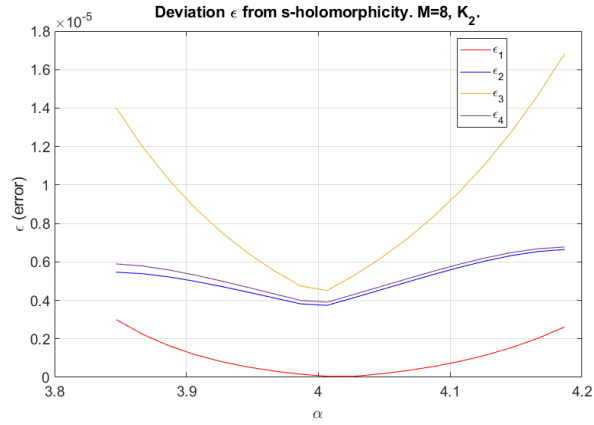


Figure 8.6: Deviation ϵ from s-holomorphicity in the four directions of the unit cell in figure 8.1, $M = 8$, $K = K_2$, branch 2.

As the final calculation, I will study how $F_{K_{c_2}}(k, m)$ behaves when the number of columns (lattice size) M is increased from $M = 7$ to $M = 8$. Motivated by the results above, I use the values $K_{c_2} = \sqrt{2}$, $n = 2$ and $K_{c_2} = 0.5774$, $n = 1$. These results are given in Appendix C.

Chapter 9

Conclusions

In chapter 2 I explained how the loop $O(n)$ model is derived from the $O(n)$ model, after making a certain approximation.

In chapter 6 I gave a new method for the construction of the transfer matrices for the loop $O(n)$ model, for the partition function and the expectation value of the parafermionic observable. This construction can be used for the calculation of correlation functions.

I consider the results given in chapter 7 are valuable. Examining the distances of normalized correlation functions to the critical correlation functions, seems to be an accurate measure of the critical behaviour: finding and characterizing the fixed points and understanding the physics near the fixed points. It seems to be an advancement compared to the classic transfer matrix approach that uses the two largest eigenvalues.

Results in chapter 8, concerning s-holomorphicity are reasonable, but not as clear as in chapter 7. The results in chapter 8 prove that the numerical transfer matrix calculations are valuable even for such deep theoretic questions as s-holomorphicity.

Bibliography

- [1] LANDAU, L. D., LIFSHITZ, E. M. *Statistical Physics. Volume 5 of Course of Theoretical Physics (3.ed)*. Elsevier Butterworth-Heinemann, 1980.
- [2] SMIRNOV, S., DUMINIL-COPIN, H. Conformal invariance of lattice models. In *Probability and statistical physics, in two and more dimensions*, Clay Math. Proc., 15, Amer. Math. Soc. (2012), 213-276.
- [3] NIENHUIS, B. Exact Critical Point and Critical Exponents of $O(n)$ Models in Two Dimensions. *Phys Rev. Letters*, 49(15) (1982), 1062-1065.
- [4] MUSSARDO, G. *Statistical Field Theory. An introduction to Exactly Solved Models in Statistical Physics*. Oxford University Press, 2010.
- [5] CARDY, J. Holomorphic Parafermions in Loop Models and SLE. *A talk given in Florence*. <https://www.ggi.infn.it/talkfiles/slides/talk694.pdf>. (2008).
- [6] CARDY, J. *Scaling and Renormalization in Statistical Physics*. Cambridge University Press, 1996.
- [7] KAWASHIMA, N. . *Lecture notes in "Advanced Statistical Mechanics"*. Lectures at Tokyo University. <https://kawashima.issp.u-tokyo.ac.jp/wp/wp-content/uploads/2020/09/StatisticalMechanics.pdf>. (2019).
- [8] DUBAIL J., JACOBSEN J. L., SALEUR H., Conformal boundary conditions in the critical $O(n)$ model and dilute loop models. *Nuclear Physics B* 827, (2010), 457-502.
- [9] LAVIS, D. A., BELL, G. M. *Statistical Mechanics of Lattice Systems. Vol 2: Exact, series and Renormalization Group Methods*. Springer, 1999.

- [10] NIENHUIS, B. Loop Models. In *Les Houches 2008, Session LXXXIX : Exact Methods in Low-Dimensional Statistical Physics and Quantum Computing.*: Oxford University Press, 2008, pp159-195.
- [11] CARDY, J. Conformal field theory and statistical mechanics (Lecture - 01). *Lecture given at the International Centre for Theoretical Sciences.* Video at: <https://www.youtube.com/watch?v=8uFLDxGzvwQ>. 2017.
- [12] DOMB, C. On the theory of cooperative phenomena in crystals. *Advances in Physics*, 9 (34), (1960), 149-244.
- [13] ASTALA, K. *Kompleksianalyysi I. Lecture notes at the University of Helsinki.* 2016.
- [14] AHLFOR, S L. *Complex analysis.* McGraw-Hill, 1979.
- [15] DUMINIL-COPIN, H. Parafermionic observables and their applications to planar statistical physics models, *Ensaio Matemáticos*, 25 (2013), 1-371.
- [16] BLÖTE, H., NIENHUIS, B. The phase diagram of the $O(n)$ model. *Physica A* 160 (1989), 121-134.

Appendix A

Algorithms

Algorithm A.0.1. (*Formation of V_1*)

Let $M > 0$.

First possible state, the zero vector $W_N = (0, 0, \dots, 0)$, has no loops.

If M is odd, there may be $(M - 1)/2$ loops. If M is even, $M/2$ loops. Let this maximal number of loops be m .

States with one loop are formed in the following way:

Algorithm 1 states with with one loop

```
 $W_N = \text{zeros}(M, 1);$   
for  $j=1:M-1$  do  
   $W_n(j) = -2;$   
  for  $k=j+1:M$  do  
     $W_N(k) = 2;$   
     $W_N$  ready, store it;  
     $W_N(k) = 0;$   
  end for  
   $W_n(j) = 0;$   
end for
```

States with two loops are formed in the following way:

Algorithm 2 states with with two loops

```
 $W_N = \text{zeros}(M, 1);$   
for  $j_1=1:M-1$  do  
   $W_n(j) = -2;$   
  for  $k_1=j_1+1:M$  do  
     $W_N(k_1) = 2;$   
    for  $j_2=j_1+1:k_1-2$  do  
       $W_n(j) = -3;$   
      for  $k_2=j_2+1:k_1-1$  do  
         $W_N(k_1) = 3;$   
         $W_N$  ready, store it;  
         $W_N = \text{zeros}(M, 1);$   
      end for  
    end for  
  end for  
  for  $j_2=k_1+1:M-1$  do  
     $W_n(j) = -3;$   
    for  $k_1=j_2+1:M$  do  
       $W_N(k_1) = 3;$   
       $W_N$  ready, store it;  
       $W_N = \text{zeros}(M, 1);$   
    end for  
  end for  
   $W_N(k_1) = 0;$   
end for  
 $W_n(j_1) = 0;$   
end for
```

Appendix B

Additional figures for chapter 8 (s-holomorphicity)

The first 6 figures are for the two branches, two values for K , and for two values for M , $M = 7$ and $M = 8$. Thus there would be 8 figures representing the results of which 2 are given in section 8.

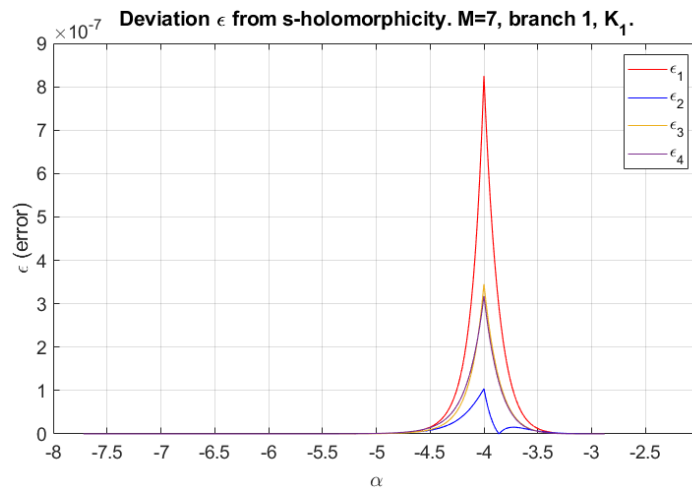


Figure B.1: Deviation ϵ from s-holomorphicity in the four directions of the unit cell in figure 8.1, $M = 7$, $K = K_1$, branch 1

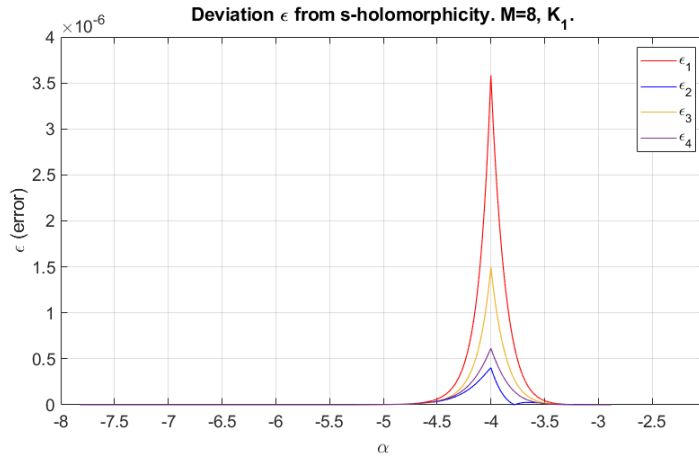


Figure B.2: Deviation ϵ from s-holomorphicity in the four directions of the unit cell in figure 8.1, $M = 8$, $K = K_1$, branch 1

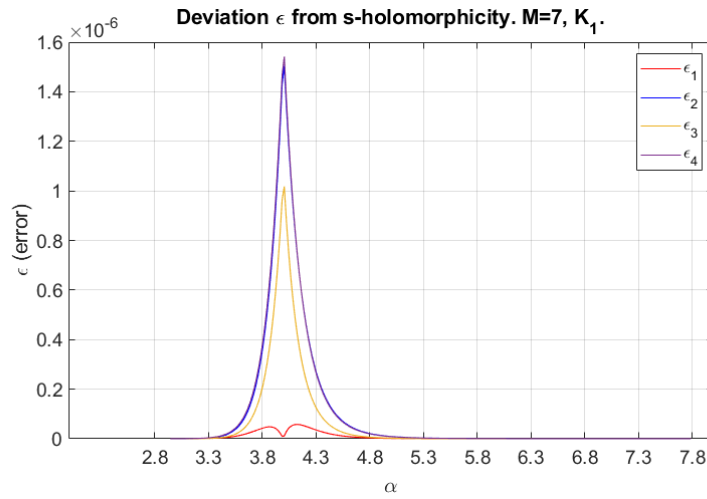


Figure B.3: Deviation ϵ from s-holomorphicity in the four directions of the unit cell in figure 8.1, $M = 7$, $K = K_1$, branch 2

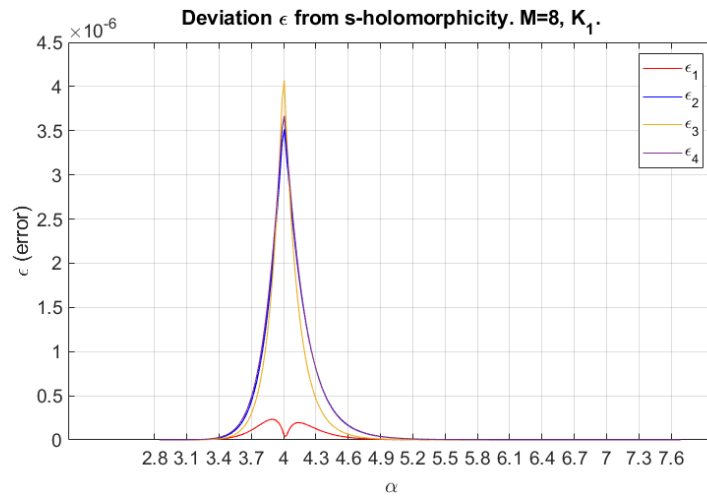


Figure B.4: Deviation ϵ from s-holomorphicity in the four directions of the unit cell in figure 8.1, $M = 8$, $K = K_1$, branch 2

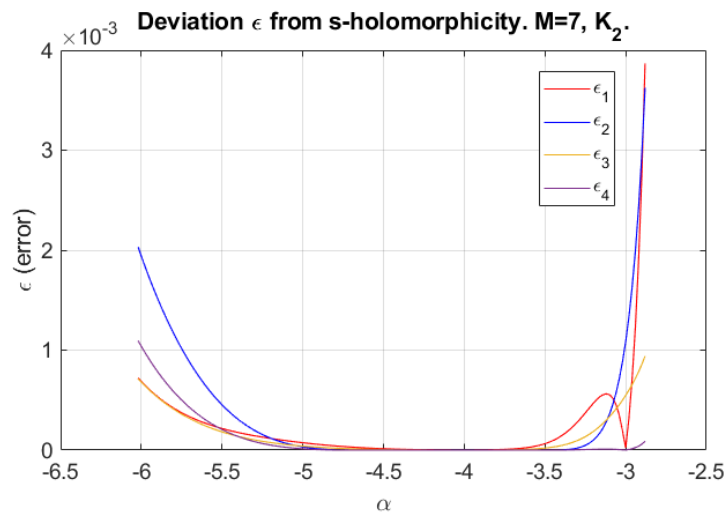


Figure B.5: Deviation ϵ from s-holomorphicity in the four directions of the unit cell in figure 8.1, $M = 7$, $K = K_2$, branch 1

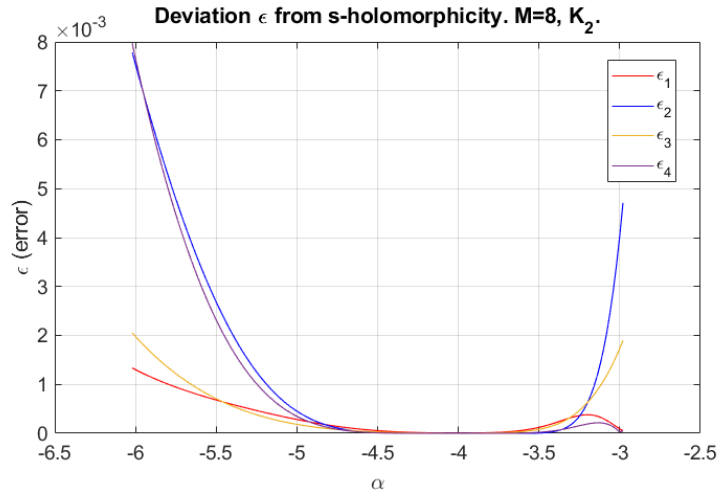


Figure B.6: Deviation ϵ from s-holomorphicity in the four directions of the unit cell in figure 8.1, $M = 8$, $K = K_2$, branch 1

I did also a calculation with set 2 (8.6), $M = 7$, $K = K_{c2}$. It gave the same results as set 1 (8.5). But calculation with set (8.7) gave a somewhat different result to set (8.5).

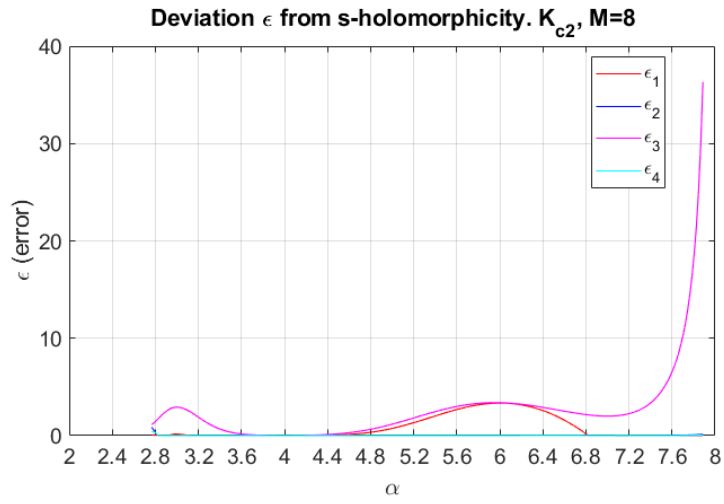


Figure B.7: Deviation ϵ from s-holomorphicity in the four directions of the unit cell in figure 8.1. $M = 8$, $K = K_{c2}$. Point set (8.5).

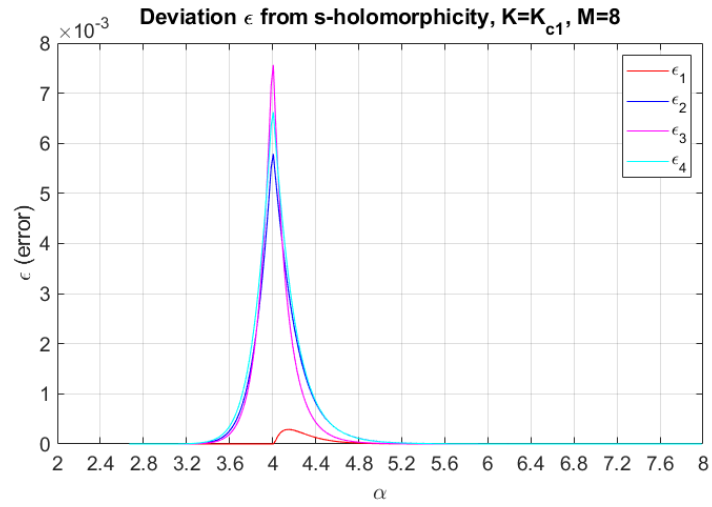


Figure B.8: Deviation ϵ from s-holomorphicity in the four directions of the unit cell in figure 8.1. $M = 8$, $K = K_{c1}$. Point set (8.5).

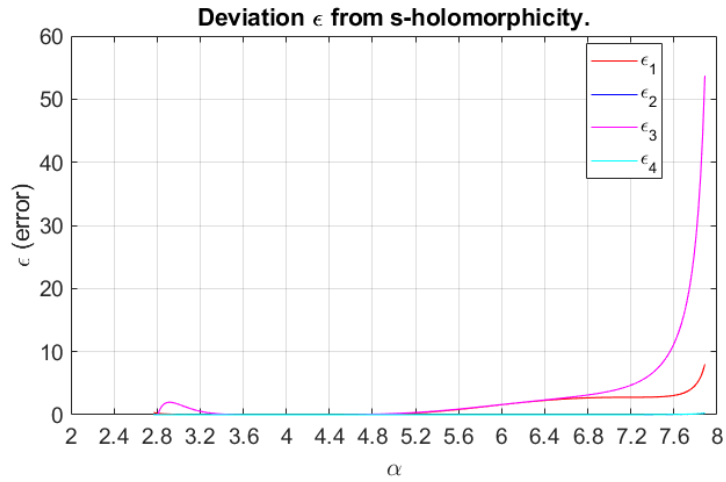


Figure B.9: Deviation ϵ from s-holomorphicity in the four directions of the unit cell in figure 8.1. $M = 7$, $K = K_{c2}$. Point set (8.7).

Appendix C

Additional figures for chapter 8 (parafermion)

Figures C.1-C.4 for $K_c = \sqrt{2}$, $n = 2$ and $M = 7, 8$ show that there may be convergence as M increases. Figures C.5-C.8 for $K_{c_2} = 0.5774$, $n = 1$ and $M = 7, 8$ show that there is no convergence when M increases. As in all similar figures in chapter 7, $F(k, 4)_K$ are normalized so that $F(10, 4)_K = 1$.

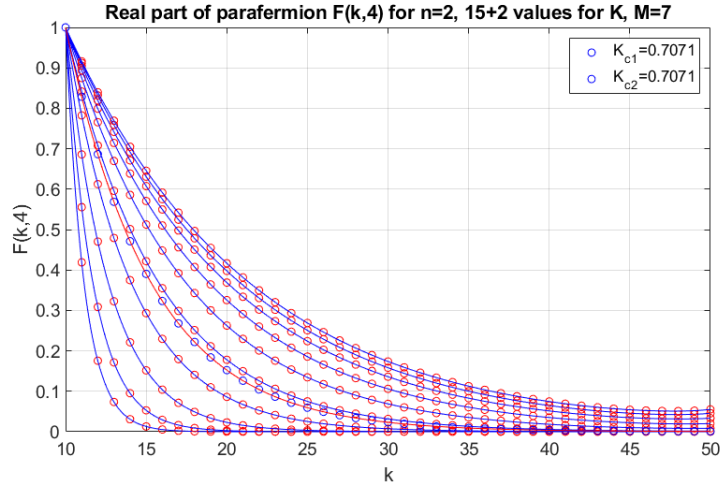


Figure C.1: $ReF(k, 4)$, $M = 7$, $n = 2$, $K_c = \sqrt{2}$

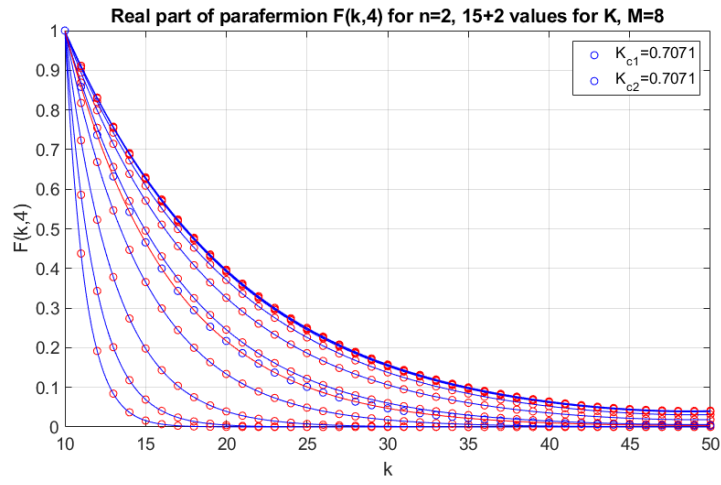


Figure C.2: $ReF(k,4)$, $M = 8$, $n = 2$, $K_c = \sqrt{2}$

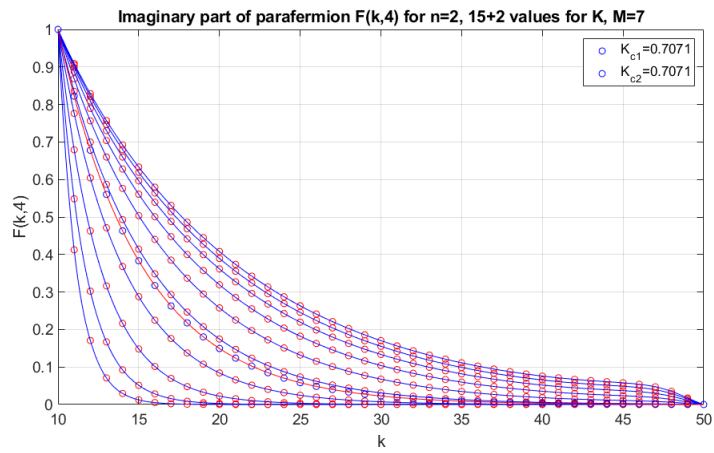


Figure C.3: $ImF(k,4)$, $M = 7$, $n = 2$, $K_c = \sqrt{2}$

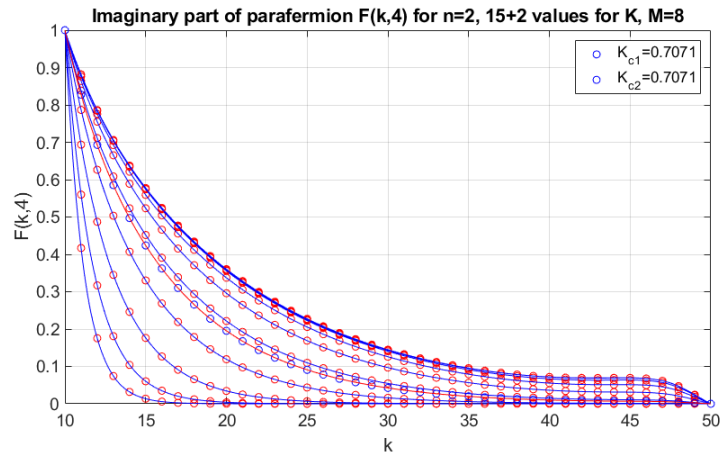


Figure C.4: $ImF(k,4)$, $M = 8$, $n = 2$, $K_c = \sqrt{2}$

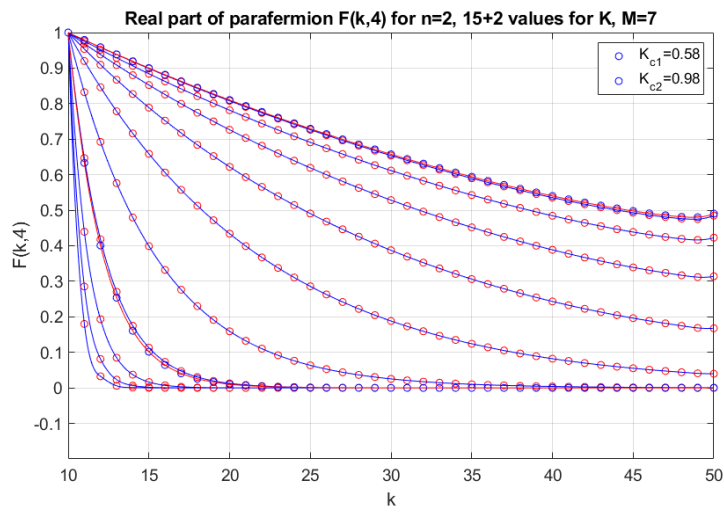


Figure C.5: $ReF(k,4)$, $M = 7$, $n = 1$, $K_{c1} = 0.5774$

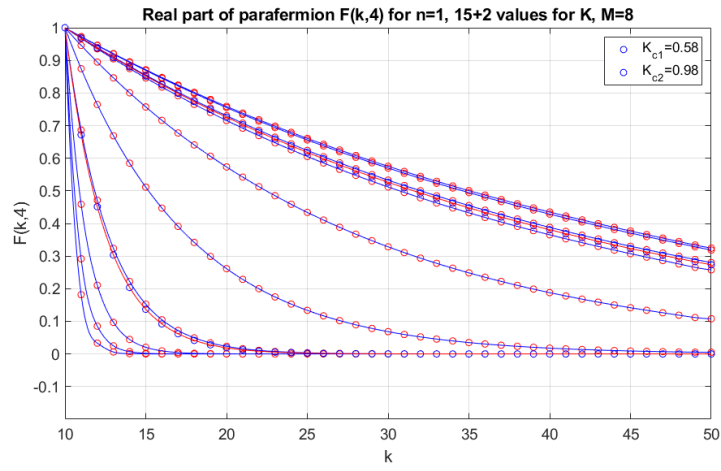


Figure C.6: $ReF(k,4)$, $M = 8$, $n = 1$, $K_{c1} = 0.5774$

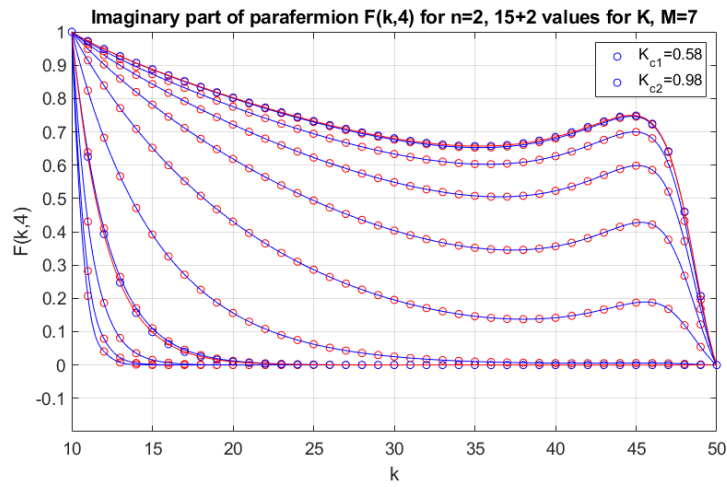


Figure C.7: $ImF(k,4)$, $M = 7$, $n = 1$, $K_{c1} = 0.5774$

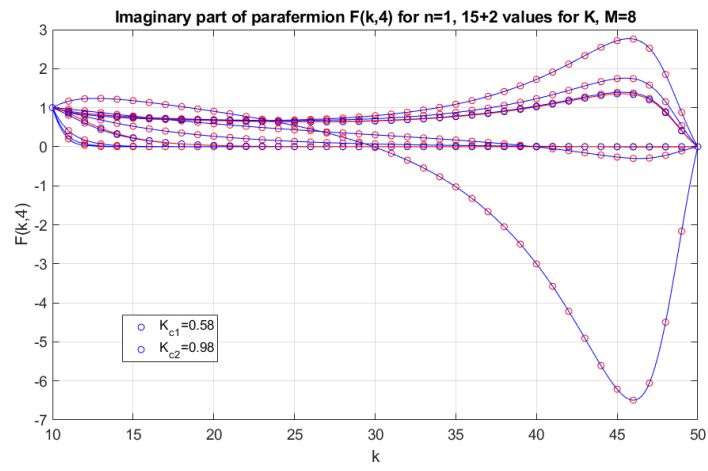


Figure C.8: $ImF(k, 4)$, $M = 8$, $n = 1$, $K_{c_1} = 0.5774$